UNIVERSITY OF MINES AND TECHNOLOGY, (UMaT)

TARKWA

FACULTY OF MINERAL RESOURCES TECHNOLOGY

DEPARTMENT OF GEOLOGICAL ENGINEERING

A PROJECT REPORT ENTITLED

DESIGN OF OPTIMAL SLOPE PARAMETERS FOR THE PROPOSED KOBEDA PIT AT GOLD FIELDS GHANA LIMITED, TARKWA MINE

BY

MOHAMMED MWENE SOMA BALEGHA

SUBMITTED IN PARTIAL FULFILMENT OF THE REQUIREMENTS FOR THE AWARD OF MASTER OF SCIENCE DEGREE IN GEOLOGICAL ENGINEERING

PROJECT SUPERVISOR

…………………………………………

ASSOC PROF MICHAEL AFFAM

TARKWA, GHANA

MAY, 2019

DECLARATION

I declare that this thesis is my own wok. It is being submitted for the degree of

……………………………………………………………………………………………..
in the University of Mines and Technology (UMaT), Tarkwa. It has not been submitted for any degree or examination in any other university.

……………………………………

(Mohammed Mwene Soma Balegha)

………………. day of …………………………..2019

ABSTRACT

Tarkwa Gold Mine (TGM) is depleting its reserves to the east of the mine. It has, as a result embarked on vigorous near mine exploratory work to the west of the concession for reserve generation. Results indicate gold mineralisation of economic interest. TGM seeks to provide slope design that would satisfy shareholders and employees in the context of safety, ore recovery, and financial returns for the proposed Kobeda Pit.

Rock Mass Rating (RMR) and subsequent adjustment to obtain the Mining Rock Mass Rating (MRMR) was done for rock mass characterisation. The rock mass ratings for the various geotechnical zones ranged from 40.91 to 67.72 and rated from fair to very good.

Kinematic stability analyses were performed for all the three design sectors using stereographic techniques to determine the failure modes that are kinematically possible in bench and/or multi-bench scale slopes. Multi-bench scale planar and wedge failures are kinematically possible in all sectors.

Limit equilibrium analysis gave factors of safety that exceeded the minimum acceptable factor of safety of 1.05 for completely weathered material and 1.20 for fresh rock. The probability of failure was however less than 5%.

Pit wall architecture for the geotechnical domains were 8 meters, 18 meters, 75 degrees for the berm width, bench height, and bench face angle respectively. Indicative overall slope angles fell between 50.02 to 59.21 degrees and rated from fair to very good.

ACKNOWLEDGEMENT

To God be the glory, for great things he has done. I thank God for His immeasurable grace upon me. Your grace alone brought me this far. I am eternally grateful ‘Papa’.

I will use this opportunity to thank my thesis Supervisor, Assoc Prof Michael Affam for his patience, encouragement, timely direction, and tutelage during this course. He was more than a father.

I equally appreciate the direction, pieces of advice and encouragement of all lectures of the department of Geological Engineering of the University of Mines and Technology, most especially Dr Anthony Ewusie, Dr Asare Annor, Dr Douglas Oti, and Mr Seidu Jamil.

My gratitude goes to the management of Gold Fields Ghana, Tarkwa Mine, for paying my fees, and to my Head of Department, Mr Godfred Baba Avane for his support. Sampson Owusu deserves my mention for the opportunity to even partake in this program in the mist of heavy work load.

Mr Conduah Ebenezer, the chief Geologist (Geotechnical Engineering), my boss and mentor deserves my gratitude for the quality time he spent on me amidst his busy schedule. Boss, I am grateful. Mr Clement Acheampong, I can’t forget of you after I worried you severely for data and technical support. Thanks mate.

Mr Martin Kufuor, you encouraged me to take up an MSc programme earlier than I had planned. It was worth it. Thank you Kufuor. To all my course mates and all who helped in one way or the other, I say God Bless you.

To my wife, Monica Balegha and Son, Jesse Ansin Mwene Balegha, who lost due access to my time, care and love, I say thank you for that huge sacrifice.

TABLE OF CONTENT

Content **Page**

LIST OF FIGURES

LIST OF TABLES

CHAPTER 1

INTRODUCTION

1.1 Statement of Problem

Tarkwa Gold Mine (TGM), of Gold Fields Ghana Limited, over the past eighteen (18) years, was mining extensively from the eastern part of its concession, thereby depleting the reserve to that part of the Mine. Some of its existing active open pits have been mined to a high depth leading to an increase in the stripping ratio.

Neighbouring communities to the east of the mine are the University of Mines and Technology, and the Brahabobom Township. Mining activities close to these communities have the potential of causing community agitation and putting the company into problem with the regulatory bodies. On a number of occasions, there were reports of excessive blast vibration and incidence of fly rocks into the Brahabobom community.

To avert the aforementioned issues and maintain its vision as the global leader in sustainable gold mining, TGM embarked on vibrant near mine exploratory work to the west of the concession for reserve generation.

Results from such work indicate some gold mineralisation of economic interest. This intervention is anticipated to reduce the stripping ratio, increase and consolidate its gains with stakeholder communities, increase the reserve base of the company and, therefore, the Life-of-Mine.

It is against this background that the design of a new Open Pit (Kobeda Pit) was proposed. It is worth designing optimal slope parameters for the pit slope architecture required for the new Open Pit Mine.

1.2 Objectives

The objectives of this thesis are to:

- Design optimal slope parameters for the various sectors of the Pit
- Identify the potential failure modes and the presence of adverse structures
- Determine the groundwater regime of the new Pit area
- Identify the appropriate slope monitoring tools that could provide real time movement alert and support systems

1.3 Scope of Work

- Establish Rock mass characteristics
- Design optimal slope parameters using probabilistic and deterministic slope design criteria and optimise with numerical modelling approach
- Propose a slope management and monitoring programme compatible with the structural complexity of the pit walls

1.4 Methods used

The methods to be used include:

- Review previous relevant literature
- Structural and geotechnical logging of rock core samples
- Laboratory test on the rock core samples
- Assessment of the groundwater conditions using piezometric measurements
- Evaluate design parameters using Rocscience Dips, Slide, and Phase 2

1.5 Facilities used

The facilities required for this research include:

- The Rock and Soil Mechanics laboratory of UMaT
- Software from Tarkwa Gold Mine of Gold Fields Ghana Limited and UMaT
- UMaT Library

1.6 Organisation of thesis Report

This thesis is organised into seven (7) chapters. Chapter 1 is the introduction and it outlines the problem statement, objectives, and the methods used to achieve solutions to the stated problems.

Chapter 2 outlines the relevant information of the mine and geological setting which elaborates the regional and local geology of the study area.

Chapter 3 considers the overview of slope design considerations in an open pit mine. The fundamentals of slope design criteria and slope Management and Monitoring forms part of this chapter.

Chapter 4 outlines data collection, laboratory work and geotechnical slope design investigations. Data analysis is presented in Chapter 5.

KNOWLEDGE, TRUTH AND EXCELLENCE

Chapter 6 evaluates the slope design model for the proposed Kobeda pit. Empirical and structural analysis, probabilistic slope design approach, and numerical modelling are also considered. Chapter 7 presents the conclusions and recommendations.

CHAPTER 2

RELEVANT INFORMATION ABOUT THE MINE

2.1 Location

Gold Fields Ghana Limited (GFGL) is located to the north and northeast of Tarkwa in the Tarkwa-Nsuaem Municipal of the Western Region of Ghana. Tarkwa is about 90 km north of Takoradi, 278 km south of Kumasi and 315 km to Accra, the capital city of Ghana (Figure 2.1).

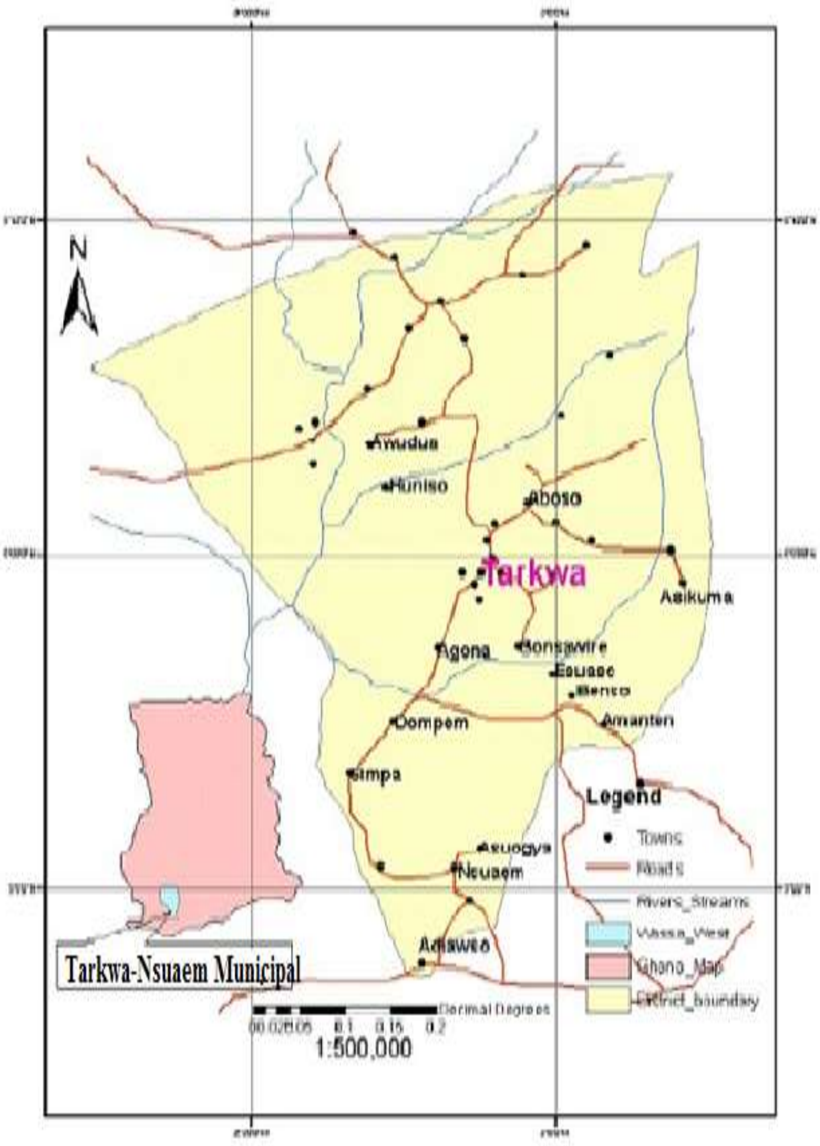

Figure 2.1 Map of Tarkwa-Nsuaem Municipal Showing the Location of Tarkwa, (Source, Ziggah et. al., 2012).

The concession is located between (latitude 5° 15'N - 5° 30'N and longitude 2° 05'W - 1° 50'W), and covers a land area of 294.6 km² extending from the town of Tarkwa in the south, for a distance of approximately 25 km to Huni Valley in the northeast limit (Anon, 2006a) as illustrated in Figure 2.1.

2.2 Historical Background of Gold Fields Ghana Limited, Tarkwa Mine

The Tarkwa area has been mined almost continuously since 1880 and prior to that by artisinals since 1850. The area first attracted European interest when J. Bonnat, a Frenchman, visited the area in 1877 with General Wray and saw extensive artisinal workings in the vicinity of the present Tarkwa. In 1878, Mr Bonnat took out concessions within the Tarkwa area and started mining (Junner, 1942).

In 1888 the concessions passed into the hands of the British who operated till 1935 when the Amalgamated Banket Area (A. B. A) legally acquired the mining concession. This group became the last to operate till Ghana attained independence, when the then government took over in 1961 and established Tarkwa Goldfields Limited as one of the State Gold Mining Corporations (SGMC) (Junner, 1942).

Tarkwa Goldfields Limited had four shafts through which it carried out its operations namely Akoon Vertical Shaft, Apinto Shaft, Fanti South Shaft and Ferguson Shaft, However, there was lack of political will on the part of Central Government to invest significantly into its operations. This led to its near collapse. Therefore, in 1992 the then government took the decision to divest the Mine (Anon, 2006b).

In 1993 Gold Fields Ghana Limited (GFGL), a South African company successfully took over the operations of Tarkwa Goldfields Limited which was essentially underground. In 1997, African Mining Services (AMS), a joint venture between Henry Eltin Limited and Ausdrill Limited was contracted for surface and other mining related activities (Anon, 2006b).

In December 1999, GFG closed down all its underground operations and concentrated on only surface mining operations. GFG then acquired the northern portion of Teberebie concession and Abosso Goldfields limited (Damang Mine) in August 2000 and November 2001 respectively. The company took over all its mining activities in June 2004, a transition from contract mining to owner mining (Anon, 2006b).

KNOWLEDGE, TRUTH AND EXCELLENCE

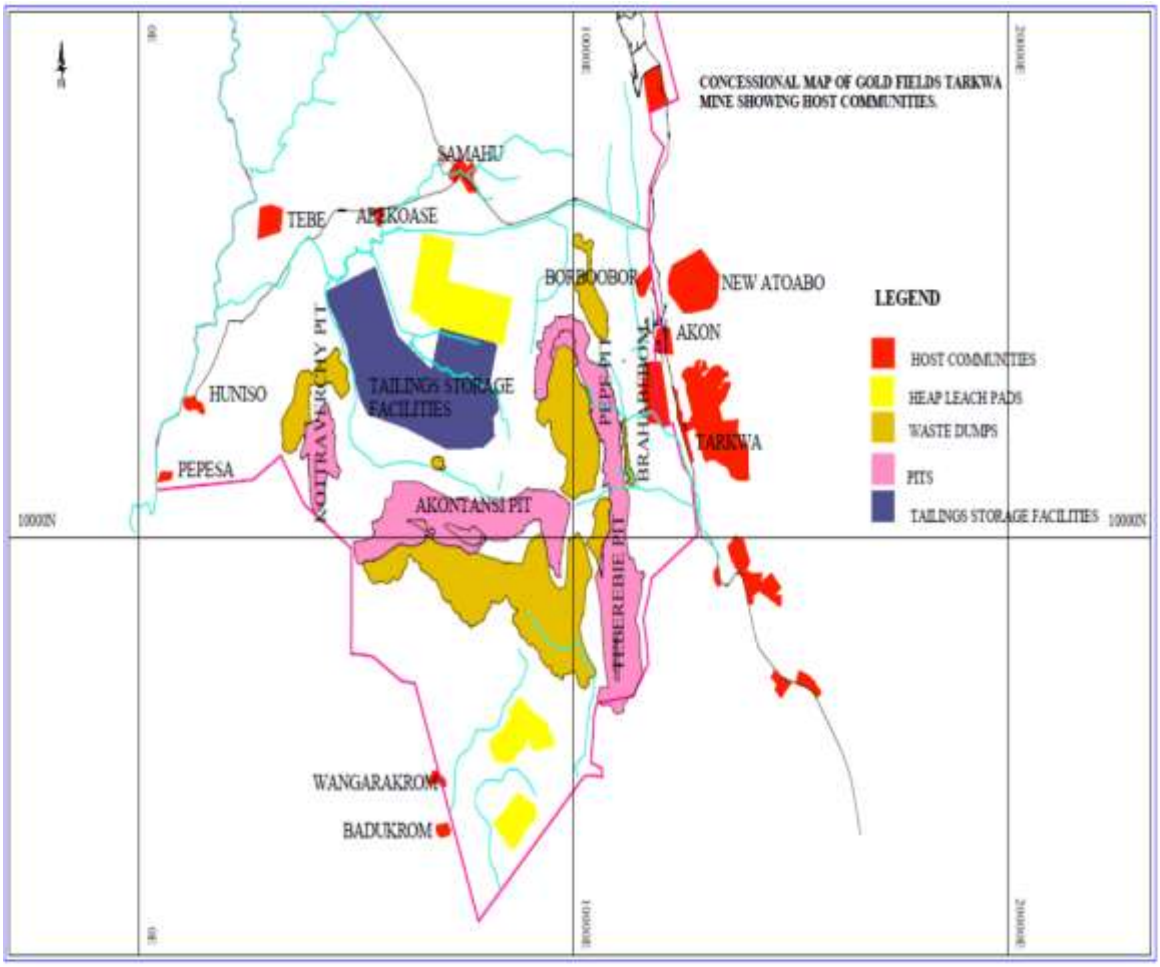

Figure 2.2 Map of Tarkwa Gold Mine Concession, (Anon, 2015)

2.3 Climate and Environment

The Mine falls within the south-western equatorial climate zone, with seasons primarily influenced by moist south-west monsoon winds from the South Atlantic Ocean and dry dust-laden north-east trade winds known as the Harmattan which blows over the Sahara Desert from the northern sub-tropical high pressure zone. The Inter-tropical Convergence zone crosses over the area of the lease two times per year, causing hydro-meteorological data including rainfall to peak during two periods: April to June and October to November. Average monthly temperature ranges from 22 °C to 32 °C with the highest temperatures recorded during February and March (Anon, 2006a).

The primary forests occurring in the area have been replaced by secondary forests and early successional vegetation due to human activities in the area such as galamsey mining, timber exploitation, firewood collection, charcoal production and various farming activities. There are few ridges and swampy areas which have not been disturbed (Anon, 2006a).

2.4 Topography and Drainage

The topography of the lease area comprises ragged ridges with peaks of 320 m above mean sea level in some areas, interspersed by undulating valley bottoms. Elevations in the area range from approximately 45 m to 320 m (based on survey data available). The central areas of the lease is low lying and flatter and does not show the variations in elevation typical of the southern and eastern areas near Tarkwa and Akontansi (Anon, 2006a).

The lowest point of the catchment area lies to the northwest of Tarkwa. Here the smaller rivers draining the areas of the lease flow into the Huni River, which runs in a south-westerly direction into the Ankobra River. This river and its tributaries drain the eastern, northern and western areas of the lease. The extreme southern portions of the lease are drained by the Bonsa River and associated tributaries (Anon, 2006a).

2.5 Regional Geology

In Ghana, the Birimian greenstone belt sequence occurs as irregular basins of predominantly metasedimentary strata, separated by a series of north-east trending belts of metavolcanics in which most of the gold deposits are clustered on the south-west north-east trending Ashanti belt (Griffiths *et al*., 2002).

The Birimian greenstone belts are uncomformably overlain by Proterozoic age Tarkwaian metasediments which host the gold mineralisation at the Tarkwa mine. This gold mineralisation is concentrated in conglomerate reefs, similar to that of the Witwatersrand system (Hirst 1938). The gold deposits at Tarkwa are composed of a succession of flat dipping stacked tabular palaeoplacer units, consisting of quartz pebble conglomerates within Tarkwaian sedimentary rocks (Hirst,1938). Approximately 10 such separate economic units occur in the concession area within a sedimentary package that is between 40 and 110 meters thick. Low grade to barren quartzite units are interlayered with the Au-reefs (Hirst, 1938). The Volcanic belts are typically up to 40 km wide and 90 km apart and dominated by volcanic and volcanoclastic sediments of tholeiitic basaltic (81%), andesitic (16%), and dacitic (3%) composition (Griffiths et al., 2002).

The meta-sedimentary rocks comprise of turbiditic wackes and argillites with similar chemistry to the volcanic rocks (Hirst 1938). No quartz-rich, craton-derived, border sediments are found except in the west of Cote d'Ivoire, suggesting an intra-oceanic plate origin (Hirst, 1938).

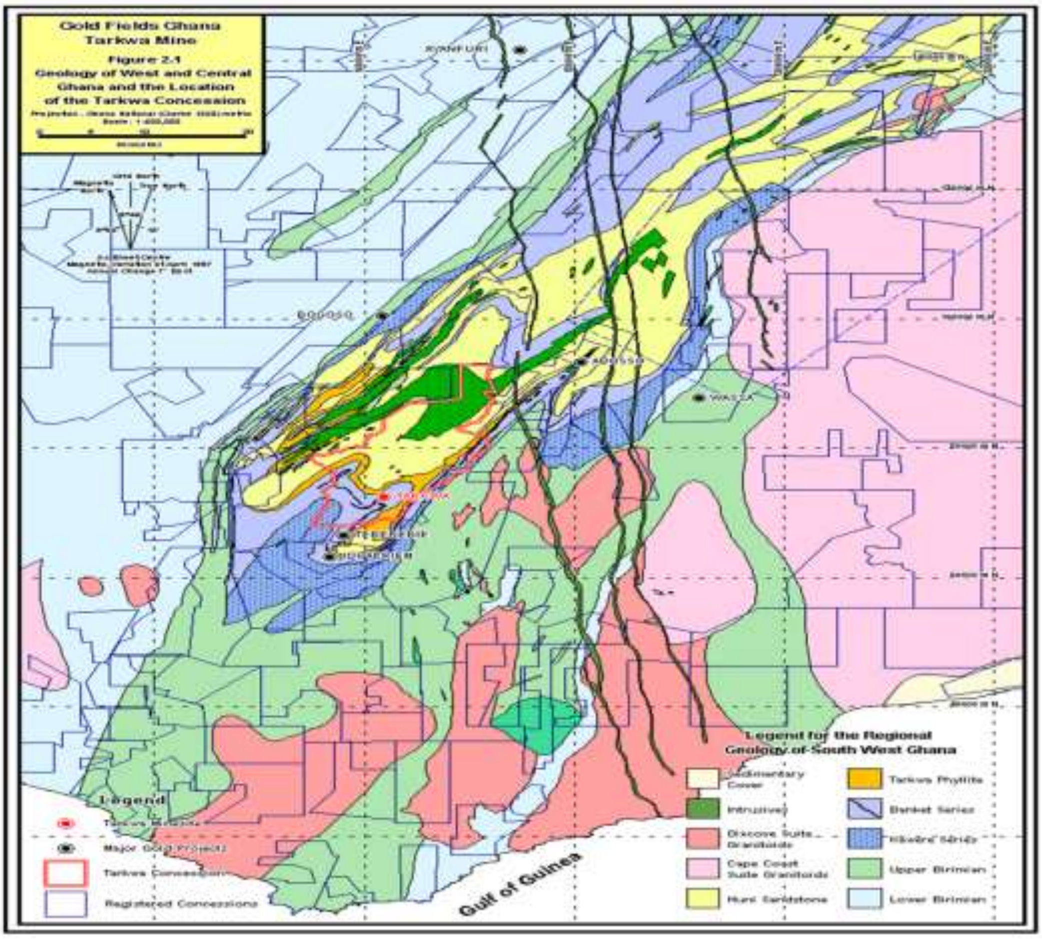

Figure 2.3 Geology of West and Central Ghana

2.6 Regional Stratigraphy

The Tarkwa basin is filled with coarsening-upward sequence of clastic sedimentary rocks, The Tarkwaian Group of Proterozoic age (2132 to 2095Ma), comprise of the Kawere, Banket, Tarkwa phyllite and Huni 'series' (Table 2.1), and rest uncomformably on the Birimian (Hirst, 1938). The Kawere 'Series' consists of between 250 and 700 meters of repeated fining upward sequence of erosively-based, polymictic, poorly sorted, often matrix supported conglomerates grading up through immature pebbly quartzite to parallel-laminated or cross-bedded feldspathic quartzites. Clasts comprise mainly of basic lavas with subordinate felsic lavas, chert, pyroclastics rocks, quartz and granitoids (Griffiths et al., 2002).

Magnetite is the dominant detrital heavy mineral. Limited palaeocurrent information is unimodal, indicating derivation from the east. The overlying Banket 'Series' is the main gold bearing unit in the Tarkwa area and consists of up to 15 meters of relatively more mature quartzites and conglomerates. Four gold bearing conglomerates were originally distinguished, the Sub-basal Reef, the Basal (main Reef), the Middle (west Reef) and the Breccia Reef (Anon, 1991).

Table 2.1 Summarized Stratigraphy of the Ashanti Belt (Kesse, 1985)

Group	Series	Thickness (m)	Lithology
Tarkwaian	Huni Sandstone	1370	Quartzite, Minor Phyllite
	Tarkwa Phyllite	120 - 400	Chloritic and Sericitic Phyllite and Schist
	Banket Series	120 - 160	Quartzite, Grits, and Conglomerates
	Kawere Conglomerates	250 - 700	Quartzite, Grits, and Conglomerates
Major Unconformity			
Birimian	Birimian		Meta-Volcanics, Volcanoclastic and Sediments

2.7 Pre Mining Land Use

The area of the Tarkwa mining leases was originally covered by tall virgin forest. At the time of the Tarkwa Gold Mine Environmental Impact Statement (EIS), however, these original forests had been totally removed because of timber harvesting, agricultural practices, and earlier mining activities. Forest land in the lease area had been reduced to secondary forest because of slash and burn, and 'galamsey' (illegal mining) operations (Anon, 2006a).

Prior to the initiation of large-scale surface mining, a number of villages and hamlets were located in the lease area. People here were into activities such as firewood collection, charcoal burning, palm wine tapping, distillation of local gin, harvesting of forest-cane for weaving baskets, hunting, wood harvesting for timber, and other minor subsistence-level activities.

Some of the low-lying areas within the Tarkwa mining leases were farmed for both food and cash crops, such as cassava, maize, pineapple, rubber and oil palm. Food crop production was generally at a subsistence level with slash and burn methods of land preparation being used for cultivation of cassava, maize and assorted minor crops.

GFGL personnel and independent consultants Renner & Associates conducted a comprehensive survey of buildings and crops that would be affected by the planned open pit mining operation. Based on these surveys, it was estimated that there were approximately 1400 farms in the area to be affected by mining activities. The most frequent crop combinations were oil palm/cassava/maize or oil palm/pineapple/maize mixtures. Maize and cassava or pineapples were usually intercropped with oil palm during the initial stages with limited quantities of plantain in the mixture (Anon, 2006a).

Areas such as the location of the heap leach pads were previously swamp forest; conditions generally found in low lying well-watered portions of the Tarkwa mining lease area. The steeper side slopes and tops of the ridges occurring in the lease area were generally not being actively farmed at the time of the Environmental Impact Statement (EIS). Some of these areas were the sites for 'galamsey', which resulted in the destruction of most natural vegetation and left with only grass species. The predominant pre-mining land use of the Tarkwa mining lease prior to the initiation of large-scale surface mining was wildlife habitat and minor commercial subsistence uses of secondary forest, swamp and bush. It is estimated that only 22% of the land area of the Tarkwa mining leases has agricultural potential (Anon, 2006a).

2.8 Mining Activities

Mining is undertaken by conventional open pit methods using hydraulic excavators and haul trucks. Bulldozers are used for clearing vegetation; topsoil stripping, waste dump construction and general pit/road maintenance. Topsoil is either stockpiled for use in future for reclamation or hauled directly to areas that are being rehabilitated for placement. Waste from open pits is hauled to waste dumps or to in-pit backfill dumps. Wherever practicable, waste dumps are constructed in 15 m lifts at an overall slope of 22° to ensure long-term stability and that minimal work is required for rehabilitation (Anon, 2006a).

Ore is hauled to one of two primary crushers, where it is either dumped directly into the crusher or stockpiled at an adjacent location for future processing. Mining operation is conducted 24 hours per day, 7 days per week (Anon, 2006a).

2.9 Structural Deformation

The Ashanti belt is a member of the extensively researched Eburnean orogenic event that metamorphosed, deformed, faulted and fractured the Birimian Super Group and the Tarkwaian Goup rocks. Five phases of structural deformation (D0 to D4) have been identified in the Tarkwa region (Karpeta, 2001). The systematic deformations in this section are not to scale.

2.9.1 D0 Deformation

The D0 event produced the Tarkwa depositional basin as an extensional half-graben. A north-east striking master fault (the Prestea lineament) formed the west margin that sourced small alluvial fans. Subsidiary faults and rollovers on the eastern margin sourced extensive fluvial systems that fed sands and gravel into the basin. East-west cross structures (Summang, N1 and Fanti Abosso break) acted as transfer faults between normal fault segments and compartmentalized the basin (Karpeta, 2001).

2.9.2 D1 Deformation

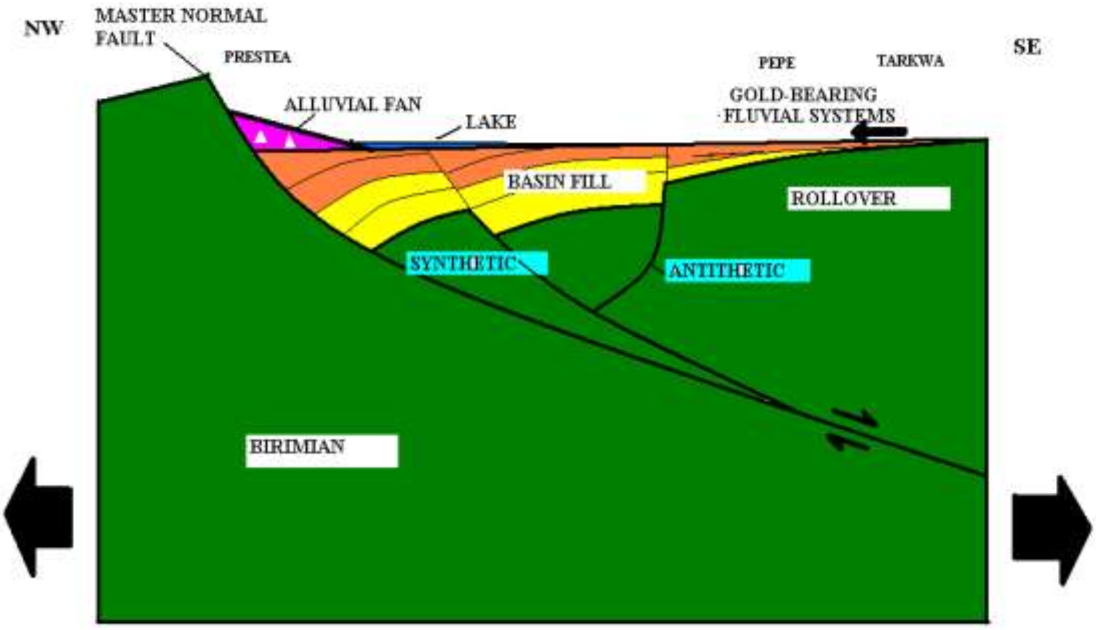

Figure 2.4 Normal Faulting associated with D0/D1 Extension (Karpeta, 2001)

The D1 event was prolongation of the D0 event resulting in normal faulting of the basin fills itself. These D1 synthetic and antithetic normal faults acted as buttresses to the D2 compression and were inverted (reactivated as steep reverse faults (see figure 2.4). Bedding planes parallel to basic sills were also introduced during D1 tectonics (Karpeta, 2001).

2.9.3 D2 Deformation

D2 deformation involved NW-SE sub-horizontal compressive stress producing NE striking thrusting and folding. Early D2 deformation was thin-skinned and was concentrated in the basin fill. It produced NW and SE verging bedding plane parallel thrust and back thrust in the more competent horizons like the Footwall quartzite (FW), the B quartzites (B) and the Hanging Wall quartzites (HW) which ramped up through the reefs at buttresses, forming imbricate thrust (Karpeta, 2001). Major structures in the Midlap and Underlap pit were formed during D2 deformation (Karpeta, 2001).

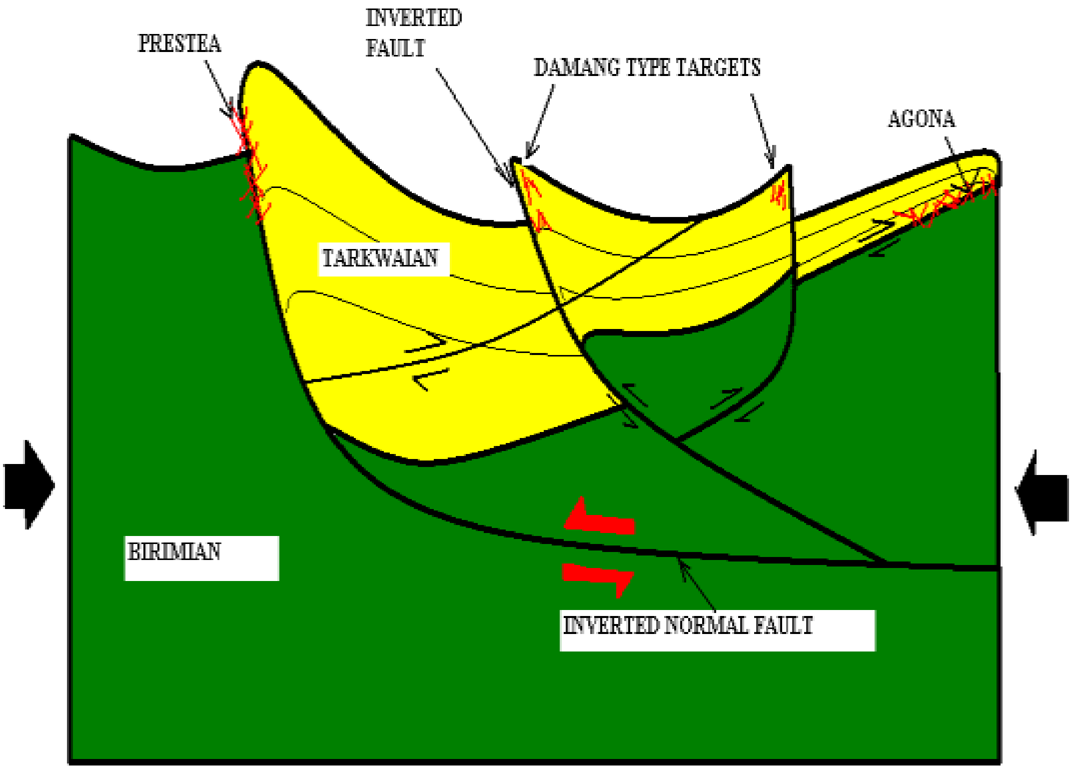

Figure 2.5 D2 Inversion of Basin-fill Sediments (after Karpeta, 2001)

Subsequent D2 deformation impacted on both the basin fill and the basement rocks, producing thick skinned deformation. Basement deformation resulted in the inversion of the D0/D1 normal faults as steep and the basin fill was folded into open, cylindrical flexural slip folds (Karpeta, 2001). The Tarkwa Syncline and the Pepe Anticline are examples of this type of deformation. The final D2 deformation phase caused large SE verging thrusts, locally named the Kottraverchy and Plateau thrusts as well as the basement decollement (Karpeta, 2002). These are interpreted as “out of the graben” thrusting associated with partial expulsion of the basin fill (Karpeta, 2001).

2.9.4 D3 Deformation

D3 deformation involved a sub vertical NE-SW oriented sinistral shear couple, which produced strike-slip movement on the basin-margin faults resulting for example in the Prestea lineament. South to south-east verging thrusts (for example the Muva and Syncline faults) and minor faults occurred within the basin. The east-west cross structures may have acted as buttresses concentrating thrust ramps around them (Karpeta, 2002).

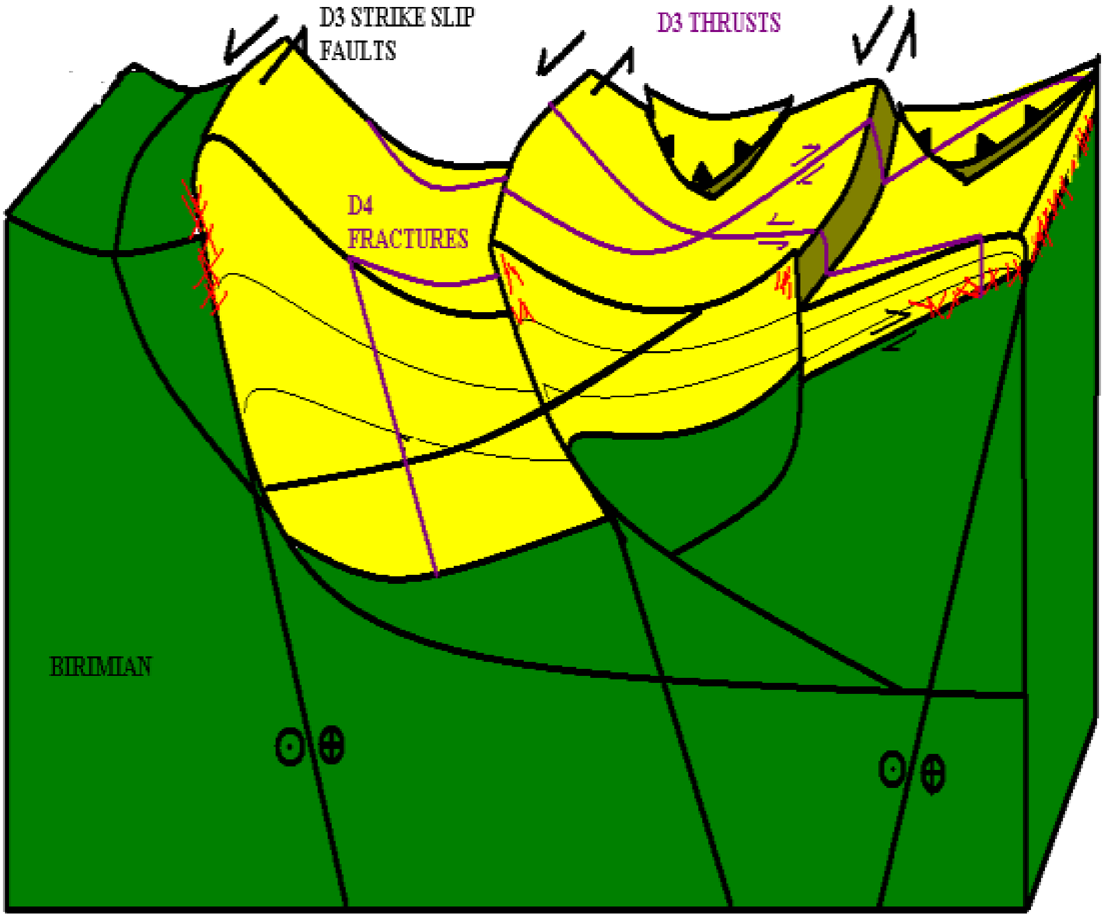

Figure 2.6 Thrust Faulting and Folding due to D3/D4 Deformation (Karpeta, 2001)

2.9.5 D4 Deformation

The D4 event involved renewed sub horizontal NW-SE compression, which produced sub vertical arrays of WSW and NNW striking conjugate fractures and faults, locally named “Franks Faults”. The D4 event also involved the final movement on the cross structures and the intrusion of a basic dyke along the Summang river (Karpeta, 2002).

CHAPTER 3

GEOTECHNICAL CONSIDERATION IN OPEN PIT MINING

3.1 Pit Slope Stability

The stability of a slope is defined as the ratio of the strength forming the slope to the stresses which develop in the slope (Call, 1982). The strength of the rock mass that forms the slope is influenced by the intact strength of the rock mass, and also depends on the strength defects within the rock mass.

Detailed geological interpretation of the rock mass is therefore necessary to identify potential failure mechanisms. Structural data is needed to be combined with results from extensive testing of the rock in order to make an assessment of the strength of the rock mass. If the stress exceeds the strength, the slope is unstable. On the other hand, if the strength exceeds the stress, the slope is stable. This ratio is the factor of safety and has been the basis for stability analysis in ground engineering (Call, 1982).

Call, (1982) also indicated that the stresses and strengths used in stability assessment are estimates of populations with significant distribution rather than single values. This is because of the variability of rock properties, uncertainty in the measurement of these properties, and the influence of quasi-random events such as earthquakes and rainfall. For this reason, safety factors greater than one have been used for slope design.

Alternatively, slope stability is also analysed by the reliability method, where the probability of whether or not a slope will be stable is calculated from the distribution of input values (Sjőberg, 1999). Slope instability does not necessarily mean slope failure from the operational perspective. In the mining environment, an unstable slope that will result in significant cost to the mine operation will depend on the;

- rate of movement,
- type of mining operation and,
- relationship of the unstable material to the mining operation.

Unstable areas with rates of displacement over 100 mm/day have not indicated slope failure in some sections of mines (Call, 1982).

According to Call (1982), millimetres of displacement of the rock under a crusher, conveyor, or building may require extensive repair. When the rate of displacement is such that it disrupts the operation or the movement produces damage to mining facilities, it is considered an operational slope failure.

3.2 Slope Management

In an optimised slope, some slope failure can be expected but the specific location and time of instability cannot be identified with any certainty. Also, the stability analysis utilised in design, with very few exceptions, are static solutions that do not provide estimates of the rate or magnitude of displacement (Krishna, 2006). Therefore, to provide safe working conditions, and minimise the economic impact of slope failure, there should be a programme of displacement monitoring to provide advance warnings of major slope displacement, accompanied by design of remedial measures. With an appropriate slope management programme, it should be possible to mine steep with an equal or greater safety record (Kliche, 1999).

Once it is determined that there is a movement on a slope face, the area is continuously monitored and managed to prevent loss of equipment and lives. There are several failure management options to choose from; the most obvious approach is to leave the unstable area alone if it is located in an inactive area or in an area of the pit that can be avoided. If mining must continue nearby but the area of instability is small, partial clean-up can be conducted as slope failure occurs (Call, 1982). This approach may be effective when a slide is small and its displacement is low and predictable and may only cover the immediate working area, part of a ramp, or haul road. If, however, the slide is large but its displacement is low and predictable, the reaction of the mine to slope instability may be controlled by:

- Dewatering the slope by drilling horizontal drain holes into the pit slope face
- Reinforcing or supporting the unstable ground with rock bolts, anchors, wire mesh and bolt, and shotcrete.
- Reducing the slope height segmenting the slope in step-outs to provide safer slope angles

Buttressing or placing waste material at the toe of the failure zones; this helps to slow and control pit slope movement (Call, 1982).

3.2.1 Pit Slope Geometry

The mine operating environment is comprised of three major components of a pit slope namely, bench configuration, inter-ramp slope, and overall slope. The bench configuration is defined by the bench face angle, the bench height, and the bench width. The inter-ramp angle is the slope angle produced by a number of benches.

Where there are haul roads, working levels, or other wide benches, the overall slope angle is the angle of the line from the toe to the crest of the pit; the slope angle will be flatter than the inter-ramp angle. It is important in slope design to consider these components (Call, 1982) as shown in Figure 3.1.

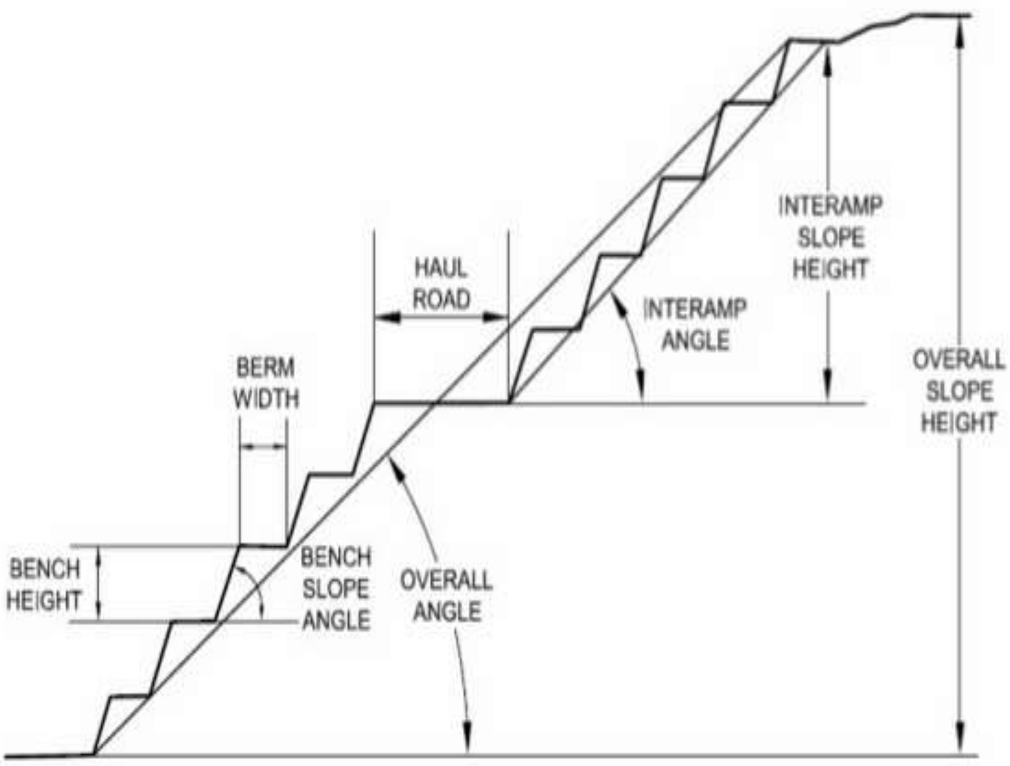

Figure 3.1 Cross Sectiona and Terminologies of Open Pit Slope (Source Sullivan, 2006)

For any one slope and any one mine, one or all of these elements could be the critical design elements, requiring analysis and design. In some mines, consideration of all three is essential and they may form competing design elements (Sullivan, 2006).

3.3 Slope Failure

Unstable slopes are an inherent part of the modern approach to open pit mining. Designs are predicated on an accepted probability of failure. Economic pressure can result in higher risk designs being adopted, either intentionally to improve project finances or unintentionally, as a result of less detailed geotechnical investigations driven by smaller investigation budgets. Either way, the management of geotechnical slope risk generally falls back to site personnel to resolve what the best course of action is (Sullivan, 2006).

A slope is geotechnically stable if it does not physically collapse. The factor of safety is a measure of confidence that a slope will not collapse. Depending on the mine operations, certain generalised criteria can be used as guide in the selection of acceptable slope angles.

The conditions that may control the stability will always be site specific and it may require due care when applying these criteria (O' Bryan, 2007). However, slope failure is rarely attributed to a single cause, and rarely occurs via a single mechanism. Blasting influences are often cited as contributing to failure, but it is virtually difficult to quantify its involvement (Sullivan, 2006).

3.3.1 Slope Failure Mechanism

Potential hard rock slope failure mechanisms are determined predominantly by the orientation and strength of the defects present in the rock mass forming the slope. Un-dissipated groundwater pressure tends to destabilise slopes and will potentially promote all failure mechanisms (O' Bryan, 2007).

Two forms of slope failure mechanisms are known i.e. slope failures for which a factor of safety can be calculated and slope failures for which factor of safety cannot be calculated. Failures of the former type involve movement of a mass of material on a failure surface. Analysis of failure or calculation of factor of safety requires that shear strength of the failure surfaces be known. Slope failures for which a factor of safety cannot be calculated are the type of failures which cannot be analysed for factor of safety even if the strength parameters of the material are known since failure does not involve simple sliding (Hoek and Bray, 1981).

Slope failures are also categorised into continuum or discontinuum mode. Where failure has been created through rock mass, the slope instability is said to be a continuum. A discontinuum mode of failure occurs by the presence of specific pre-existing discontinuities.

Even though soil slopes are discontinuous in nature, majority of rock slope instabilities are caused by individual discontinuities as strength of intact rock can be high (Hoek, 1981).

3.4 Types of Slope Failure

Because of its geometry, rock slopes expose two or more free surfaces. Thus, as a rule, constituent rock blocks contained within the rock mass have a relative high kinematic potential for instability (Hoek and Bray 1974).

As indicated by Kovari and Fritz (1989), the type of failure is primarily controlled by the orientation and spacing of discontinuities within the rock mass, as well as the orientation of excavation and the angle of inclination of the slope. Below are the general types of slope failure which are controlled by the above factors.

3.4.1 Circular Failure

This type of failure generally occurs in soil, completely weathered rock, tailings and waste dumps. True circular failures rarely occur in pit walls; despite an often-high degree of weathering, slope failure in weathered material usually initiates from or along relict defects (Hoek and Bray 1981).

Figure 3.2 Typical Circular Failures (Source O' Bryan, 2007)

The failure surfaces are not defined by defects and follows the line of least shear resistance through the slope. Such failure break-out near or possibly below and beyond the slope toe with the head some distance behind the pit crest. Pseudo-circular failure can occur in highly fractured rock masses, where the step-path failure surface may resemble a circular failure surface (O' Bryan, 2007).

3.4.2 Planar (step-path) Failure Mode

According to Hoek and Bray (1981), a plane failure occurs when a geological discontinuity such as a bedding plane strikes parallel to the slope face and dips into the excavation at an angle greater than the angle of friction. Naturally, side release is needed, but will typically be provided by cross-cutting defects, and possibly some intact rock failure (O' Bryan, 2007).

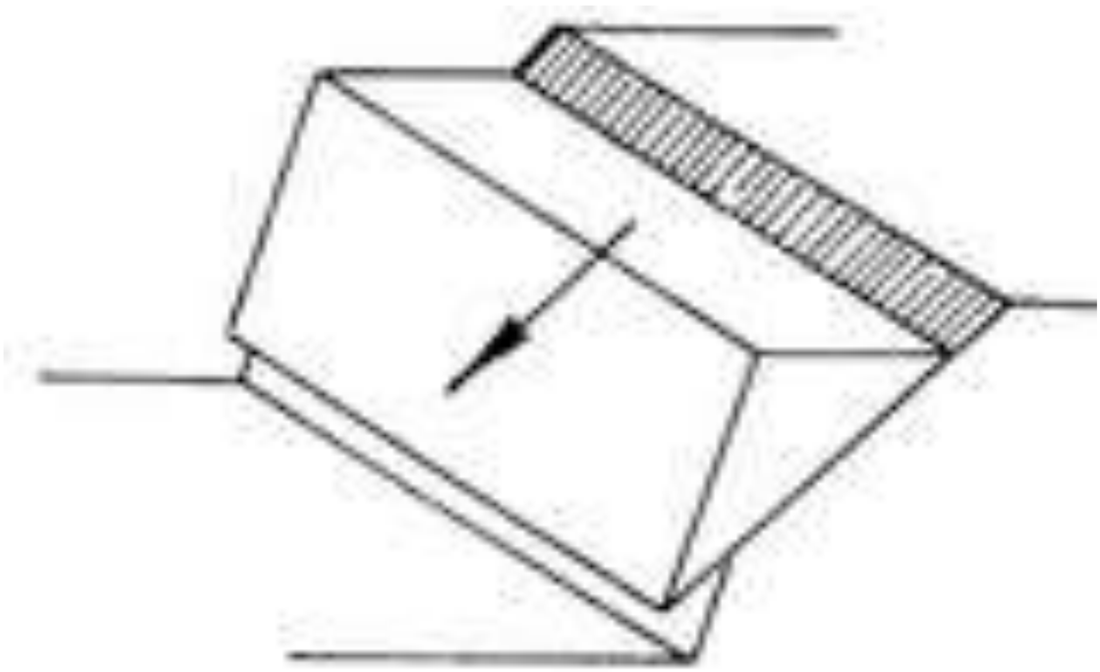

Figure 3.3 Planar Failures (Source O' Bryan, 2007)

The major disturbing force is the weight of the block (potentially mobile). The shear strength of the defect consists of the friction between the two surfaces of the defect, and the cohesion of the defect. The degree of friction will depend on the shape and roughness of the defect, and load acting across the defect (overburden load). Cohesive strength derived from zones within the defect which are unbroken or re-healed may or may not exist.

Where there is no cohesion, sliding will occur when the dip of the "daylight" defect exceeds the friction angle of the defect. The onset of a simple planar failure can be aided by the presence of a tension crack at the crest of the slope.

However, a step-path failure occurs where the failure surface is defined by series of steps formed by pervasive defects of limited persistence which dip into the pit and cross-cutting defects and or rupture through intact rock bridges (Muller, 1963). The favourable conditions of plane failure are as follows:

- The dip direction of the planar discontinuity must be within (±20^0)
- The dip of the planar discontinuity must be less than the dip of the slope face (Daylight)) of the dip direction of the slope face.
- The dip of the planar discontinuity must be greater than the angle of friction of the surface.

The study of planar failure mechanism provides insight knowledge of the behaviour of rock slopes and is particularly valuable for investigating the sensitivity of slope behaviour to variations in parameters such as shear strength of failure surfaces and groundwater conditions.

3.4.3 Wedge Failure Mode

When two discontinuities strike obliquely across the slope face and their line of intersection daylights in the slope face, the wedge of rock resting on these discontinuities will slide down the line of intersection, provided that the inclination of this line is significantly greater than the angle of friction (Hoek and Bray, 1981).

More complex shaped wedges can be formed by the intersection of more than two defects and the slope. It is also possible for wedge failure to develop progressively. A step wedge is similar to the wedge except that one or both of the failure surfaces are step paths (Call, 1982).

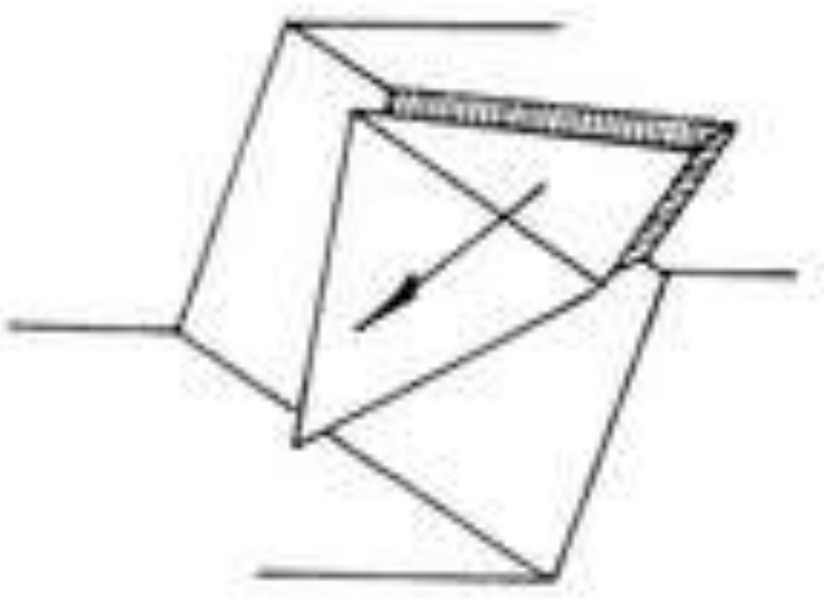

Figure 3.4 Wedge Failure Mode (Source; O' Bryan, 2007)

The necessary structural conditions for wedge failure are summarized as follows:

- The trend of the line of intersection must approximate the dip direction of the slope face.
- The plunge of the line of intersection must be less than the dip of the slope face. The line of intersection under this condition is said to daylight on the slope.
- The plunge of the line of intersection must be greater than the angle of friction of the surface (O' Bryan, 2007).

3.4.4 Toppling Failure Mode

Toppling failures of slopes have been observed in a wide range of rock masses and can occur in both natural and excavated slopes (Muller, 1963; Goodman and Bray, 1976). Four principal types of toppling failure, namely: block, flexural, block-flexural and secondary toppling, are recognised by Goodman and Bray (1976).

Toppling failure occurs when bedding or passive point sets dip into the slope and the bedding planes can slip relative to each other (Figure 3.5).

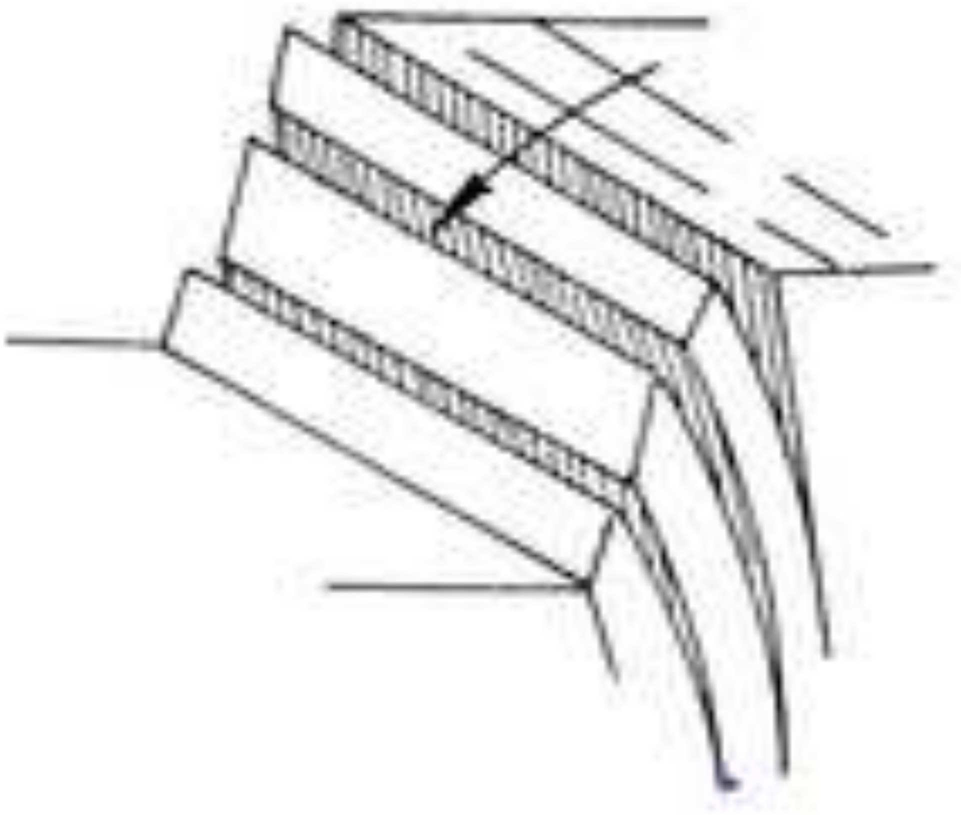

Figure 3.5 Toppling Failure Mode (Source; Gordon 2006)

The potential for toppling failure is dictated by the following factors (Gordon, 2006);

- Dip of bedding relative to slope: - the steeper the bedding and/or steeper the slope, the greater the potential for failure
- Frictional characteristics of bedding plane: - the lower the friction angle, the higher the potential for failure (water also plays a significant role in reducing friction along planes).
- Strength of intact rock: - for columns to snap and crush intact rock failure must take place (toppling more likely to take place in weathered zone).
- Presence of flat dipping defects: - if present, the rock columns will preferentially snap off on base.
- Slenderness of rock column:- tall, thin columns are likely to topple than short, squat blocks i. e. closely bedded (or jointed) horizon are more likely to topple.
- Swelling pressure due to slaking of clay infills due to water ingress.
- Dilation forces caused by shear along bedding/joint places.
- Pore pressure due to water ingress.

For the purposes of slope design, no deterministic or probabilistic methods exist for the analysis of toppling failure. This is due to the complex nature of the mechanics of toppling and many (often unquantifiable) factors that influence failure. Slopes prone to toppling are designed using empirical or experience-base methods (Gordon, 2006).

According to Bucek (1995), there were few case histories dealing with toppling published before 1976. Some early descriptions of toppling were given by Zaruba and Mencl (1969), De Freitas and Waters (1973), and Bokovansky et al. (1974). None of these publications attempted to analyse the mechanisms which triggered failure.

In 1976, Goodman and Bray presented the first classification of toppling in which they classified toppling modes into flexural toppling, block toppling, and block flexural toppling

Flexural toppling occurs in rocks with the preferred discontinuity system oriented to form a rock slope composed of semi continuous cantilever beams (Bucek 1995).

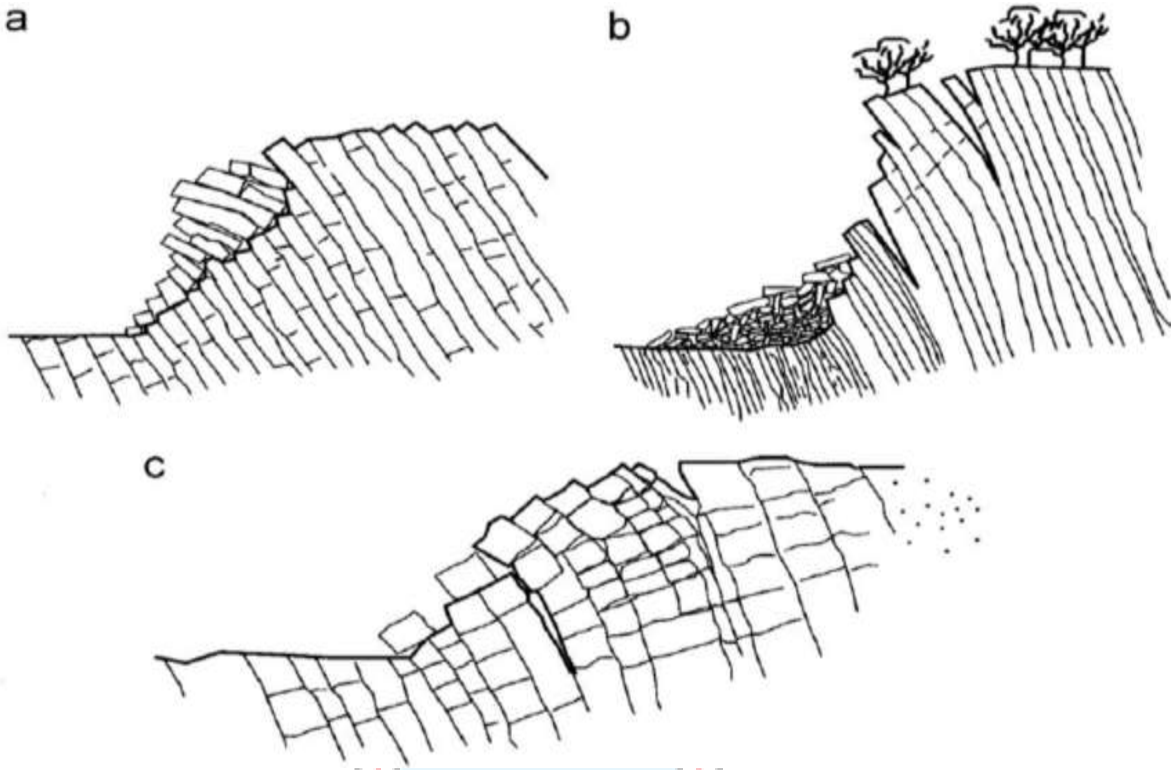

Figure 3.6: Classification of Toppling Failures (a) Block (b) Flexural and (c) Block flexural toppling (Goodman and Bray, 1976)

Erosion or mining activity can trigger this mechanism. Failure starts at the toe and progresses backwards, creating a wide deep tension crack. The lower portion of the slope is covered with disoriented and disordered blocks. The bending and cracking continue until the line of tension crack intercepts the crest of the slope, provided that the geology did not change through the slope. The bending is gradual and according to Bucek (1995), there is an obvious base of this mechanism that could be discovered by drilling. Flexural toppling occurs most notably in slates, phyllites, and schists (Goodman and Bray, 1976).

Block toppling on the other hand occurs in rocks with more than one system of joints, typically with one system of bedding planes and two systems of widely spaced joints (Bucek, 1995). Longer, overturning columns at the crest of the slope lean on shorter blocks at the toe creating system of toppling and sliding blocks.

Goodman and Bray, (1976), indicated that, the base of this disturbing mass is better defined than in the case of flexural toppling, it consists of a stairway which, generally, rises from one layer to the next. Block toppling occurs mostly in thick bedded sedimentary rocks such as limestone and sandstone, as well as in columnar jointed volcanic rocks.

Block flexural toppling is characterized by pseudo-continues blocks in highly jointed rock (Bucek, 1995). Sliding is concentrated at the toe and there is a combination of sliding and toppling in the rest of the unstable slope. Sliding occurs either directly as a result of the thrust applied by an upper overturning block on a lower resting block, or as a result of steepening of the joint angles of the toppling column, or as a combination of the two mechanisms.

The character of the disturbed zone is such that, it is widely opened, but with fewer edges to face contacts than in the case of block toppling. Typical rocks susceptible to block flexural toppling are interbedded sandstone and shale, interbedded chert and shale and thin bedded limestone (Goodman and Bray, 1976).

3.4.5 Rockfall

Rockfall consist of free –falling blocks of different sizes, which are detached from a steep rock face. The block movement includes bouncing, rolling, sliding and fragmentation. The detachment of relatively small fragments of rock from the face is known as ravelling. In the design of rock slopes, the problem of Rockfall is the prediction of the paths and the trajectories of the unstable blocks, which detach from the rock slopes so that suitable protection can be constructed (O' Bryan, 2007).

Rockfall is generally initiated by some climatic or biological event that causes a change in the forces acting on a rock. These events may include pore pressure increase due to rainfall infiltration, erosion of surrounding material during heavy rain storms, freeze-thaw processes in cold climates, chemical degradation or weathering of the rock, root growth or leverage by roots moving in high winds.

In an active mining environment, the potential for mechanical initiation of a Rockfall is of a higher magnitude than the climatic and biological initiating events.

Rockfall are a major hazard in an active open pit mine. Once movement of a rock perched on the crest of a pit slope has been initiated, the most important factor controlling its fall trajectory is the geometry of the slope (O' Bryan, 2007).

3.5 Open Pit Slope Design

A number of steps and levels of analysis are required in the process of open pit slope design. These range from local bench design to overall stability of the walls, to evaluation of the design performance and calibration of parameters through back-analysis. The process requires the use of a variety of methods of analysis and software ranging from limit equilibrium methods to more involved numerical analysis such as distinct element, which can capture detailed geology and handle mix failure modes (Anon, 2008a).

Before the design and analysis stage, a considerable amount of field work is carried out to provide the required data. The data gathering and interpretation process is extremely important and its quality and thoroughness is usually responsible for the success of the design.

The aspects of preliminary data collection required prior to design are as follows;

- Regional geology, regional faulting and emplacement of the ore are important factors worthy of consideration. These usually define the lithological and structural domains in the pit.
- Hydrogeology and understanding of the groundwater regime impact overall stability.
- Structural mapping of the different domains and rock types control both bench design and overall stability. This includes both joint sets, dykes, faults and lithological contacts among others.
- Identification of alteration zones within the pit is important. Alteration affects rock strength; therefore, different alterations within the same rock should be grouped separately.
- Laboratory testing of the different rock types with the results grouped per the degree of alteration.

Stability analyses are routinely performed in order to assess the safety and functional design of an excavated slope and equilibrium conditions. The analysis technique chosen depends on both site conditions and the potential mode of failure, with careful consideration being given to the varying strengths, weaknesses and limitations inherent in each methodology.

The difficulty in predicting failure velocity also necessitates an accompanying development of a design methodology for cases in which precise prognosis cannot be made (Sjoberg, 1999). Slope design is categorised into deterministic and probabilistic approach.

The methods considered under deterministic approach are;

- Empirical and classification methods.
- Limit analysis and limit equilibrium analysis.

- Kinematic analysis using stereonet.
- Numerical methods

In the deterministic approach, a point estimate of each variable is assumed to represent the variable with certainty (Coates, 1977). The analysis is based on the concept of factor of safety where a single hypothetical value for each input parameter is used without considering the extent of uncertainty. However, uncertainty is not formally recognized since in conventional analysis, one is not much concerned with reliability associated with this unique value.

3.5.1 Empirical and Classification Methods

Empirical design method was developed on the basis of past slope performance and is calibrated based on known slope failures. Due to the complexity of rock mass, a number of studies have been conducted to correlate rock slope design with rock mass parameters. Many of these methods have been modified over the years and are now being used in practice for preliminary and sometimes final design.

Rock mass classification has been developed as a useful tool for preliminary assessment of slope stability which gives some simple rules about modes of instability and the required support systems. In recent times, rock mass classification has been providing systematic design aid in an otherwise haphazard 'trial-and-error' procedure.

The objectives of the rock mass classification are to:

- Identify the most significant parameters influencing the behaviour of rock mass
- Divide a particular rock mass formation into groups of similar behaviour, thus rock mass classes of varying quality.
- Provide a basis for understanding the characteristics of each rock mass class
- Relate the experience of rock conditions at one site to the conditions and experience encountered at others.
- Provide common basis for communication between engineers and geologists.
- Derive quantitative data and guidelines for slope engineering design.

According to Duran and Douglas (2000), the empirical rock mass rating techniques that can be utilised in the design of slopes include the following (Table 3.1):

- RMR – Rock Mass Rating (Bieniawski, 1976, 1989).
- MRMR – Mining Rock Mass Rating (Laubscher, 1977, 1990).

- SMR – Slope Mass Rating (Romana, 1985).
- SRMR – Slope Rock Mass Rating (Robertson, 1988).
- RMS – Rock Mass Strength (Selby, 1980).

The rating values for each method vary slightly depending on their intended usage since a number of these methods were developed for the design of support in underground excavations; the parameters and or weighting may not be applicable to the stability of large slopes.

Adjustment factor to the basic rock mass rating are applied to most empirical rating methods, which account for such factors as defect orientation, excavation method, weathering, induced stresses and major planes of weakness.

The RMR requires a summation of ratings assessed for intact rock block strength, rock mass block size, defect condition and ground water. The block size is assessed using Defect Spacing and Rock Quality Designation. The method has been updated a number of times.

Table 3:1 Comparison of Weights for Various Rock Mass Rating Methods

	References	**RMR_{76}**	**RMR_{89}**	**MRMR**	**SMR**	**SRMR**	**RMS**
BASIC ROCK MASS RATING	Intact Strength	0-15	0-15	5-20	0-15	0-20	0-20
	Block Size	8-50	8-40	0-40	8-40	8-30	0-20
	-Spacing	*	*	*	*	*	*
	-RQD	*	*	*	*	*	*
	Defect Condition	0-20	0-30	0-40	0-30	0-30	3-14
	-Persistence	*	*	*	*	*	*
	-Aperture	*	*	*	*	*	*
	-Roughness	*	*	*	*	*	*
	-Infilling	*	*	*	*	*	*
	-Weathering	*	*	*	*	*	*
	Groundwater	0-10	0-15	*	0-15	-	1-16
ADJUSTMENT	Defect Orientation	(60)-0	(60)-0	63-100%	(60)-0		5-20
	-Strike	*	*	*	*		*
	-Dip	*	*	*	*		*

	-Slope dip-defect dip						
	Excavation Method	-	-	80-100%	(8)-15		-
	Weathering	-	-	30-100%	-		3-10
	Induced Stresses	-	-	60-120%	-		-
	Major Plane of Weakness	-	-				
	TOTAL RANGE	(52)-100	(52)-100	0-120	(60)-115	8-100	25-100

Bieniawski (1876, 1989) subtracted the adjustments from the rock mass rating. From table 3.1, it is shown that, defect orientation adjustment can dominate the RMR. If the defect orientations are deemed “very unfavourable”, an adjustment of minus sixty (-60) is applied to the basic rock mass rating. Even for defect orientations denoted as “fair”, an adjustment of minus twenty-five (-25) is applied. There are no guidelines as to what “very unfavourable” means.

The MRMR method, developed by Laubscher (1977), applies adjustment, multipliers to the basic rock mass rating. The multipliers were developed primarily for underground excavations but are also used for slopes. A similar, though less comprehensive approach to slope stability classification was proposed by Haines and Terbrugge (1991), who based their classification on MRM. The method combines the groundwater parameter with defect condition.

Bieniawski (1989), recommends the use of the Romana (1985) SMR corrections for slopes. The SMR according to equation 3.1 is obtained by subtracting adjustment factors (F_1, F_2, F_3) of the joint-slope relationship and adding a factor (F_4) depending on the method of excavation; this requires an iterative approach for design.

$$SMR = RMR_{89} – (F_1\, F_2\, F_3) + F_4 \qquad (3.1)$$

Where,

(i) F_1 depends on the parallelism of joints and slope face strikes. It ranges from 0.15 to 1.0. It is 0.15 in cases where the angle between the critical joint plane and the slope face is more than 30^0 and the failure probability is very low, whereas it is 1.0 when both are near-parallel. These values were initially established empirically and subsequently found to approximate the relation:

$$F_1 = (1 - \sin A)^2 \quad (3.2)$$

Where A, denotes the angle between the strike of the slope face and that of the joint ($\alpha_{s} - \alpha_j$).

(ii) F_2 refers to the joint dip angle (β_j) in the planar failure mode. Its value ranges from 0.15 to 1.0. It is 0.15 when the dip of the critical joint is less than 20^0 and 0.1 for joints with dip greater than 45^0. For toppling mode of failure, F_2 remains equal to 1.0. F_2 is a measure of the probability of joint shear strength (Romana, 1985).

$$F_2 = \tan \beta_j \quad (3.3)$$

(iii) F_3 refers to the relationship between the slope face and joints. In planar failure mode, F_3 refers to the probability of joints “day lighting” in the slope face. Conditions are fair when slope face and joints are parallel, however, when the slope dips 10^0 more than the joints, the condition is termed unfavourable. For the toppling mode of failure, unfavourable conditions depend upon the sum of dips of joints and the slope $\beta_{j} + \beta_s$.

According to Hudson (1993), unfavourable or very unfavourable conditions for toppling failure cannot happen as there are very few sudden failures and many toppled slopes remain standing. The Goodman–Bray (1976) condition has been used to evaluate toppling probability with the hypothesis that this failure is more frequent in weathered slopes and there is a small reduction (-50) of shear strength due to rotational friction. The values of adjustment factors F_1, F_2 and F_3 for different joint orientations (Figure 3.2).

Table 3.2 Adjustment Factors for different Joint Orientation (after Romana, 1985)

Case		Very Favourable	Favourable	Fair	Unfavourable	Very unfavourable
P	$a_j - a_s$	> 30°	30° – 20°	20 - 10°	10° – 5°	< 5°
T	$a_j - a_s - 180^o$					
P/T	$F_1=[1- \sin(a_j - a_s)]^2$	0.15	0.40	0.70	0.85	1.00
P	B_j	$<20^0$	$20 – 30^0$	$30 – 35^0$	$35 – 45^0$	>45
P	$F_2 = \tan^2 B_j$	0.15	0.40		0.85	1.00
T	F_2	1.0	1.0	0.70	1.0	1.0
P	$B_j - B_s$	$>10^0$	$10 - 0^0$	1.0	$0 – (-10^0)$	$< -10^0$
T	$B_j + B_s$	$<110^0$	$110 – 120^0$	$>120^0$	-	-
P/T	F_3	0	-6	-25	- 50	- 60

P – Planar failure a_s - *Slope dip direction* a_j *– Defect dip direction*

T – Toppling failure B_s – *Slope dip* B_j *– Defect dip*

According to Romana (1985) the adjustment factor for the method of excavation F_4 (Table 3.3) has been empirically established as:

(i) Natural slope are more stable because of long time erosion and built-in protection mechanism (vegetation and grass desiccation): $F_4 = +15$

(ii) Normal blast applied with sound method do not normally change slope stability condition: $F_4 = 0$

(iii) Pre-splitting increases slope stability for half a class: $F_4 = +10$

(iv) Smooth blasting when well-done also increases slope stability $F_4 = +8$

(v) Mechanical excavation of slopes usually by ripping can be done only in soft and or much fractured rock and is often combined with some preliminary blasting. The plane of slope is often difficult to finish: $F_4 = 0$

(vi) Poor or deficient blasting damages the slope stability: $F_4 = -8$

Table 3.3: Adjustment Factor for Method of Excavation of Slope (after Romana, 1985)

Methods of Excavation	Natural Slopes	Pre-splitting	Smooth Blasting	Normal blast or Mechanical excavation	Poor blast
F_4 Value	+15	+10	+8	0	-8

Robertson (1988) developed SRMR based on RMR, for weak rock masses. Robertson increased the rating for intact strength by 15. This allowed for a broader range of weightings for rocks with uniaxial compressive strength (UCS), less than 1 MPa.

The RQD and defect spacing was measured from "handled" core. According to Robertson (1988), groundwater parameter should not be included in any rock mass rating, as it would be included in the analysis of the slope. The effect of moisture should be accounted for in the intact rock strength and the defect condition parameter if it is considered that a moisture change may reduce the strength of the rock or cause softening of any infill (Duran and Douglas, 2000).

According to Selby (1980), RMS includes defect orientation and weathering in the basic rock mass rating. Selby (1980), did not use RQD as he was assessing existing natural slopes where spacing was readily available. RQD was primarily used for the design of support in underground excavations it is not a good parameter to use for large rock slopes. RMS suggested the use of only defect spacing instead of block size (Duran and Douglas, 2000).

The weighting was reviewed at regular intervals in the development of the system and is now accepted as being as accurate as possible. The range of 0 to 100 is used to cover all variations in jointed rock masses from very poor to very good. The classification is divided into five classes (Table 3.4).

Table 3.4: Rock Mass Classification (Bieniawski, 1989)

Class	I	II	III	IV	V
Rating	100 - 81	80 - 61	61 - 41	40 - 21	20 - 0
Description	Very Good	Good	Fair	Poor	Very Poor

However, on the strength of intact rock, a vast amount of information has been published during the past fifty years. Hoek and Brown (1988), reviewed the published information on intact strength and proposed an empirical failure criterion for rock. In developing their empirical failure criterion, Hoek and Brown attempted to satisfy the following conditions:

a. The failure criterion should give good agreement with rock strength values determined from laboratory triaxial tests on core samples of intact rock. These samples are typically 50 mm in diameter and should be oriented perpendicular to any discontinuity surfaces in the rock
b. The failure criterion should be expressed by mathematically simple equations base, to the maximum extent possible, upon dimensionless parameters.
c. The failure criterion should offer the possibility of extension to deal with the failure jointed masses.

The most general form of the Hoek – Brown failure criterion, which incorporates both the original and the modified form is given by the equation:

$$\sigma_1^{'} = \sigma_3^{'} + \sigma_{ci}\left(m_b \frac{\sigma_3^{'}}{\sigma_{ci}} + s\right)^a \qquad (3.4)$$

Where,

m_b is the value of the constant m for the rock mass

S and a are constants which depend upon the characteristics of the rock mass

σ_c is the uniaxial compressive strength of the intact rock pieces and

σ_1 and σ_3 are the axial and confining effective principal stresses respectively.

The original criterion has been found to work well for most rocks and good reasonable quantity in which rock mass strength is controlled by tightly interlocking angular rock pieces. The failure of such rock masses can be defined by setting a =0.5 in Equation (3.4).

For poor quality rock masses, in which the partially interlocking has been destroyed by shearing or weathering, the rock mass has no tensile strength or "cohesion" and specimens will fall apart without confinement. For such rock masses, the modified failure criterion is more appropriate and is obtained by putting s =0 into Equation (3.4).

However, it is practically impossible to carry out triaxial or direct shear tests on rock masses at a scale which is appropriate for underground or surface excavations in mining or civil engineering. Numerous attempts have been made to overcome this problem by testing small scale models made up from assemblages of blocks or elements of rock or of carefully designed model materials.

The processes used by Hoek and Brown in deriving their empirical failure criteria were one of trial and error. The justification for choosing this particular criterion over the numerous alternatives lies in the adequacy of its prediction of observed rock fracture behaviour and the convenience of its application to range of typical engineering problems.

3.5.2 Limit Analysis

This approach is used to model materials assumed to behave as continuum in nature such as soil. Assumptions on perfectly plastic material with associated flow rule are made to determine the collapse load. Two plastic bonding theorems (lower and upper bounds) are used to calculate the collapse load (Chen, 1995).

According to the upper bound theory, if a set of external loads acts on a failure mechanism and the work done by the external load in an increment of displacement equal the work done by the external stresses, the external loads obtained are not lower than the true collapse loads. It is noted that the external loads are not necessarily in equilibrium with the internal stresses and the mechanism of failure is not necessarily the actual failure mechanism

The lower bound theorem states that if an equilibrium distribution of stress covering the whole body can be found that balances a set of external loads on the stress boundary and is nowhere above failure criterion of the material, the external loads are not higher than the true collapse loads. It is noted that in lower bound theorem, the strain and displacement are not considered and that the state of stress is not necessarily the actual state of stress at collapse.

3.5.3 Limit Equilibrium Analysis

The limit equilibrium technique has become the routine method for analysing slope stability problems in soil and rock mechanics. The method assumes that soil at failure obeys the perfectly plastic Mohr-Coulomb failure criterion to determine shear strength along a sliding surface. None of the basic equations of continuum mechanics regarding equilibrium, deformation and constitutive behaviour are satisfied completely (Sjőberg, 1999). The deformation of the material is not taken into account, and the condition for equilibrium is normally satisfied only for forces.

The limit equilibrium is based on the principles that the stress at which a soil fails in shear is defined as the shear strength of the soil. According to Janbu (1973), a state of limit equilibrium exists when the mobilised shear stress is expressed as a fraction of the shear strength.

As cited in Krishna (2006), Nash (1987) stated that, the shear strength at the point of failure is fully mobilised along the failure surface when the critical state conditions are reached.

The available shear strength depends on the type of soil and the effective normal stress whereas the mobilised shear stress depends on the external forces acting on the soil mass. This defines the Factor of Safety (FoS) as a ratio of the shear strength to shear stress in a limited equilibrium analysis (Janbu, 1973).

However, the factor of safety can be defined in three ways; as limit equilibrium, force equilibrium, and moment of equilibrium. The first definition is based on the shear strength. It can be obtained either by the total stress approach or the effective stress approach (Abramson et. al., 2002).

The type of strength consideration depends on the soil type, the loading conditions and the time elapsed after excavation. The total stress strength approach is used for short-term conditions in clay soil, whereas the effective stress strength approach is applied for long-term conditions in all kinds of soil or any conditions where pore pressure is known (Janbu, 1973). The second and third definitions are based on force equilibrium and moment of equilibrium conditions for resisting and driving forces components respectively (Krishna, 2006).

The limit equilibrium analysis approach has been applied to circular, planar, wedge and toppling failures. Limit equilibrium analysis for circular failures is applicable to soil slopes and very weak rock that undergo circular, rotational or curvilinear slip.

Only in exceptional circumstances will instabilities occurring in a continuum have truly circular slip surfaces; they will usually be curvilinear (Hudson and Harrison, 1997).

The slip surface is curved and usually terminates at a tension crack at the upper ground surface. In the analysis for a potential slip surface, consideration is given to the location of critical slip surfaces and determination of the factor of safety for a given slip surface, which in practice is determined for assumed slip surface locations. Iterative procedures involving the selection of a potentially unstable slide mass, subdivision of the mass into slices and consideration of force equilibrium and moment of equilibrium acting on each slice as shown from Figure 3.7 to Figure 3.12 are applied.

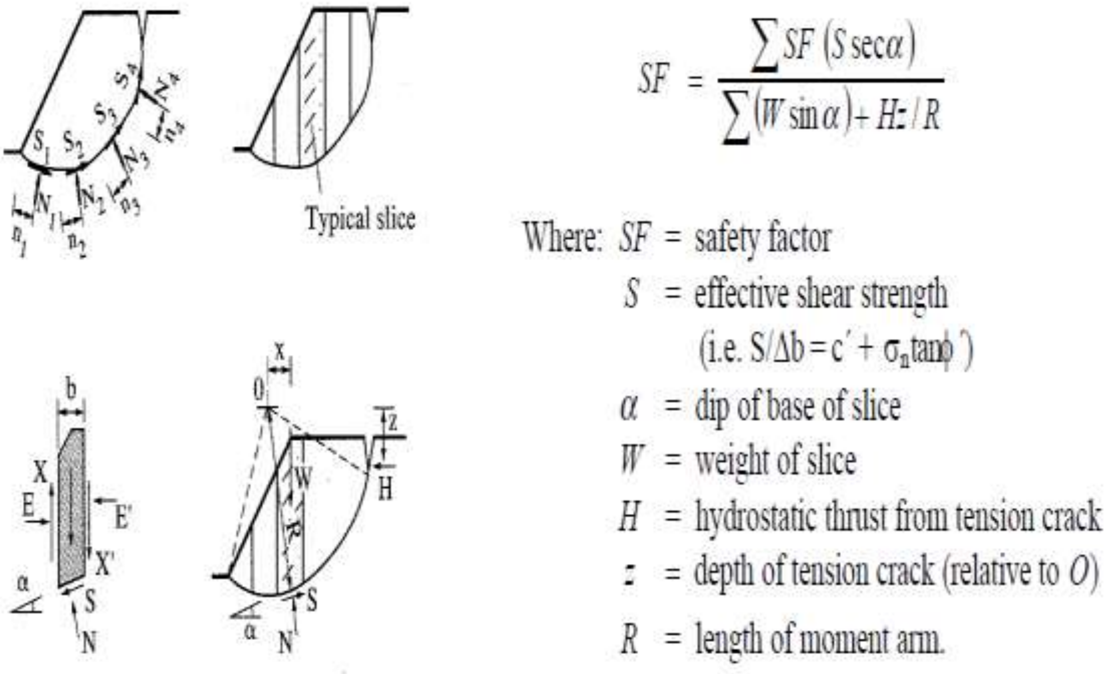

Figure 3.7: Limit Equilibrium Solution for Circular Failure (after Hudson and Harrison, 1997)

Several methods such as Bishop (1995), Spencer (1967), Janbu (1973), among others have been developed for analysis of circular slip failures with differences on how the conditions of equilibrium are satisfied and how the interslice forces are included to determine the solution of equilibrium. The limit equilibrium analysis for planar and wedge failure is statically determinate since the factor of safety can be calculated directly. The solution is straight forward which reduces the problem in two-dimension. It is assumed in planar analysis that all points along the sliding plane are on the verge of failure and that the distribution of stresses along the sliding surface is constant.

The theoretical solution for plane sliding is that, the strike of the failure plane and slope are parallel and that no end restraints are present (Hudson & Harrison 1997; Eberhardt et al. 2003). The solution further assumes that the rock mass is impermeable, the sliding block is rigid; the strength of the sliding plane is given by the Mohr-Coulomb failure criterion and that all forces pass through the centroid of the sliding mass (Figure 3.8)

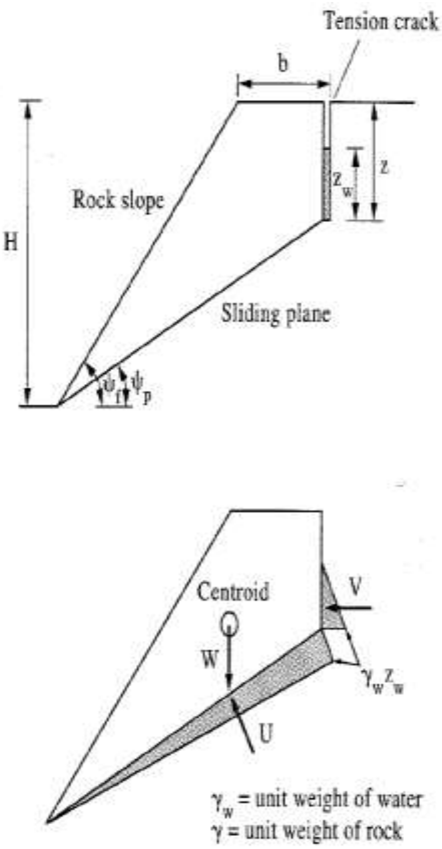

$$SF = \frac{c'(H-z)\csc\psi_p + (W\cos\psi_p - U - V\sin\psi_p)\tan\phi'}{V\cos\psi_p + W\sin\psi_p}$$

Where:

SF = safety factor
c' = effective cohesion
ϕ' = effective friction angle
ψ_p = dip of slide plane
W = weight of block
U = uplift force due to water pressure along slide plane
V = force due to water pressure in tension crack
H = slope height
z = tension crack depth

Figure 3.8: Limit Equilibrium Solution for Planar Failure (after Hudson and Harrison, 1997)

The dimensional method of analysing wedge failure (Figure 3.9) has been developed by Hoek and Bray (1974), and Kovari and Fritz (1989) which involves lengthy solutions.

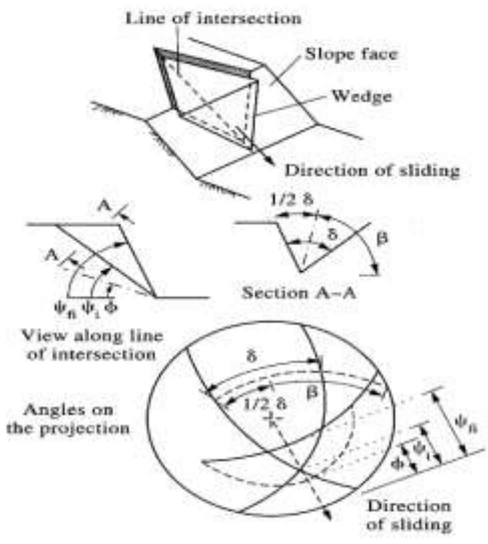

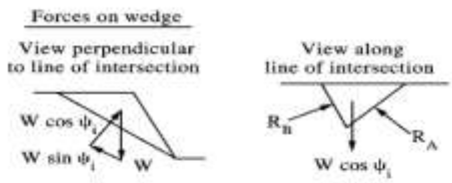

$$SF = \frac{(R_A + R_B)\tan\phi}{W\sin\psi_i}$$

and $R_A + R_B = \dfrac{W\cos\psi_i \sin\beta}{\sin(0.5\,\delta)}$

Where: SF = safety factor
ϕ = friction angle
ψ_i = dip of the line of intersection
W = weight of block
β, δ = wedge geometry factors

Figure 3.9: Limit Equilibrium Solution for Wedge Failure under Dry Conditions with Frictional Strength only (after Hudson and Harrison, 1997)

According to Bucek (1995), the first basic and till now the only limit equilibrium model of toppling is that of Goodman and Bray (1976). The presentation considered analysis of block toppling on a positively stepped base which was later upgraded several times but the core of all successive approaches were the same. The condition for sliding and or toppling for a rock block are defined in Figure 3.10.

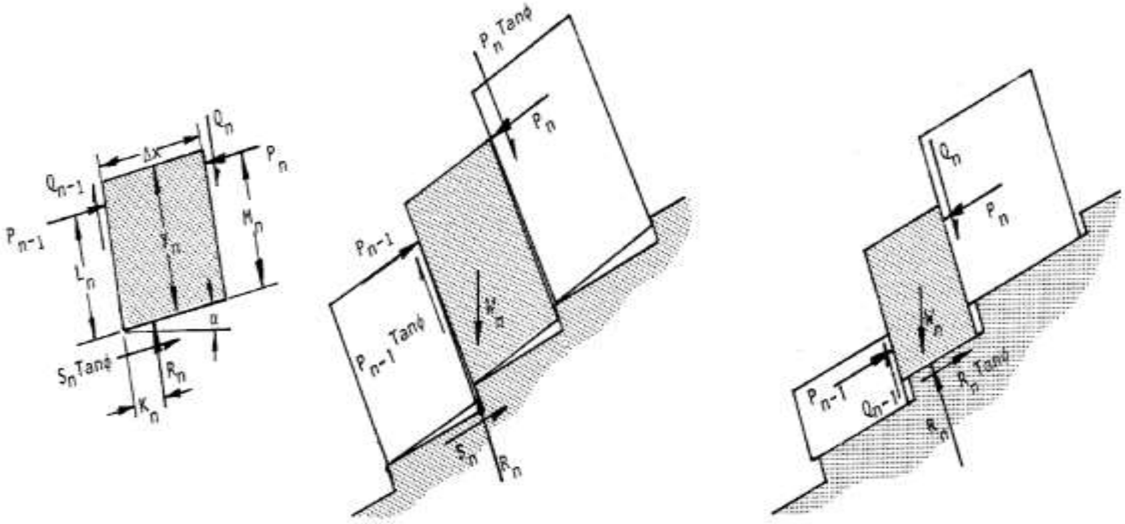

$$P_{n-1} = \frac{P_n\left(M_n - \Delta x \tan\phi\right) + \left(W_n/2\right)\left(y_n \sin\alpha - \Delta x \cos\alpha\right)}{L_n} \qquad P_{n-1} = P_n - \frac{W_n\left(\tan\phi \cos\alpha - \sin\alpha\right)}{1 - \tan^2\phi}$$

Figure 3.10: Limit Equilibrium Conditions for Toppling and Sliding, with Input Variables (after Hoek & Bray, 1981)

The line of action of force due to gravity serves to establish the equilibrium due to toppling. Four categories of equilibrium as listed below are defined in Figure 3.11.

Region 1: $\Psi < \phi$ and b/h > tan ϕ; no sliding and no toppling.

Region 2: $\Psi > \phi$ and b/h > tan ϕ: sliding but no toppling

Region 3: $\Psi < \phi$ and b/h < tan ϕ; toppling but no sliding.

Region 4: $\Psi > \phi$ and b/h < tan ϕ; sliding and toppling simultaneously.

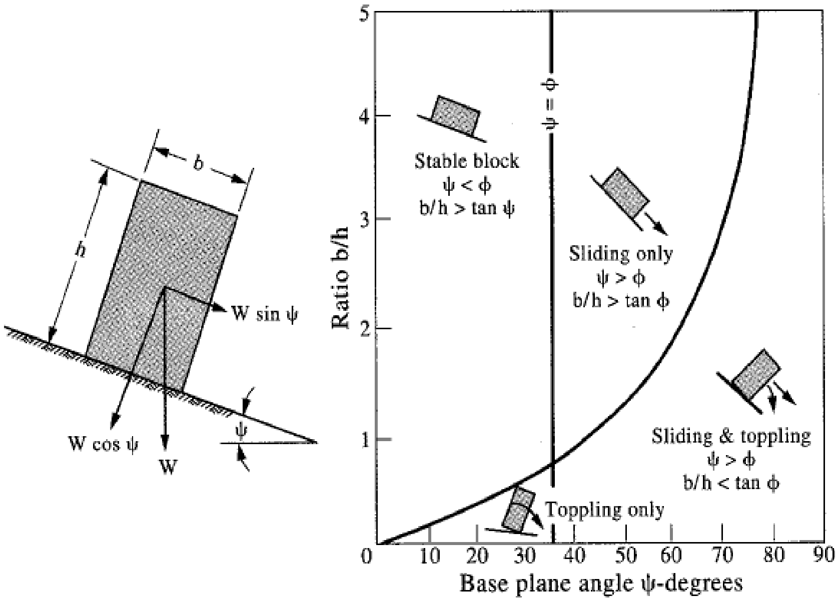

Figure 3.11: Sliding and Toppling Instability of a Block on an Inclined Plane (after Hoek & Bray, 1981)

Limit equilibrium analysis for flexural toppling will include geometric parameters (Figure 3.12) together with friction angle, which can be used to define the geometric factor of safety.

$$F = \frac{\tan \emptyset}{\tan(\Psi + \beta - 90)}$$

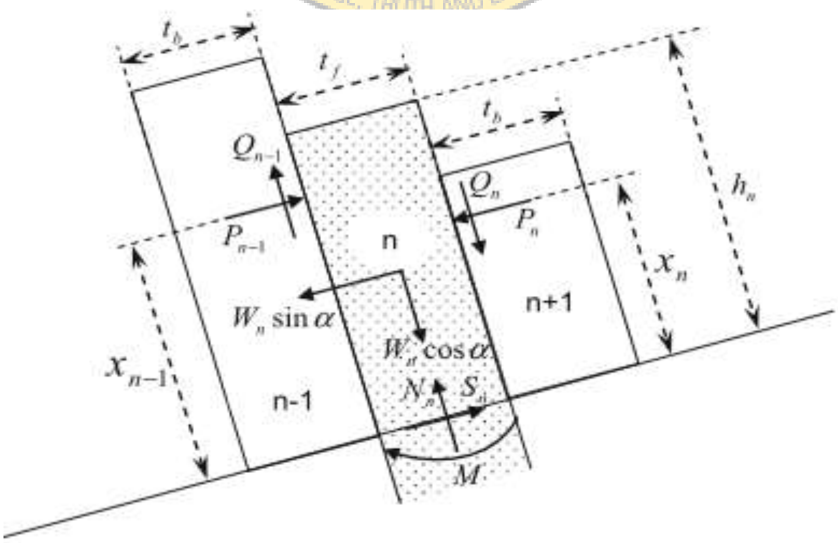

Figure 3.12: Limit Equilibrium Conditions for Flexural Toppling and Sliding (after Hoek & Bray, 1981)

3.5.4 Kinematic or Stereographic Analysis

Kinematic refers to the motion of bodies without reference to the forces that cause them to move (Goodman, 1989). According to Haswanto and Ghani, (2008), Kinematic analyses are very useful to investigate possible failure modes of rock masses which contain discontinuities. These methods consider the influence of block geometry on failure modes.

The technique includes stereographic projections commonly used to evaluate the stability of rock slopes (Goodman & Bray, 1976). Potential rock failure which involves plane sliding, wedge sliding and toppling due to the formation of "daylighting" discontinuities and geometry of the slope are identified kinematically on stereonet. The basic concepts related to estimation of maximum safe slope angles for the three basic modes of failure are discussed by Goodman (1989).

The method is used as a first hand approach to check the kinetic feasibility of rock slope system discontinuities but they do not provide a numerical measure of the degree of safety of the slopes, however sufficient information is achieved if the system is kinematically feasible.

For a kinematically plane feasibility, the following conditions must be satisfied (Hudson and Harrison, 1997).

- The dip of the slope must exceed the dip of the potential failure plane – this causes the existence of discrete blocks.
- The potential slip plane must daylight on the slope face/plane – this necessitates the discrete block formed in (a) above to move.
- The dip of the potential failure plane must be such that the strength of the plane is reached – this ensures that dip of plane must exceed friction angle of the discontinuity surface.
- The dip direction of the sliding plane should lie within approximately $\pm 20^0$ of the dip direction of the slope – occurs when the release blocks slide more or less directly out of the face.

However, wedge instability is kinematically feasible if the following criteria relating to the line of intersection are satisfied (Hudson and Harrison, 1997):

- The dip of the slope must exceed the dip of the line of intersection of the two discontinuity planes associated with the potentially unstable wedge.

- The line of intersection of the two discontinuity planes associated with the potentially unstable wedge must daylight the slope face.
- The dip of the line of intersection of the two discontinuity planes associated with the potentially unstable wedge must be such that the strengths of the two planes are reached.

Toppling generally occurs in two modes, direct and flexural toppling. The same kinematic instability technique for plane and wedge instability is used except that there will be the need to analyse the intersections which define the edges of the block and the poles which defines the basal planes on which toppling occurs.

The nature of direct toppling is determined from the block geometry of the rock mass relative to the geometry and the strength parameters, even though the latter can be used to establish toppling only and sliding plus toppling. The question of direct toppling is whether a block resting on an inclined surface will be stable, or slide, or topple. According to Goodman, (1989) two conditions are required kinematically:

- There are two sets of discontinuity planes whose intersections dip into the slope to provide rock block formation.
- There is a set of discontinuity planes to form the bases of the toppling blocks to combine with above condition to complete rock block formation.

For flexural toppling to occur, the creation of excavation surface leads to the establishment of principal stresses either parallel or perpendicular to the excavated face. Kinematic feasibility analysis of this type is dependent on the geometry of the layer and the potential for inter-layer slip (Hudson and Harrison, 1997).

3.5.5 Numerical Modelling

It has been established that limit equilibrium can be misleading when used to compute factor of safety as they generally do not provide information about the development of failure. The numerical methods are however, used to show how failures are initiated and the likely failure mechanism. These methods are relatively recent compared to limit equilibrium. They are used to obtain stress and strain distribution and are useful for analysis of slope stability when it is subjected to various types of loading or when the slope has complex geometry, material anisotropy and non – linear behaviour. Numerical methods for rock slope stability can be used to distinguish between the continuum and discontinuum and hybrid modelling and they serve different purposes in rock mass modelling (Sjőberg, 1999).

A continuum model regards the rock mass as a uniform medium where the material properties are the average of the intact rock blocks and the joints that separate them. The stress and deformation is distributed evenly through the whole rock mass. This type of modelling is the best solution when there are no or only a few joints in the rock mass, or if the rock mass is heavily jointed. Most continuum model programs allow for the modelling of a few distinct joints where a joint slip criterion may be assigned to the joint elements. The continuum approach used in rock slope stability includes the finite-difference and finite-element methods. In these, the entire problem domain is discretized into elements (Anon, 2008b).

The available program for majority of continuum modelling in slope engineering has been the finite difference code, FLAC (Itasca, 1996). According to Eberhardt et al. (2001), the code allows a wide choice of constitutive models to characterize the rock mass to incorporate time dependent behaviour, coupled with hydro-mechanical and dynamic modelling. Two-dimensional continuum codes assume plane strain conditions, which are frequently not valid in inhomogeneous rock slopes with varying structure, lithology and topography. The recent advent of 3-D continuum codes such as FLAC 3D enables the engineer to undertake 3-D analyses of rock slopes on a desktop computer (Anon, 2008b).

The distinct-element method using distinct-element codes such as UDEC and 3DEC (Itasca, 1996) are among the commonest codes used in slope engineering analysis. These use a force-displacement law specifying interaction between the deformable joint bounded blocks and Newton's second law of motion and provide displacement induced within the rock slope.

3.5.6 Probabilistic Methods

Geotechnical parameters are associated with uncertainties and as such care is greatly taken in selecting appropriate values for the design of slope stability. This has suggested the replacement of the traditional deterministic slope stability methods by probabilistic methods (Priest and Brown, 1983, McMahon, 1975) with all attempts emphasizing on geological structures on slopes. Considering probabilities of failure rather than the safety factors is an acknowledgement that there is a finite chance of failure, although it can be very small (Sjőberg, 1999).

A probabilistic approach requires that a deterministic model exists (Tapia et al, 2007). The parameters used in this case are described as probability distribution instead of point estimate values. The probability of failure is estimated by combining the distribution within the deterministic model used to calculate the factor of safety. Monte Carlo simulation technique is usually used to combine the distribution. Each input parameter is randomly sampled from its distribution and factor of safety is determined for each set of random input. The probability of failure is calculated from the ratio between the number of iterations yielding a factor of safety less than unity and the total number of simulations. The overall probability of failure is the product of the probability that failure is possible and the probability that the strength is exceeded (Sjőberg, 1999).

However, risk analyses are used to access the main drawback of the slope design methods with the consequences that risk criteria are acceptable. Risk can be defined as the probability of occurrence of an event (slope failure) combined with the consequence or potential loss associated with the event.

Risk = (Probability of Failure) × (Consequence of Failure)

The consequence associated with the risk can be personnel and economic impact. Because the risk analysis sets the acceptability criteria on the consequences rather than on the likelihood of failure, a complete evaluation of the probability of slope failure is required in addition to other uncertainty not encountered with the slope stability model. This requires the inclusion of engineering judgement and expert knowledge into the process.

3.6 Effects of Groundwater on Slope Instability

High groundwater table is one of the most important factors known to produce movement of stable and unstable slopes in an open pit; that is high pore pressure ratio above slip surface. This effect of water pressure creates an uplift on the potential failure surface and thus reduces the pore water pressure along the slip surface.

In all pit slope stability problems, it is necessary to determine the pore water pressure from a prescribed phreatic surface. Phreatic surface in the open pit slope area is not constant and it depends on different factors (Mandzic, 1999). In order to include the effects of pore pressure in stability analysis, the pore pressure ratio, (*ru*), is used. The pore pressure ratio is defined as the ratio between total upward force due to pressure and total downward force due to the weight or overburden pressure.

According to Archimedes principle, the upward force is equal to the weight of water displaced or the volume of sliding mass under water multiplied by the unit weight of water. The downward force is equal to the weight of sliding mass.

According to Mandzic (1999), the pore pressure ratio, *ru*, can be determined from the relation:

$$ru = \frac{(\text{Volume of sliding mass under water}) \times (\text{unit weight of water})}{(\text{Volume of sliding mass under water}) \times (\text{unit weight of soil})} \quad (3.17)$$

Morton et. al. (2008), states that, the stress state in a slope at any point is governed by the principal stresses and the acting water pressure. The Mohr-Coulomb equation derived from the Coulomb-Terzahi Equation states:

$$\tau = (\sigma - p) \tan\emptyset + c$$

Where: τ = shear strength

σ = total normal stress

p = pore water pressure

$\emptyset$ = internal friction angle

C = cohesion.

Strength comes from the cohesion and the weight of the formations and weakness comes from the pore water pressure and internal angle of friction. A reduction in the effective stress (σ – p) will reduce the shear strength of the rock mass. Therefore, in stability analysis, it is essential to know the distribution of pore pressures in the pit slopes.

Geological materials have hydraulic conductivity values ranging over 13 to 14 orders of magnitude (Freeze and Cherry, 1979). In an open pit slope, hydraulic conductivity is highly heterogenic and anisotropic with values varying over 3-4 orders of magnitude within the same lithology. Groundwater flow is controlled primarily by hydraulic conductivity; therefore, flow line and pore pressure have a non-uniform distribution in open pit slope formations.

The pore pressure rise may be high in the confined permeable zones following exceptional heavy rainfall. Such high pressures transmitted perhaps via rock discontinuities might aid the formation of soil pipes in saprolite (Jiao and Nandy, 2001).

According to Rowe and Beale (2007), the extent to which active mine operations are impacted by groundwater can vary considerably. In most situations, a properly planned and managed programme of water control will provide added value to a mine project and contribute to safe operating conditions. In some cases, dewatering and slope depressurization is essential to mine implementation, providing for workable conditions, improved slope performance and considerable annual operational cost savings. A robust conceptual understanding of site hydrogeological conditions and interactions with the mine plan is essential for implementation of appropriate pit dewatering measures.

Understanding the dewatering requirements for a mine involves integrated assessment and quantification of geology, geologic structure, rock mass hydraulics, rock mechanics, surface hydrology and climate. The operating plan must then be placed in the site-specific hydrogeologic context, enabling dewatering issues to be identified, predicted and managed in advance of mining.

Dewatering of open pit can involve several key components including the following:

Installation of in-pit groundwater storage removal which typically involves in-pit dewatering pumping wells to remove the groundwater occupying the pores or fractures in the rock mass within and surrounding the mine shell. Wells are installed and operated to lower groundwater levels ahead of the active benches. Wells that are within the mining footprint are at risk of mining activities.

Interceptor wells are drilled at the perimeter of the pit for interception and removal of lateral groundwater inflow into the pit. These are positioned to remove groundwater that is flowing toward the pit from the surrounding system and to lower the groundwater table behind the pit slopes. These are controlled by geologic structure in many cases; however, in some cases it may be possible to achieve considerable cost savings by intercepting groundwater flow towards the workings at shallow levels.

Depressurization of pit slope involves the installation of horizontal drains directly into the slope where elevated pore pressures can develop. Diligent operation of process facilities and infrastructure is often important for minimizing recharge at the crest of the pit wall.

Control and removal of surface water runoff generated by incident rainfall falling on the pit slopes or other contributing drainage areas. This can be considerably importance and, in some cases, is the major challenge for operations, particularly in tropical or monsoonal environments where highly intense rains occur. The pit floor is a concentration point for runoff generated from the pit slopes, so that reserves and infrastructure in the pit-floor can be vulnerable to surface water inflow.

3.7 Slope Monitoring

According to Kayesa (2006), open pit mining brings about volumetric, stress and strain changes in the rock mass in a mine opening. When the deformations surpass the limits controlled by the rock strength, instability is created around the mining excavation, which will lead to failure.

Slope failure is a business associated with safety risk to a mine, which can have devastating consequences such as loss of production, damage to equipment, injury to personal and most serious of all, loss of life. In times of serious open pit slope failure, high insurance premiums, loss of reputation as well as legal action could arise. The most important slope stability management tool is slope monitoring (Kayesa, 2006).

Slope monitoring is the recording of the stability of the rocks making up the slopes surrounding an open pit mine. The objectives of slope monitoring are to:

- Verify mine design, where measurements can be used as basis for maintaining, steepening or reducing slope angles with the resultant economic and safety benefits and source for future mine design.
- Serves as a warning system as to which areas of the pit are unstable.
- Serve as a major slope stability risk management tool for making management decisions for the safety of workers.
- Give technical assurance to production and management officials.
- Give measurement of rates of movement in the unstable zones.

3.7.1 Slope Monitoring Systems

Selecting slope monitoring instruments depends on the associated problem to be monitored. A comprehensive monitoring system may include instruments capable of measuring rock mass displacement, groundwater parameters and ground vibration.

Surface measurement of rock mass displacement is done using the electronic distance method which involves a survey network consisting of target prisms placed on the pit walls and pit crest, berms and areas of anticipated instability together with one or more non-moving survey station located on a complete stable ground. The angles and distances to the target prisms are measured from the survey station on regular basis to establish a history of movement. Measurement can be done manually or automated and continuous.

Another simple and easy method to provide some information on the extent of unstable ground is by visual monitoring of tension cracks. Measuring and monitoring the changes in the crack width and direction of crack propagation is required to establish the extent of the unstable area. The simplest method for monitoring tension cracks is to mark the ends by spraying so that new cracks or propagation along existing cracks can be easily identified on subsequent inspections. Crack measurement can be done by driving two wooden pegs, crack pins, or stakes on either side of the crack and the separation measured with measuring tape.

Wire extensometer is another common method mostly complemented with survey network to monitor movement across tension cracks. The commonest set up is comprised of a wire anchored in the unstable portion of the ground with a monitor and pulley station located on the stable ground behind the tension crack. The wire runs over the top of a pulley and is tensioned by a weight suspended from the other end. As the unstable portion of the ground moves away from the pulley stand, the weight will move, and the displacement can be recorded either electronically or manually. Electronic monitoring equipment can be programmed to set off alarms if the displacement reaches certain threshold limits.

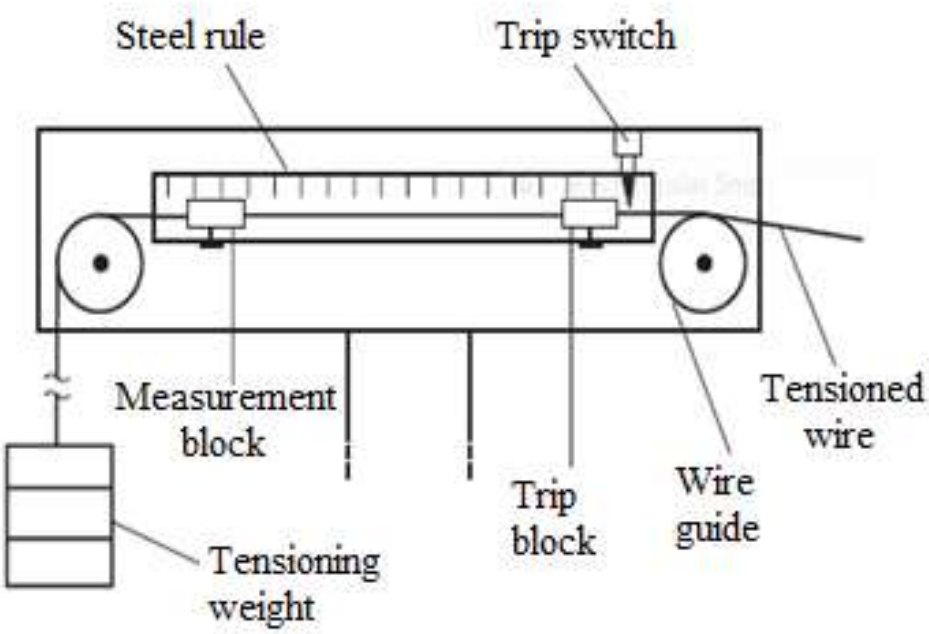

Figure 3.13 Wire Extensometer (Broadvent and Zavodni, 1982)

Borehole inclinometers, extensometers, piezometers and micro-seismic monitoring are subsurface measurement methods (Call 1982; and Savely, 1993). Borehole inclinometers measure the angular deflection of the borehole and thus the horizontal displacement in different directions (Sjöberg, 1999). It consists of casing with embedded sensors that are placed in the ground in the area of expected movement.

The end of the casing is assumed fixed so the lateral profile of displacement can be calculated. The deflection of the casing, and hence the surrounding rock mass, are measured by determining the inclination of the sensing unit at various points along the length of the installations (Sjöberg, 1999).

Information collected from inclinometers (Kliche, 1999) can be used to:

- Locate shear zones.
- Determine whether shearing is planar or rotational.
- Determine whether movement along a shear zone is constant, accelerating, or decelerating.

Borehole extensometers are used to monitor known structural features which will have a major influence on the stability of the slope. It has been established that borehole extensometer can withstand very small shear displacement. It is made up of tensioned rods anchored at different points in a borehole. Changes in the distance between the anchor and rod head provide the displacement information in the rock mass.

Piezometers are used to monitor groundwater levels and measure pore pressure behind the pit walls; they are also essential means to monitor the effectiveness of mine dewatering programs. Essential pore pressures, especially water infiltration at geologic boundaries are responsible for many slope failures (Kliche, 1999).

Open pit slope monitoring using micro-seismic methods is on the increase. Micro – seismic monitoring still has its niche in open pit mines located in seismically active areas to detect seismically active zones which might trigger slope failure (Sjöberg, 1999).

3.7.2 Slope Movement

Measurable displacement and other indications of instability such as cracks, scarp and changes in pore pressure are found to precede slope failure.

Empirical studies by Broadvent and Zavodni (1982) showed slope movement may be classified into three main types (Figure3.14) depending on the tendency for the slide to become more stable or more unstable (Table 3.5).

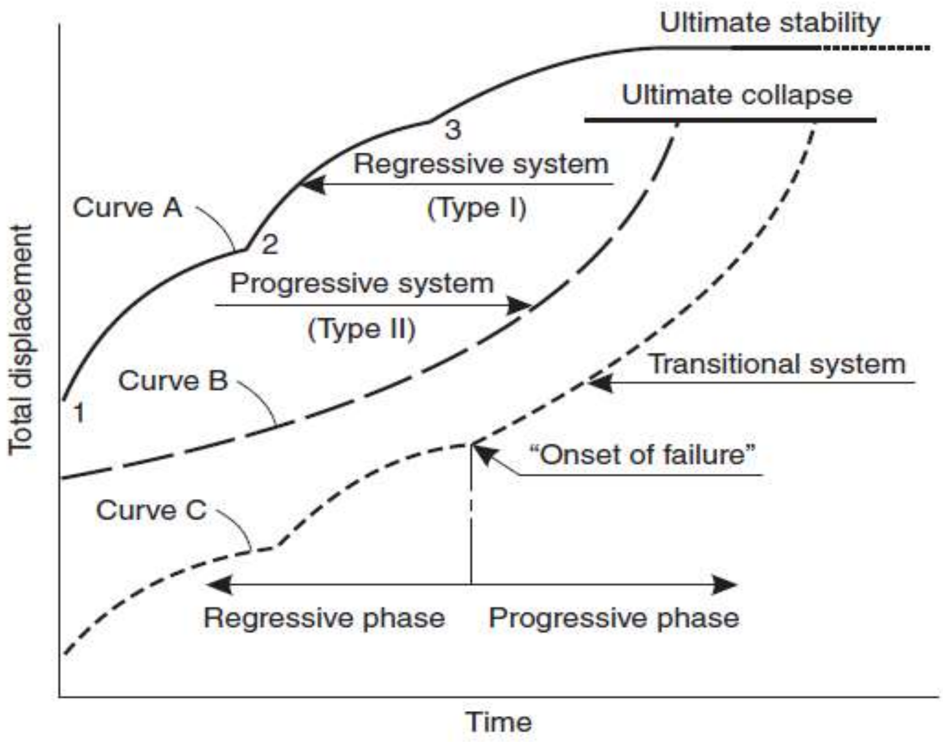

Figure 3.14: Typical Displacement Time Behaviour for Pit Slope Failures (Broadvent and Zavodni, 1982)

Table 3.5: Description of Time Behaviour for Pit Slope Failures (Broadvent and Zavodni, 1982).

Type 1	Curve A	A regressive type characterized by a series of short term decelerating movement cycles leading to ultimate stability
Type 2	Curve B	A progressive type characterized by accelerating movement leading to overall failure
Type 3	Curve C	A transitional type which starts as regressive and end as progressive type. This usually occurs as a result of change in external conditions such as groundwater or rainfall or changes in shear strength.

Detail interpretation and assessment of slope monitoring date requires specialist skills with the ultimate objectives to manage the extent, scale, time frame potential impact and consequences to mining production.

Open pit slope monitoring programs can be simple and depending on the condition can be refined and become more complex; its implementation is step-by-step from visual inspections of pit crest, accessible berms and slope face to remote monitoring using high precision slope monitoring equipment.

CHAPTER 4

METHODS USED

4.1 Borehole Logging

Rock mass logging was carried out from oriented diamond drilled cores. The rock mass parameters logged included rock types, identification of natural joints, cemented joints, quartz veins, drilling induced fractures, infill types and strength estimates. The data collected from the rock mass logging was used to determine the rock mass ratings (Figure 4.1).

In all, fourteen (14) oriented boreholes from the north wall, east wall, and south wall were geotechnically logged. From the logging exercise, the oriented boreholes at the east wall dipped at 75^0 to the west orienting at 270^0. Oriented boreholes at the north wall were found dipping to the south at 75^0 orienting at 180^0, while those to the south wall dipped at 75^0 to the north orienting at 0^0 (Figure 4.1).

Table 4.1 Parameters for the various Geotechnical Holes

HOLED ID	Y	X	Z	DEPTH	DIP	AZIMUTH
GDKD002	7395.185	8127.482	108.02	74.1	-51.16	357.02
GDKD003	7244.061	8139.389	94.54	69.02	-50.4	357.18
GDKD004	7207.669	8218.438	84.272	79.7	-50.86	215.92
GDKD005	7398.761	8055.667	78.273	79.8	-51.08	177.76
GDKD006	7250.536	8140.427	94.88	122.15	-54.28	314.07
GDKD019	7602.297	7884.635	100.801	100.98	-54.72	180.2
GDKD020	7515.763	8017.63	61.88	79.83	-53.94	180.3
GDKD021	7681.11	7884.661	87.336	118.6	-54.44	181.16
GDKD069	7559.2	7933.596	80.157	102	-65.2	340.2333
GDKD070	7436.501	8092.992	99.658	83.34	-55.05	40.475
GDKD072	7552.269	7912.444	81.141	80.13	-64.4	222.925
GDKD075	7492.373	8008.082	62.241	80.28	-64.86	219.32
GDKD076	7520.533	8031.831	62.12	85.7	-63.025	43.2
GDKD077	7423.11	8078.746	96.538	100	-63.85	218.725

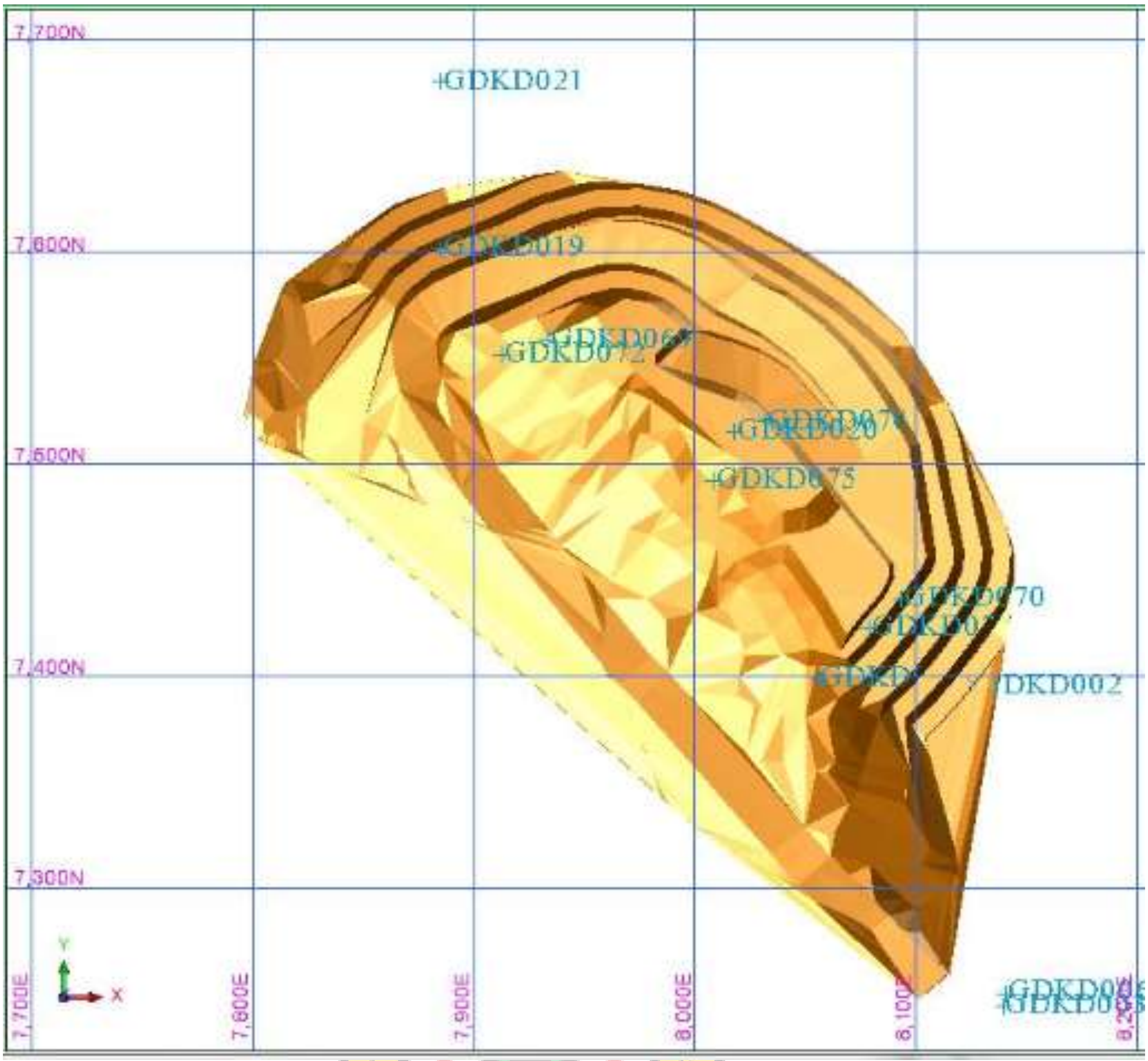

Figure 4.1 Spatial Distributions of Geotechnical Holes

4.2 Laboratory Test

4.2.1 Soil Tests

The particle size distribution, Atterberg limit, and direct shear tests were performed in accordance with British Standard BS 1377 (1990). Graphs of Shear Stress versus Displacement and Shear Stress versus Normal Stress are presented in Appendix B.

Representative samples of the various soils in the study area were taken and analysed for particle size distribution by sieving and sedimentation processes. The sieve analysis was carried out on over-size of washed material on the 63 μm sieve. Sodium Carbonate ($NaCO_3$) solution was used as dispersant during the sedimentation test.

The liquid and plastic limits of soil samples were determined from the undersized fraction over 0.425 mm sieve. The liquid limit test was performed by feeding the metal cup of the test device with soil paste and a groove was made down its centre. The cup was repeatedly dropped and the number of blows required for the groove to close for 13 mm recorded (Table 4.2a and 4.2b).

Table 4.2a Results of Atterberg Limit Test

<table>
<tr><th rowspan="2">Hole Id</th><th colspan="2">Depth</th><th rowspan="2">Lithology</th><th rowspan="2">Weathering</th><th colspan="3">Consistency Limits</th></tr>
<tr><th>From</th><th>To</th><th>LL (%)</th><th>PL (%)</th><th>PI (%)</th></tr>
<tr><td>GDKD069</td><td>0</td><td>0.16</td><td rowspan="2">SSRP</td><td rowspan="2">CW</td><td rowspan="2">54.90</td><td rowspan="2">28.90</td><td rowspan="2">26.00</td></tr>
<tr><td>GDKD069</td><td>0.6</td><td>3.7</td></tr>
<tr><td>GDKD069</td><td>5.2</td><td>5.47</td><td>SSSL</td><td>CW</td><td>28.00</td><td>25.70</td><td>2.30</td></tr>
<tr><td>GDKD069</td><td>6.94</td><td>7.09</td><td rowspan="2">SSSL</td><td rowspan="2">CW</td><td rowspan="2">26.00</td><td rowspan="2">16.40</td><td rowspan="2">9.60</td></tr>
<tr><td>GDKD069</td><td>9.12</td><td>9.32</td></tr>
<tr><td>GDKD070</td><td>0.13</td><td>0.25</td><td>SSRP</td><td>CW</td><td>55.40</td><td>38.10</td><td>17.30</td></tr>
<tr><td>GDKD070</td><td>3.4</td><td>3.59</td><td>SSRP</td><td>CW</td><td>34.50</td><td>9.60</td><td>24.90</td></tr>
<tr><td>GDKD070</td><td>3.59</td><td>3.82</td><td>SSRP</td><td>CW</td><td>28.80</td><td>20.20</td><td>8.60</td></tr>
<tr><td>GDKD070</td><td>3.18</td><td>3.34</td><td>SSRP</td><td>HW</td><td>46.50</td><td>20.10</td><td>26.40</td></tr>
<tr><td>GDKD072</td><td>0.53</td><td>0.83</td><td>SSRP</td><td>CW</td><td>55.38</td><td>26.20</td><td>29.20</td></tr>
<tr><td>GDKD072</td><td>1.32</td><td>1.5</td><td>SSRP</td><td>CW</td><td>30.50</td><td>25.50</td><td>5.00</td></tr>
<tr><td>GDKD076</td><td>3.66</td><td>3.83</td><td>SSSL</td><td>CW</td><td>33.40</td><td>16.40</td><td>17.00</td></tr>
<tr><td>GDKD076</td><td>4.15</td><td>4.22</td><td>SSSL</td><td>CW</td><td>37.90</td><td>32.50</td><td>5.40</td></tr>
<tr><td>GDKD076</td><td>4.5</td><td>5.12</td><td>SSSL</td><td>CW</td><td>32.90</td><td>27.20</td><td>5.70</td></tr>
<tr><td>GDKD076</td><td>5.66</td><td>6.02</td><td>SSSL</td><td>CW</td><td>35.60</td><td>27.60</td><td>8.00</td></tr>
</table>

Table 4.2b Results of Particle Size Distribution Test

Hole Id	Depth		Lithology	Weathering	PSD			
	From	To			% Gravel	% Sand	% Silt	% Clay
GDKD069	0	0.16	SSRP	CW	5.10	41.20	52.20	1.50
GDKD069	0.6	3.7						
GDKD069	5.2	5.47	SSSL	CW	17.35	28.05	53.24	1.37
GDKD069	6.94	7.09	SSSL	CW	1.35	57.85	40.12	0.68
GDKD069	9.12	9.32						
GDKD070	0.13	0.25	SSRP	CW	43.10	20.90	22.65	13.35
GDKD070	3.4	3.59	SSRP	CW	0.70	54.20	44.54	0.56
GDKD070	3.59	3.82	SSRP	CW	4.55	54.95	39.50	1.00
GDKD070	3.18	3.34	SSRP	HW	2.20	33.95	36.71	27.14
GDKD072	0.53	0.83	SSRP	CW	0.35	48.85	33.44	17.36
GDKD072	1.32	1.5	SSRP	CW	19.40	40.75	39.35	0.50
GDKD076	3.66	3.83	SSSL	CW	0.58	48.33	50.24	0.85
GDKD076	4.15	4.22	SSSL	CW	32.76	48.98	17.96	0.30
GDKD076	4.5	5.12	SSSL	CW	1.44	65.26	26.36	6.94
GDKD076	5.66	6.02	SSSL	CW	5.30	66.70	10.27	17.73

The plastic limit of the soil sample on the other hand was determined by mixing the soil with enough water to form a uniform paste, and rolling and kneading balls of the soil paste into thread and until threads of about 3 mm began to crumple.

The shear strength parameters c and ϕ were determined by subjecting trimmed 60 mm × 60 mm× 20 mm specimens obtained from undisturbed samples to normal loads of 2.0 KN, 4.2 KN AND 8.5 KN on a shear box assembly. The shear displacements and the vertical displacements were recorded for each load until the soil failed. Plots of the shear stress versus relative displacements were made from which the peak stress for each normal load was extracted and used for plotting of the Mohr – Coulomb envelope.

4.2.2 Rock Tests

The uniaxial compressive strength test, point load test and direct shear test were performed in accordance with International Society for rock Mechanics, ISRM, (1985) standards. Tilt test on rock cores was also conducted to determine the basic friction angle on discontinuity surfaces. The cylindrical cored specimens for uniaxial compression strength test were prepared with length to diameter ratio 2.0. The two ends of the specimen were trimmed and flattened to the desired size of the disc.

The tilt test on cored specimen was performed to determine the basic friction characteristics along artificial planar saw cut surface or solid core. The test was performed by placing two pieces of cored specimen on a horizontal base. A third piece of core was placed on top of the first two pieces of core and the base rotated about a horizontal axis until sliding of the upper piece of core began. The minimum angle at which the sliding began was recorded as the basic friction angle (ϕ).

Table 4.3 Results of Uniaxial Compressive Strength Test

Hole Id	Depth		Lithology	Weathering	UCS
	From	To			Mpa
GDKD069	22.78	23.22	SSSL	MW	5.93
GDKD069	23.22	23.46			
GDKD069	47.05	47.56	SSSS	SW	65.25
GDKD069	50.1	50.42	SSSS	SW	62.60
GDKD069	52.81	53.19			
GDKD069	53.19	53.59	IFDL	UW	90.83
GDKD069	53.91	54.18			
GDKD069	66.02	66.35	SSSS	UW	97.72
GDKD069	68.37	68.64	SSSS	UW	92.69
GDKD069	99.15	99.96	SSSS	UW	95.22
GDKD070	15.4	15.74	SSSL	MW	1.05
GDKD070	18.67	18.86	SSSL	MW	13.79
GDKD070	41.96	42.27	SSSL	MW	66.14
GDKD070	71.66	71.89	SSSS	UW	87.6
GDKD070	72.71	72.98	SSSS	UW	92.69
GDKD070	82.26	82.51	SSSS	UW	94.22
GDKD072	2.77	3.56	SSSL	MW	4.91
GDKD072	4.2	4.56	SSSL	MW	5.61
GDKD072	17.07	17.29	SSSL	CW	0.76

4.3 Hydrogeological Conditions

4.3.1 Surface water condition

A number of streams, generally referred to as “Ahuma-blue”, traversed the project area with an average flow rate of 20 litres per minute. The stream water was highly turbid and brownish-red in colour due to the presence of Fe^{3+} oxides.

4.3.2 Piezometric Water Levels

The groundwater levels behind the pit walls were determined from water level measurements in twenty-five standpipe piezometers located along the crests of the pit walls to determine the phreatic water surface for stability analysis.

The project area was highly weathered and heavily vegetated. This led to a cave in of some boreholes and loss of access to others after a heavy rainstorm. For this, groundwater level measurements could not be repeated. Consequently, permeability of the rock mass could not be determined (Table 4.4).

Table 4.4 Measuring Water Level from Piezometers.

Hole ID	Northing	Easting	Water Level (m)
GDKD009	7559.19	8041.852	61.89232
GDKD010	7512.746	7961.085	60.93096
GDKD013	7409.565	8091.486	43.57528
GDKD014	7406.332	8013.51	62.93648
GDKD016	7441.817	8010.736	59.91784
GDKD017	7547.03	7884.594	36.87528
GDKD018	7447.792	8086.345	39.90492
GDKD019	7602.297	7884.635	35.10116
GDKD020	7515.763	8017.63	61.63424
GDKD022	7526.834	8087.55	61.68364
GDKD025	7563.34	7921.551	29.89792
GDKD026	7602.923	8009.893	62.3648
GDKD027	7712.616	7839.813	50.07764
GDKD028	7631.091	7843.283	46.66052
GDKD029	7633.284	7960.16	53.04692

GDKD031	7597.098	7918.678	47.91768
GDKD032	7563.769	8006.46	62.37524
GDKD034	7523.641	8060.105	62.0366
GDKD037	7484.15	8088.78	54.53864
GDKD038	7365.847	8085.591	66.2502
GDKD039	7672.112	7842.726	50.06212
GDKD041	7769.597	7799.425	33.54604
GDKD042	7385.785	8131.459	41.09592
GDKD043	7306.578	8129.459	45.51144
GDKD044	7607.247	7801.679	48.43312

KNOWLEDGE, TRUTH AND EXCELLENCE

CHAPTER 5

ANALYSIS OF RESULTS AND DISCUSSIONS

5.1 Empirical Analysis

The methodology for the evaluation of the design parameters was to establish an initial design envelope using empirically (lower bound, conservative) and structurally (upper bound, optimistic) derived indicative slope design parameters. These two approaches provided a reliable starting point to carry out limit equilibrium analysis.

The empirical analysis provided initial estimates of the Indicative Bench Stack Angle (IBSA) and the indicative overall slope angles (IOSA). This was supplemented with comparative bench stack angles from the structural analysis in order to obtain a first pass slope design that was subsequently tested in the numerical modeling. The initial structural evaluation of the rock mass fabric determined the Spill Berm Width (SBW) and Bench Face Angle (BFA) for the various design sectors.

A limitation was also imposed on the maximum bench height and minimum berm width that can be achieved by the 2012 edition of Minerals and Mining Regulations, (LI 2182). Regulation 88 sub-regulation two (2) states that "in providing a bench under sub-regulation (1), the manager of the mine shall ensure that the maximum bench height is twenty metres and the minimum bench width is five metres that".

The empirical evaluation discussed here utilises the methodology of Laubscher's (1990) Mining Rock Mass Rating Classification System. The approach used by this system is to assign in-situ (virgin conditions) ratings to a rock mass, based on measurable parameters where an algebraic relation of the rock mass results in a representative rock mass quality.

The basic rock mass rating captures the main features that would affect the shear strength of the rock mass and subsequently the stability of slopes in the rock mass. The design process detailed the following parameters for each slope sector:

- Bench Face Angle
- Bench Height
- Spill Berm Width
- Inter-ramp Angle
- Indicative Bench Stack Angle (IBSA)
- Indicative Overall Slope Angle (IOSA)

5.2 Mining Rock Mass Rating

The empirical evaluation is based on the mining adjusted Mining Rock Mass Rating (MRMR) classification system (Laubscher, 1990). This is an extremely useful and robust method of utilizing all the relevant rock mass parameters to assist with mine design. It has been used in open pit mining from initial scoping studies through to full mine production. The in situ RMR was adjusted to take account of the expected mining environment factors, namely:

- the influence of weathering
- structural orientation
- induced stresses
- blasting effect

The adjustments are introduced in recognition of the type of excavation proposed and time dependent behavior of the rock mass. The parameters that can be expected to influence the stability of a rock mass include:

- the length and initial distribution of the geotechnical zones
- Rock Quality Designation (RQD)
- rock mass defects; faults, shear zones, intense fracturing and zones of deformable minerals
- intact Rock Strength (IRS)
- degree and nature of rock weathering
- relative orientation of structures
- spacing between the set of structures (Js)
- total number/density/frequency of structures (FF/m)
- condition of structures; roughness, wall alteration and infilling (Jc)
- groundwater condition

The parameters were assessed based on the MRMR system and allocated ratings up to the indicated below and used to determine the in situ RMR.

Intact rock strength rating (IRS).........................20

Spacing of discontinuities 25

RQD rating 15

Joint condition 40

These rating must sum up to 100. The various RMRs were calculated from the averages of these parameters. The adjusted RMR is the Mining Rock Mass Rating, (MRMR). The MRMR's were calculated based on the following percentage ratings:

- Weathering 95
- Joint Orientation 80
- Induced Stresses 100
- Blasting 94

Summaries of the MRMR's and the Indicative overall slope angles (IOSA) for each pit sector are tabulated in Table 5.1 to Table 5.4.

Table 5.1 RMR, MRMR and IOSA values for the Geotechnical Domains

Domain	RMR	MRMR	IOSA
OXIDE			
North Wall	42.73	31.43	45.12
East Wall	42.50	31.30	45.20
South Wall	43.82	32.70	46.10
TRANSITION			
North Wall	57.05	41.03	50.51
East Wall	56.89	40.91	50.45
South Wall	57.32	41.22	51.11
FRESH ROCK			
North Wall	64.05	50.85	55.51
East Wall	63.23	50.07	55.03
South Wall	67.72	53.58	56.79

The empirical values above were determined from the Haines and Terbrugge chart (1991) using Equation 5.1 below.

$$IOSA = (0.5 * MRMR) + 30 \tag{5.1}$$

Table 5.2 Recommended IOSA values from adjusted RMR (After Haines and Terbrugge, 1991)

MRMR	100	90	80	70	60	50	40	30	20	10	0
IOSA	$>75^0$	75^0	70^0	65^0	60^0	55^0	50^0	45^0	40^0	35^0	$<35^0$

MRMR were also calculated for the various rock types and presented in Table 5.3;

Table 5.3 RMR, MRMR and IOSA for various Rock Types

East Wall			
Lithology	RMR	MRMR	IOSA (^{0})
Sandstone	63.13	49.31	54.66
Lithic Sandstone	52.19	40.03	50.02
Conglomerate	74.05	58.41	59.21
Intrusive	73.37	57.69	58.85
North Wall			
Lithology	RMR	MRMR	IOSA (^{0})
Sandstone	58.86	46.06	53.03
Intrusive	66.02	57.69	58.85
South Wall			
Lithology	RMR	MRMR	IOSA (^{0})
Sandstone	63.13	49.31	54.66
Lithic Sandstone	52.19	40.03	50.02
Conglomerate	74.12	58.41	59.21
Intrusive	72.02	55.34	57.67

Empirical slope design geometry (Table 5.4) was evaluated from the statistical averages. This provides the starting point for limit equilibrium analysis.

Table 5.4 Slope Parameters Generated from Empirical Studies

Pit Sector	Geotechnical Zone	Bench Height (M)	Bench Width (M)	Bench Face Angle (^{0})
FRESH ROCK				
North Wall	Un weathered	18	8	75
East Wall	Un weathered	18	8	75
South Wall	Un weathered	18	8	78
TRANSITION				
North Wall	moderately weathered	18	8	70
East Wall	moderately weathered	18	8	70
South Wall	moderately weathered	18	8	70

5.3 Structural Analysis

The structured evaluation was carried out in two parts

- Major structural evaluation
- Minor structural evaluation

The major structural evaluation was carried out to identify large scale instability, and the minor structural analysis was to determine the optimum bench and spill berm geometries.

5.3.1 Major Structural Evaluation

Structural mapping was carried out in the area to identify structures that are inclined sub-vertically and generally found to be unfavorable to stability. These can potentially cause major planar instability if frictionally unstable.

The orientation and nature of the major structures has a definite influence on the determination of the limiting bench stack height (Gibson *et. al.*, 2017). Of concern was the potential for large wedge influence, formed from the combination of major known faults and minor faulting and shearing, which can influence the stability of inter-ramp slopes where stacks of benches are at risk.

The influence of the major structures on the stability of pit walls was assessed for each design domain. These were assessed and included in the slope design architecture. Structures mapped from the boreholes were faults and shear zones.

The limiting bench stack height is a function of the frequency and attitude of the major structures relative to the pit shell. For any bench stack, it is recommended that only one major structure has the potential to influence the stability of that stack. A limit to the stack height must be imposed where it is assessed that more than one major structure, or in combination with minor or secondary structures, can adversely influence the bench stack stability (Gibson *et. al.*, 2017).

KNOWLEDGE, TRUTH AND EXCELLENCE

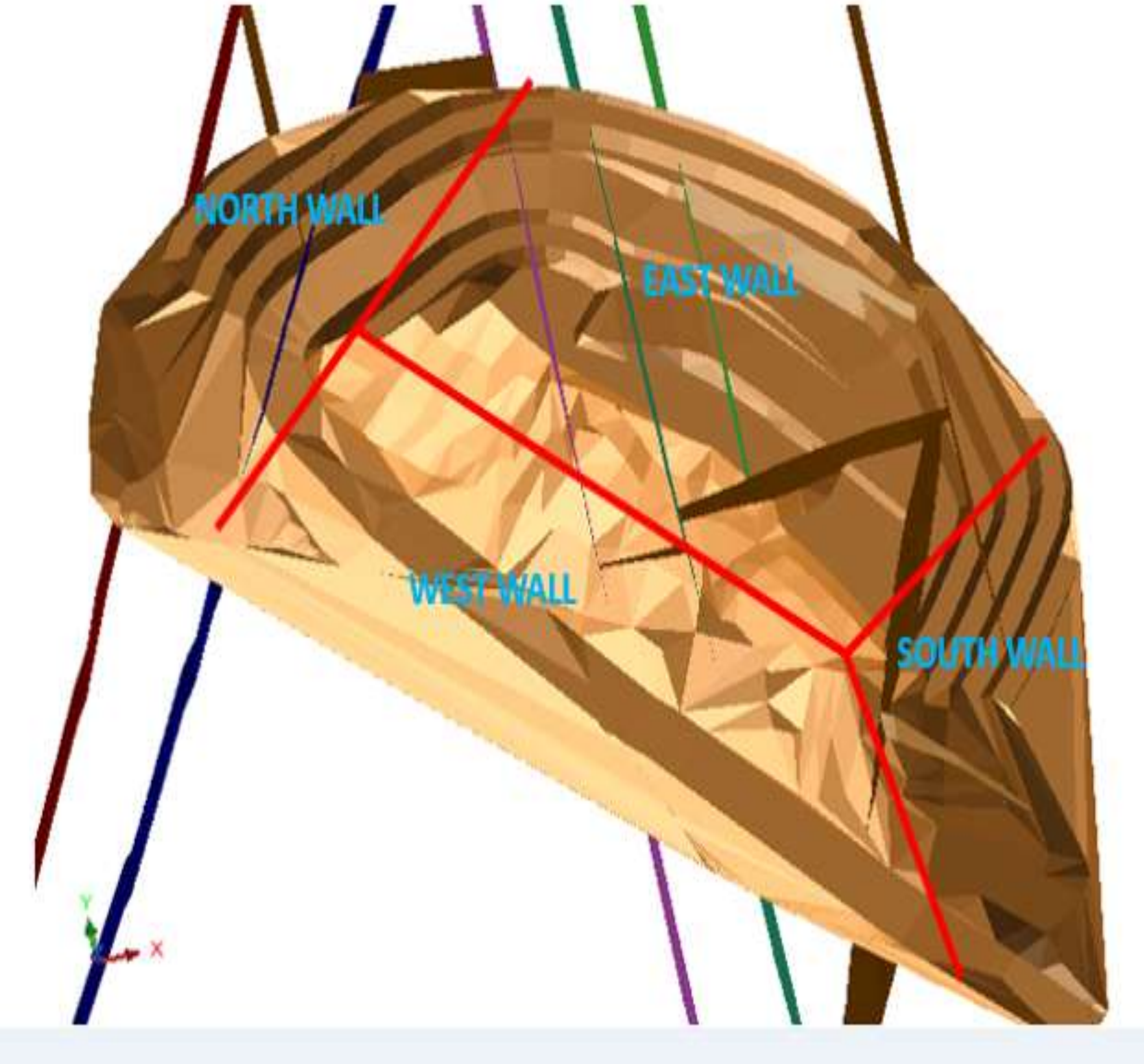

Figure 5.1 Structural Model of the Kobeda Pit

5.3.2 Minor Structural Evaluation

Dominant discontinuity sets were analysed from the oriented drill holes for each major rock type. The boreholes for investigating geotechnical conditions within the project area were drilled across an area with a north – south extent of approximately 500 meters. The Mine northings range from 7400-7900 meters. The area was divided into four domains to determine joint set variations across the pit (Table 5.6).

Table 5.5 A Summary of Drill Holes used in the Geotechnical Analysis

HOLED ID	Y	X	Z	DEPTH	DIP	AZIMUTH
GDKD002	7395.185	8127.482	108.02	74.1	-51.16	357.02
GDKD003	7244.061	8139.389	94.54	69.02	-50.4	357.18
GDKD004	7207.669	8218.438	84.272	79.7	-50.86	215.92
GDKD005	7398.761	8055.667	78.273	79.8	-51.08	177.76
GDKD006	7250.536	8140.427	94.88	122.15	-54.28	314.07
GDKD019	7602.297	7884.635	100.801	100.98	-54.72	180.2
GDKD020	7515.763	8017.63	61.88	79.83	-53.94	180.3
GDKD021	7681.11	7884.661	87.336	118.6	-54.44	181.16
GDKD069	7559.2	7933.596	80.157	102	-65.2	340.2333
GDKD070	7436.501	8092.992	99.658	83.34	-55.05	40.475
GDKD072	7552.269	7912.444	81.141	80.13	-64.4	222.925
GDKD075	7492.373	8008.082	62.241	80.28	-64.86	219.32
GDKD076	7520.533	8031.831	62.12	85.7	-63.02	43.2
GDKD077	7423.11	8078.746	96.538	100	-63.85	218.725

Data from the logging exercise was used for structural analysis to evaluate the optimum Bench Height and Spill Berm geometries for each design sector. The exercise was carried out using the Dips Software to analyse the spatial distribution of the joint set population. The stereonet analysis provided recommendations for the optimum Bench Face Angle (BFA) and optimum Spill Berm Width (SBW).

The geological discontinuities obtained from the data were plotted on a lower hemisphere equal angle stereonet.

A planar stereographic plot with great circle representing the slope angles relative to the orientation of the fractures was conducted.

Table 5.6 Slope Angles for the Pit Sectors

Pit Section	Batter Angle (^{0})		
	Oxide	Transition Rock	Fresh Rock
North	55	70	75
East	55	70	75
South	55	70	78

5.4 Laboratory Test Results

The results of the soil classification, Atterberg Limits, direct shear test, uniaxial compressive strength test are summarized in the tables below. The soil of the catchment can best be described as silty- sand with a Plasticity Index of 14.26 (Table 5.7a and 5.7b).

Table 5.7a Summary of laboratory Test Results

Lithologies – Shear Strength (Mpa)			
Sandstone	Lithic Sandstone	Intrusive	Dolerite
88.40	20.00	92.40	-
Geotechnical Zones – UCS (Mpa)			
CW - HW	MW	SW	UW
1.1	16.24	61.45	93.95
Particle Size Distribution (%)			
Gravel	Sand	Silt	Clay
9.38	47.27	37.26	6.10
Atterberg Limits			
LL	PL	PI	
38.44	24.18	14.26	

LI – Liquid Limit, PI – Plasticity Index, PL – Plastic Limit, UW – fresh rock, CW – completely weathered, MW – slightly weathered, SW – moderately weathered.

Table 5.7b Summary of Direct Shear Strength Results

Geotechnical Zone	Shear Strength	
	C (KN/m^2)	ϕ (^{0})
CW - HW	20.65	35.30
MW	0.00	41.50
SW	0.00	38.82
UW	0.00	41.91

5.5 Hydrogeological Model

Ten Casagrande standpipe piezometers were installed in the boreholes to record piezometric pressures within the monitored horizons. The provided groundwater profile data was input into slope stability analysis and was also used in generating the phreatic water surface. The groundwater level was estimated to be some 56 meters from the surface (Figure 5.2).

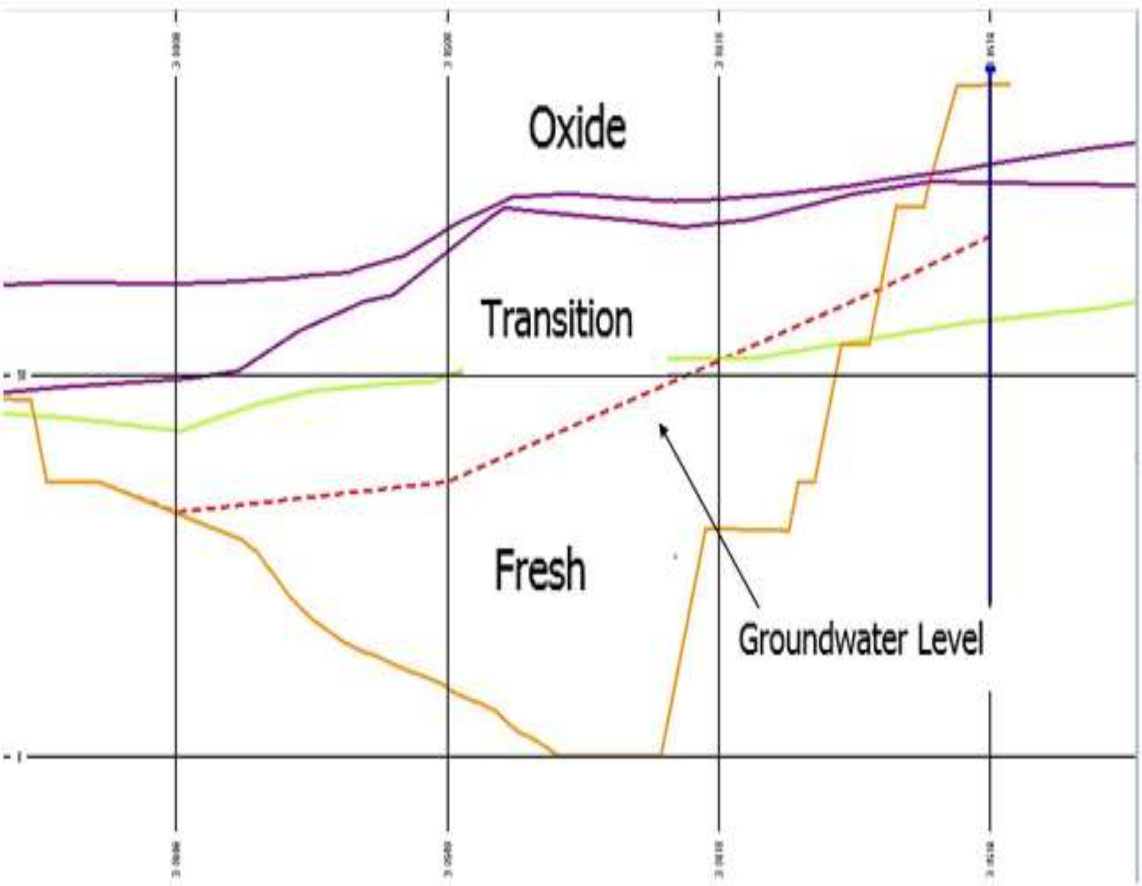

Figure 5.2 Hydrogeological Model showing the Phreatic Water Surface

CHAPTER 6

SLOPE STABILITY ANALYSIS

6.1 Rock Mass Stability Analysis

The two-dimensional limit equilibrium slope stability analysis was carried out on the pit slope sectors using the "SLIDE 6.0 computer software". The "Spencer and Bishop Method of slices" was used in the analysis for the various slope sectors. The SLIDE analysis was conducted to determine the Factor of Safety (FoS) for each pit sector. The minimum factor of safety for which failure occurred was obtained depending on the stabilising forces against the destabilising forces.

For increased overall accuracy, the analysis was done for both circular and non-circular modes of failure. The pore water pressure was also factored into the analysis.

The stability of each model was analysed under dry and saturated ground water conditions. The minimum acceptable factor of safety was 1.05 for completely weathered material and 1.20 for fresh rock throughout the analysis in keeping with Gold Fields Ghana acceptance criteria.

Table 6.1 Summary of input Parameters for Slide Analysis

Material type	Bulk Unit Weight (KN/m^3)	Cohesion (KN/m^2)	Friction Angle (Degrees)	Strength type
Oxide	18.00	20.00	25.30	Mohr-Coulomb
Transition	22.00	14.00	29.40	Mohr-Coulomb
Fresh Rock	27.00	0.07	35.50	Hoek-Brown

6.2 Slide Analysis

The proposed pit area was divided into four sectors in the optimization of the slope design. The sectors are; North, East, South, and West walls.

The ore body was emplaced on the west wall at an angle of 23^0. This was less than the angle of repose (35^0) of the material. Therefore, there was no need for any slope design for the west wall.

Slope design models were formulated from each sector and tested using limit equilibrium analysis. Each geotechnical zone was modeled with the parameters generated from the empirical studies. Each model was defined by a specific cross section with material boundaries separating zones within the model which have different material properties.

6.2.1 Analysis for North Wall

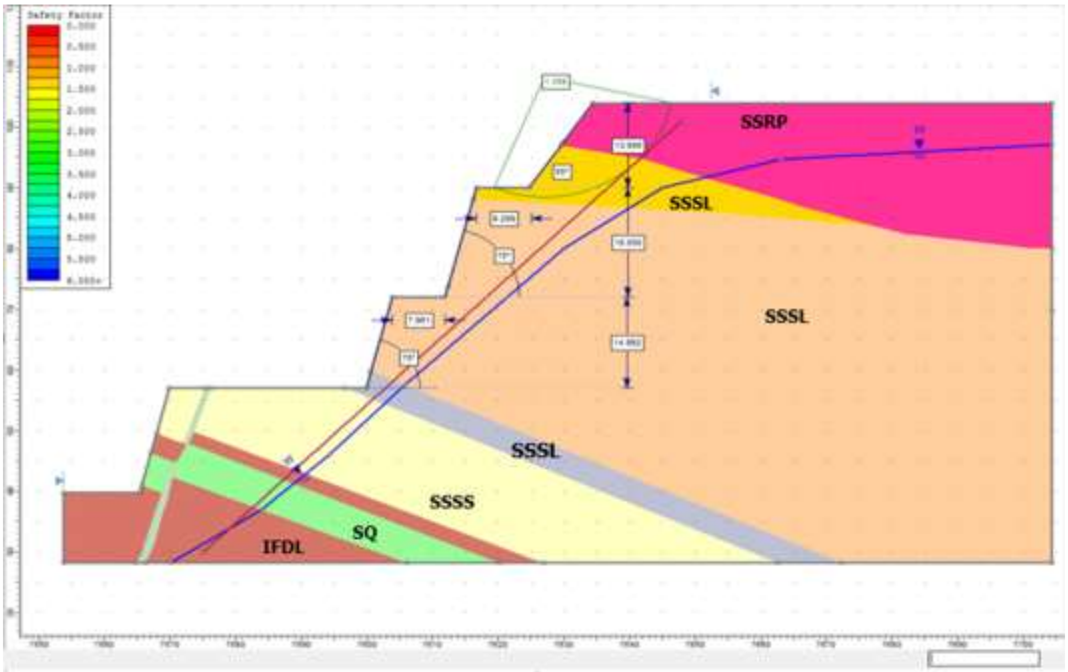

Figure 6.1a Stability Analysis for North Wall under Dry Conditions

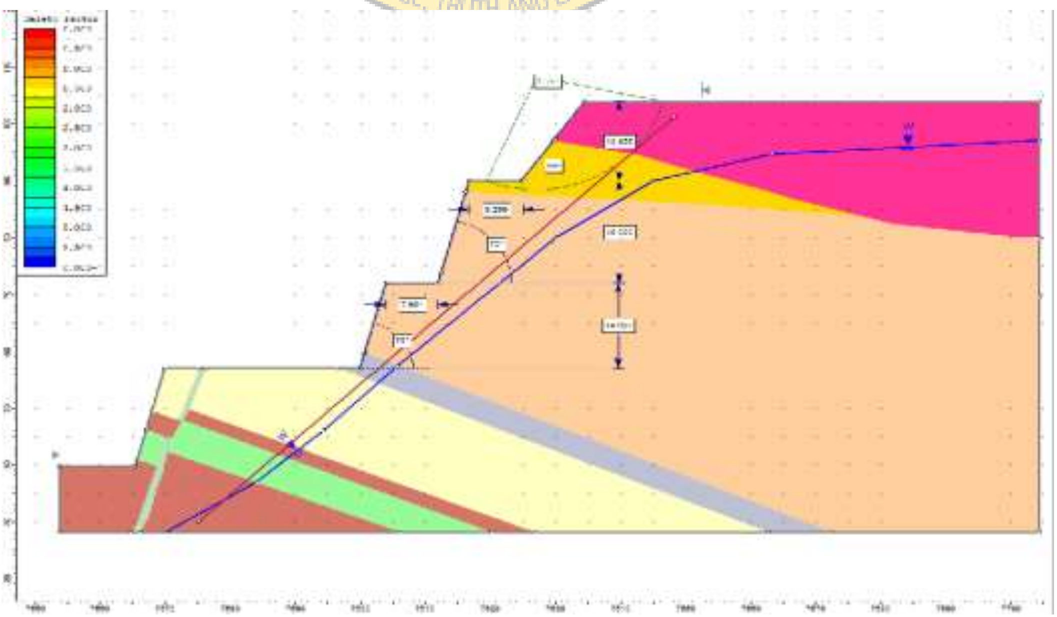

Figure 6.1b Stability Analysis for North Wall under Partially Saturated Conditions

In analyzing the sectors, a partially saturated condition of the slope was considered. Circular mode of failure was analyzed using the grid search method. This indicated a factor of safety of 1.35 – 1.59 for an overall slope failure (Figures 6.2a and 6.2b).

6.2.2 Analysis for East Wall

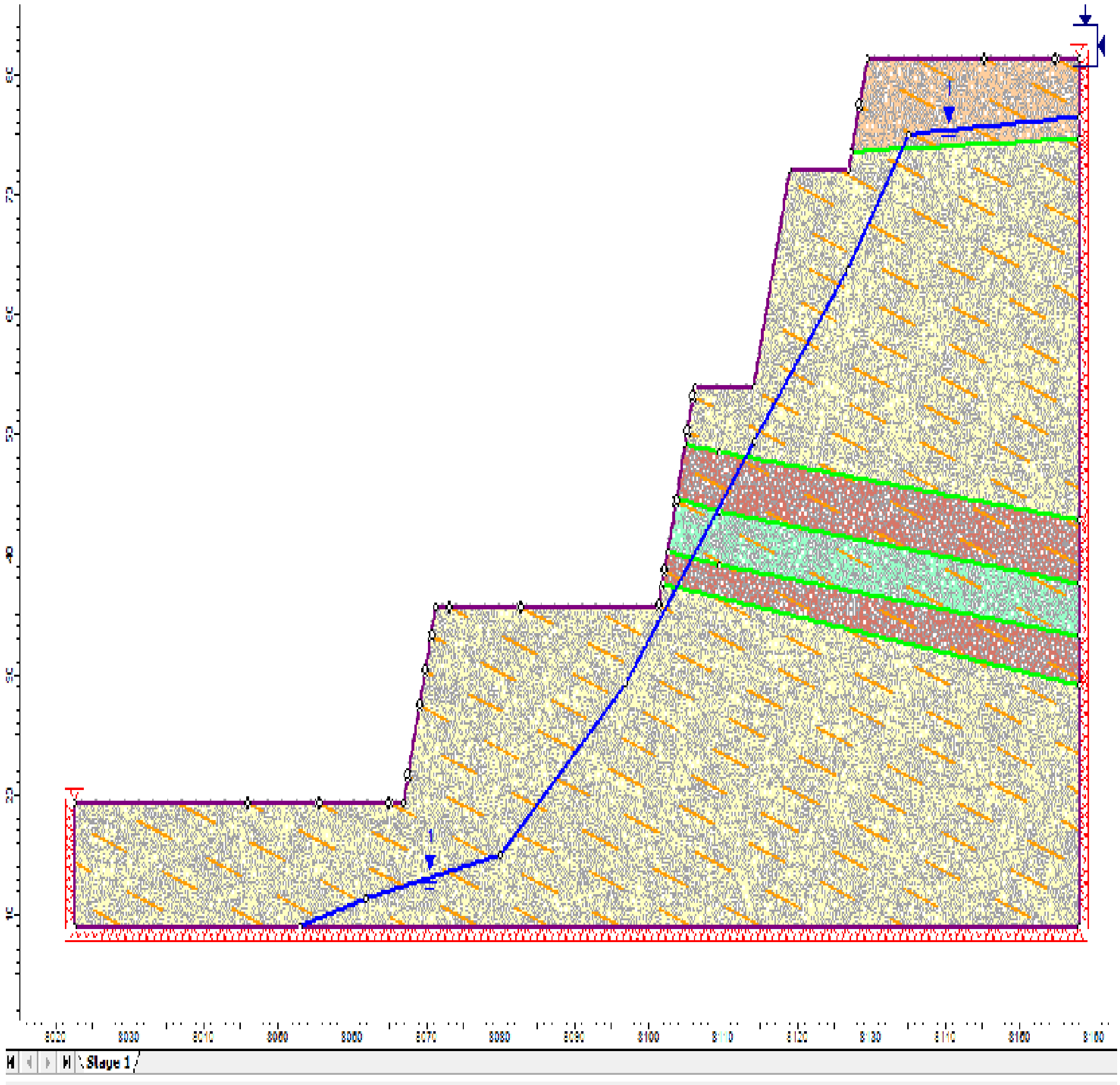

Figure 6.2a Stability Analysis for East Wall under Dry Conditions

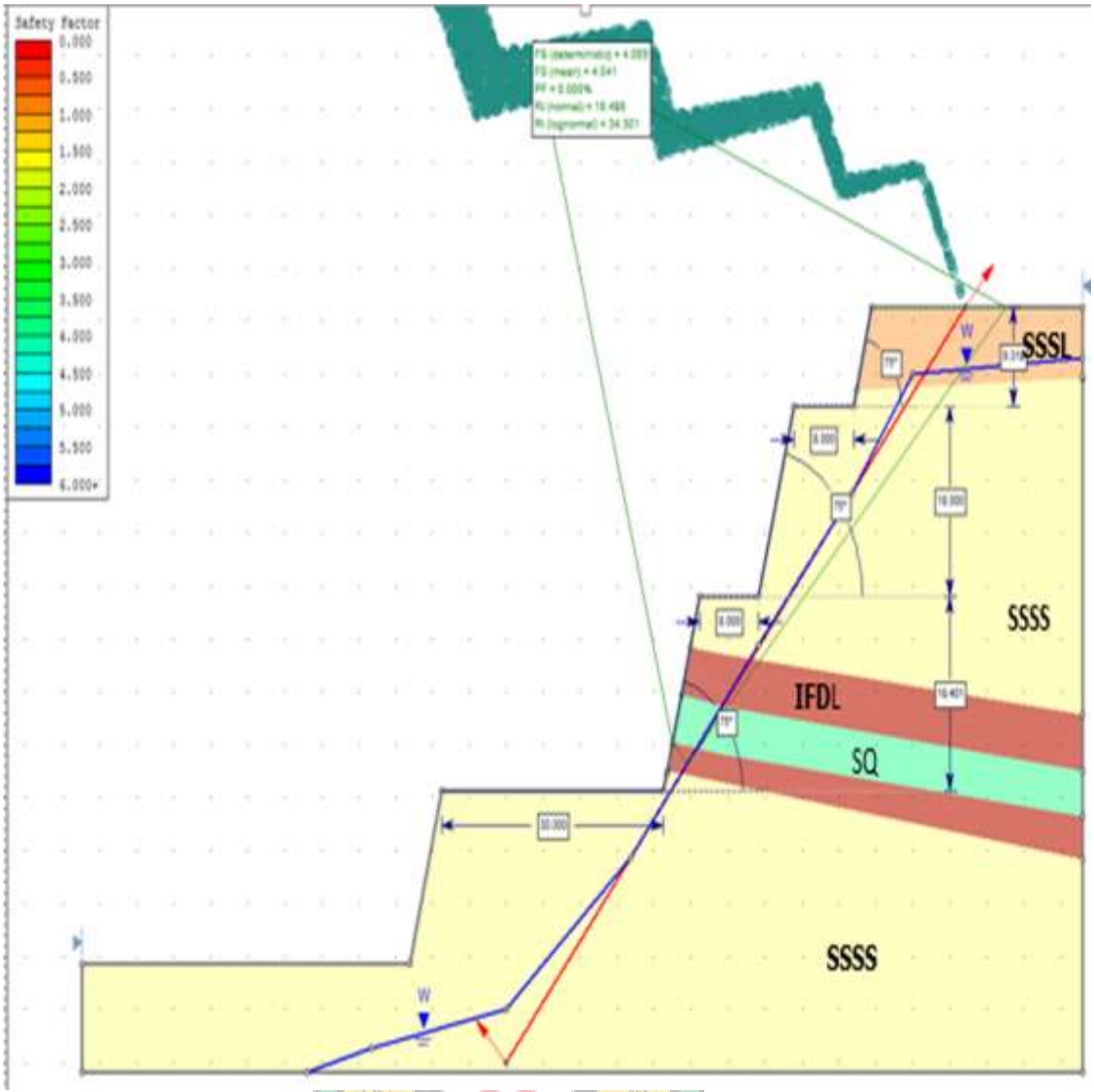

Figure 6.2b Stability Analysis for East Wall under Partially Saturated Conditions

In the analysis, a partially saturated slope considered a path search from the oxide to fresh rock domain. This indicated a factor of safety of 1.61 – 2.00 for overall slope search.

6.2.3 Analysis for South Wall

This analysis considered a partially saturated condition using the grid search method. This indicated a factor of safety of between 1.55 – 1.60 for circular analysis and 1.60 – 1.68 for non-circular analysis of the south wall (Figures 6.3a and 6.3b).

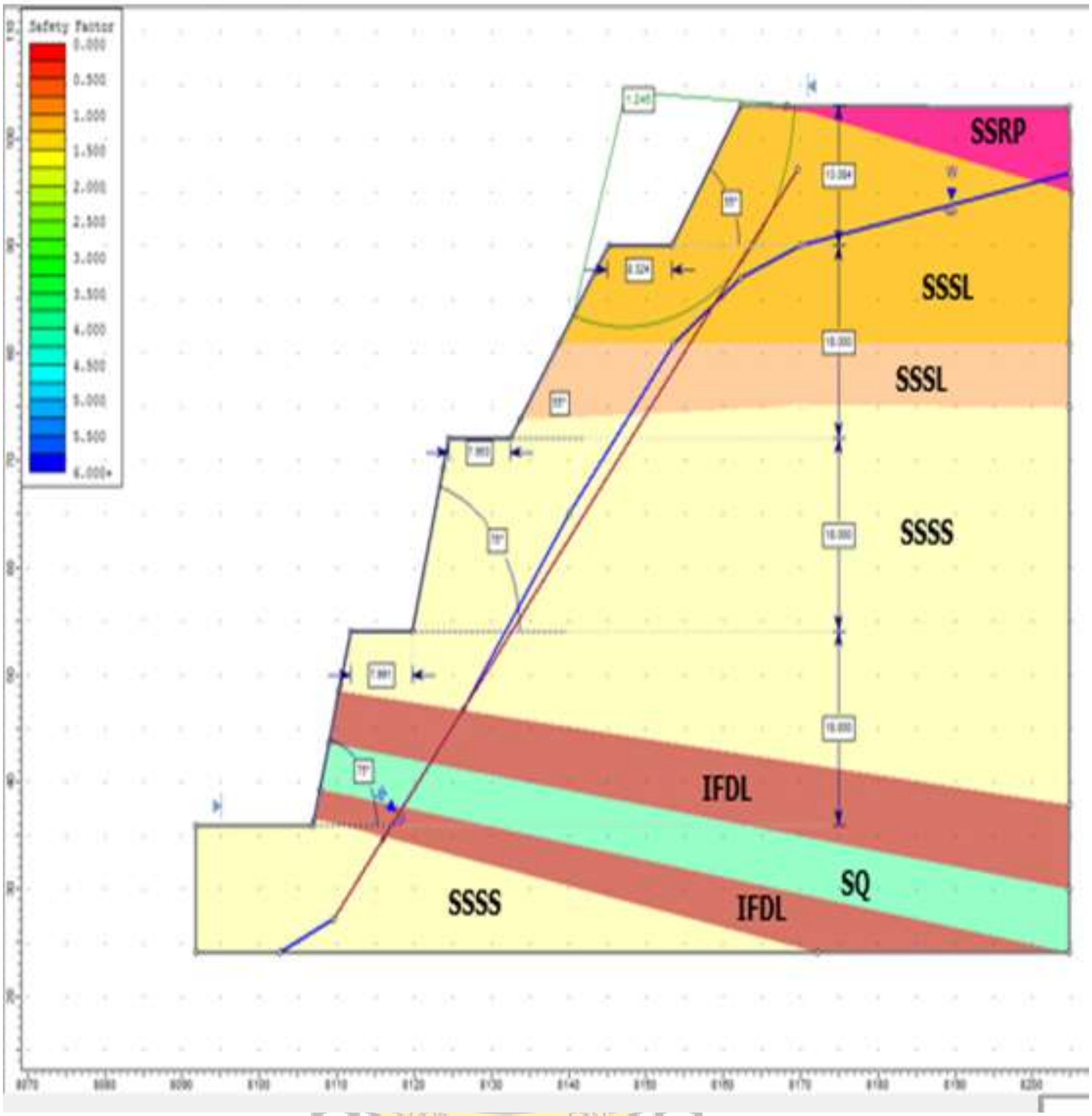

Figure 6.3a Stability Analysis for South Wall under Dry Conditions

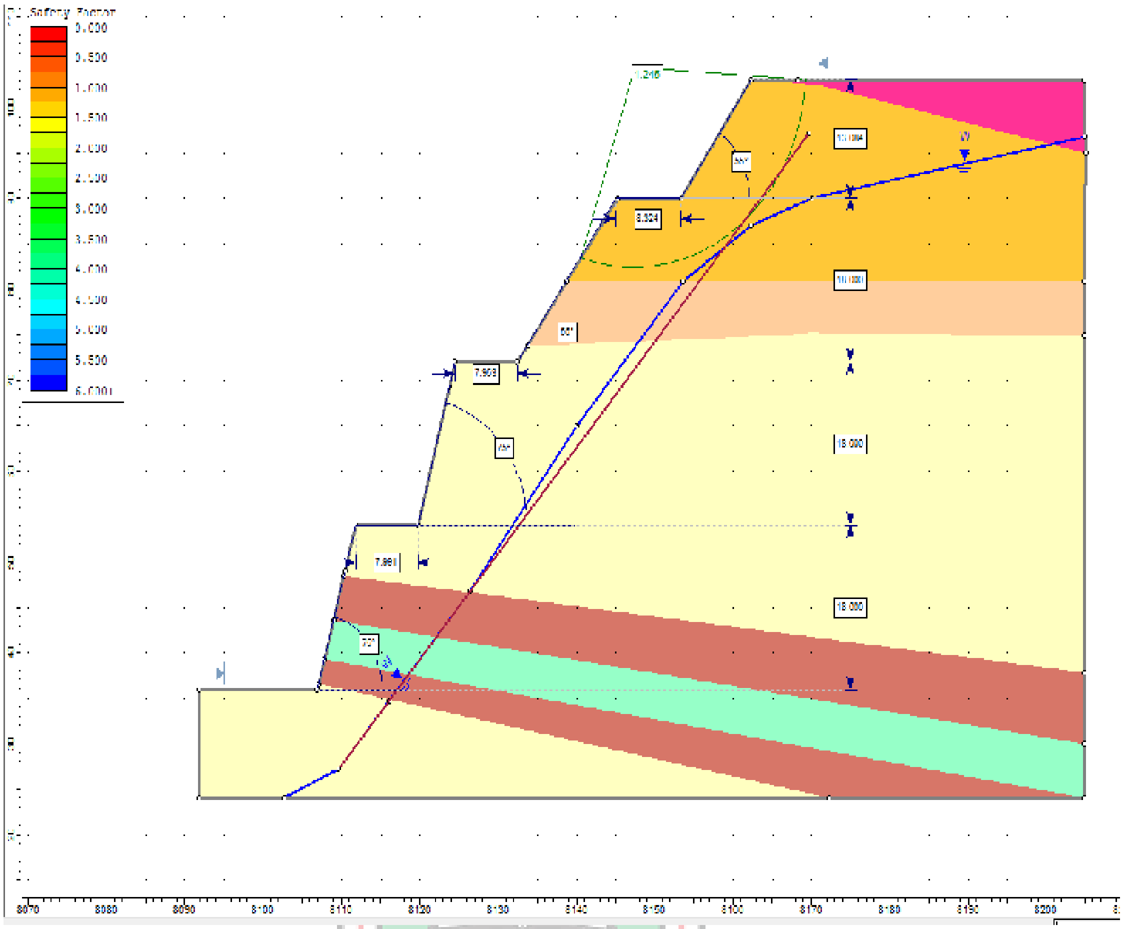

Figure 6.3b Stability Analysis for South Wall under Partially Saturated Conditions

Table 6.2 Summary of Factors of Safety for the Pit sectors

Sector	Domain	Height	Condition	Mode of Failure	OSA(^{0})	FoS
North	A	90	Dry	Circular	55	1.59
	A’’		Partially Saturated	Non–Circular	55	1.35
East	A	79	Dry	Circular	55	1.61
	A’’		Partially Saturated	Non–Circular	55	2.00
South	A	106	Dry	Circular	56	1.55
	A’’		Partially Saturated	Non–Circular	56	1.68

From Table 6.2, it could be observed that the factors of safety achieved for both circular and non-circular analysis of failure was greater than the minimum acceptable FoS of 1.05 for partially saturated circular failure and 1.20 for non-circular failure under partially saturated conditions in all sectors of the proposed pit.

At Gold Fields Ghana Limited, Tarkwa Mine, benches are excavated in multiples of three (3) meters. This is based on equipment availability and the method of ore selectivity. As a result, production drill and blast holes, as well as wall control blasts are done to either six, nine or twelve meters in depth.

Hence, aside the rock mass classification systems applied in determining the requisite parameters for rock slope stability analysis, attention was also given to the equipment availability and mining method, and drill and blast capacity.

From the stability analysis, the recommended pit slope geometry is as shown in Table 6.3.

Table 6.3 Recommended Bench Configurations

Pit Sector	Slope Angle (^{0})	Bench Height (m)	Berm width (m)
Oxide	55	12	6
Transition	70	18	8
Fresh Rock	75	18	8

6.3 Kinematic Analysis

Kinematic analysis was carried out to evaluate the various potential modes of failures. The stability assessment was performed for the following failure modes using the mean discontinuity orientations and the proposed bench face angles:

- Toppling
- Wedge and
- Planar

6.3.1 Toppling Failure Mode

Potential toppling instability was carried out on the slope sectors. Great circles representing pit wall angles and a slip limit were added to the polar plots. The slip limit was added upon the assumption that discontinuity planes cannot topple if they cannot slide against each.

The angle of dip of slip limit was obtained by subtracting the mean discontinuity friction angle from the pit wall angle. Variability cones representing joint set populations and one and two standard deviation of orientation uncertainty were added around the discontinuity mean sets orientation.

Finally, a frictional cone was introduced to determine the shearing resistance. The crescent shaped zone formed between the slip limit and the frictional cone is the zone of toppling influence. All poles falling within this zone are potentially feasible to toppling. From the analysis, there is 10% toppling potential to the south of the pit (Figure 6.4).

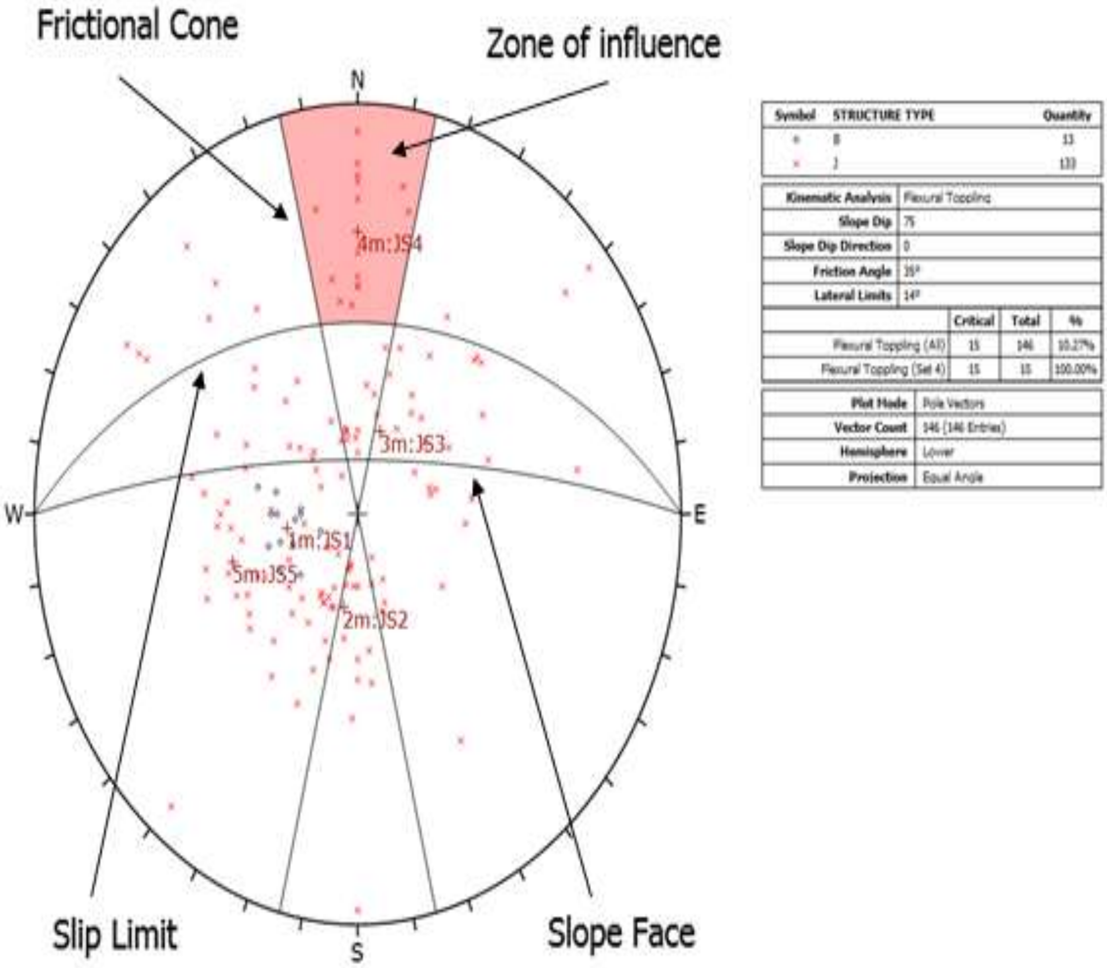

Figure 6.4 Toppling Potential Analysis for the South Wall

6.3.2 Wedge Failure Analysis

The inclination of the main structures was assessed for each sector, taking into consideration the probable orientation of the pit wall. The planes representing the mean orientation of joint sets were plotted on the stereonet. Major planes plot for wedge analysis was considered. A planes friction angle was determined by subtracting the discontinuity friction angle from the equator of the stereonet.

Wedge sliding would occur if the mean joint set orientation intersections fall within the zone defined by the friction cone and the pit slope. The zone outside the plane representing the pit wall and enclosed by the friction cone represents the zone of wedge sliding.

From the analysis, the east wall is 30^0 susceptible to wedge failure. The volume of the wedge material produced in the event of a wedge failure is a function of the geometry of the individual wedges, the persistence of the wedge forming discontinuities, the height and width of the bench, and the bench face angle.

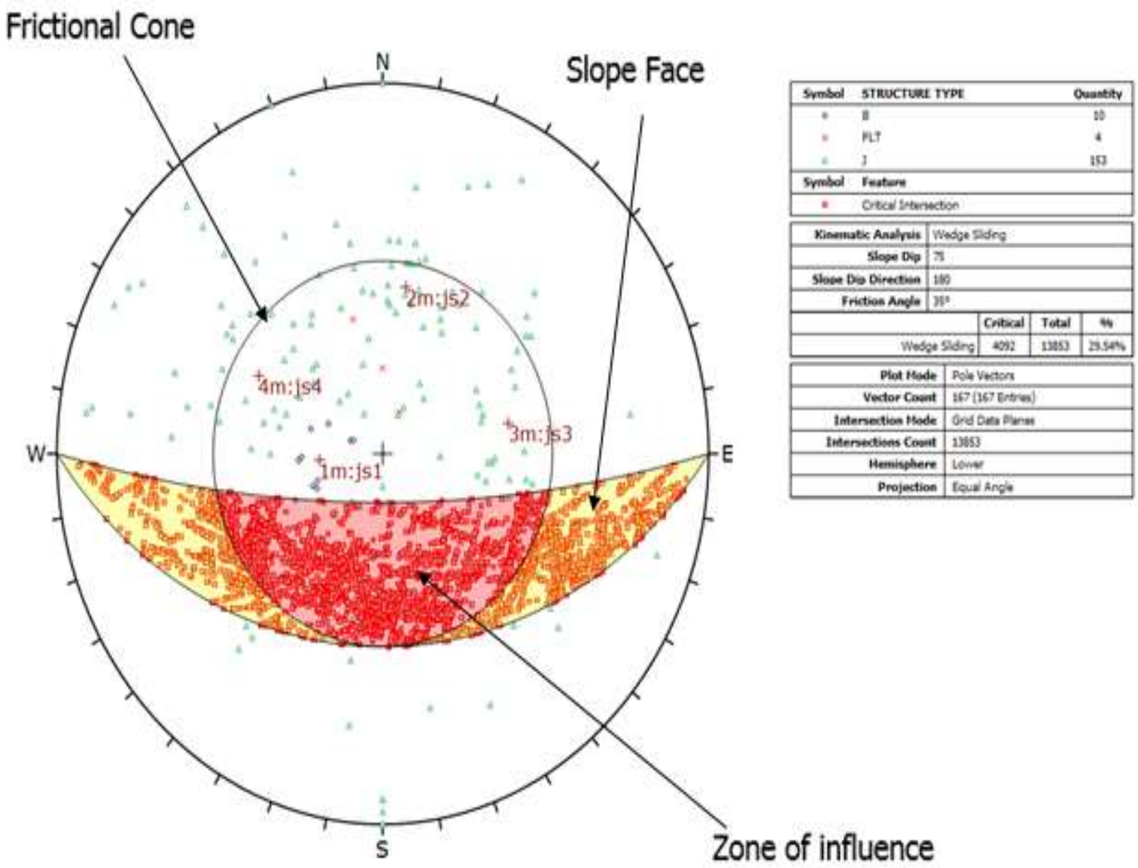

Figure 6.5 Wedges Sliding Potential Analysis for the East Wall

6.3.3 Planar Sliding

Planar sliding analysis was also carried out to determine the potential for planar sliding. This analysis uses variability cones to determine the joint set population, frictional cone and daylight envelope to test for combined frictional and kinematic possibilities. The crescent shape formed between the daylight envelope and the frictional cone indicates the region of planar sliding.

A bench face angle of 70^0 was applied. From the analysis, 40% of the theoretical population of poles fell within the region of planar influence. These have the tendency of sliding if kinematically feasible and frictionally unstable (Table 6.4).

Table 6.4 Pit Walls and their potential Mode of Failure

Pit Sector	Failure Mode (%)		
	Toppling	Planar	Wedge
North Wall	4	40	15
East Wall	7	18	30
South Wall	10	15	10

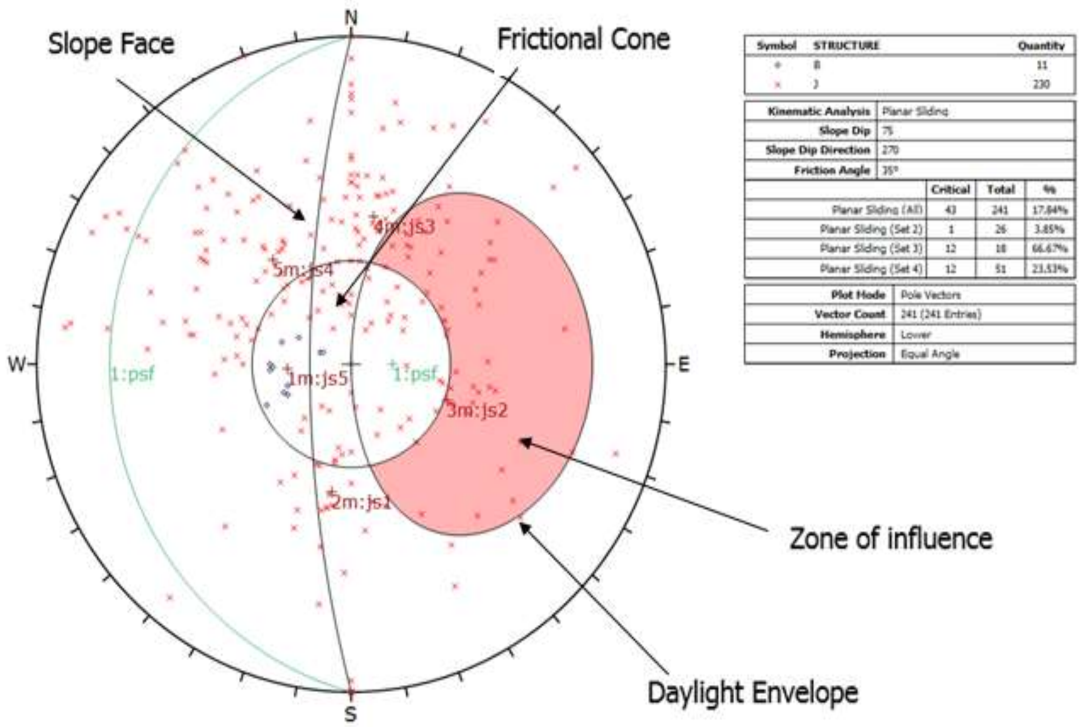

Figure 6.6 Planar Sliding Potential Analyses for the North Wall

6.4 Spill Berm Width Determination

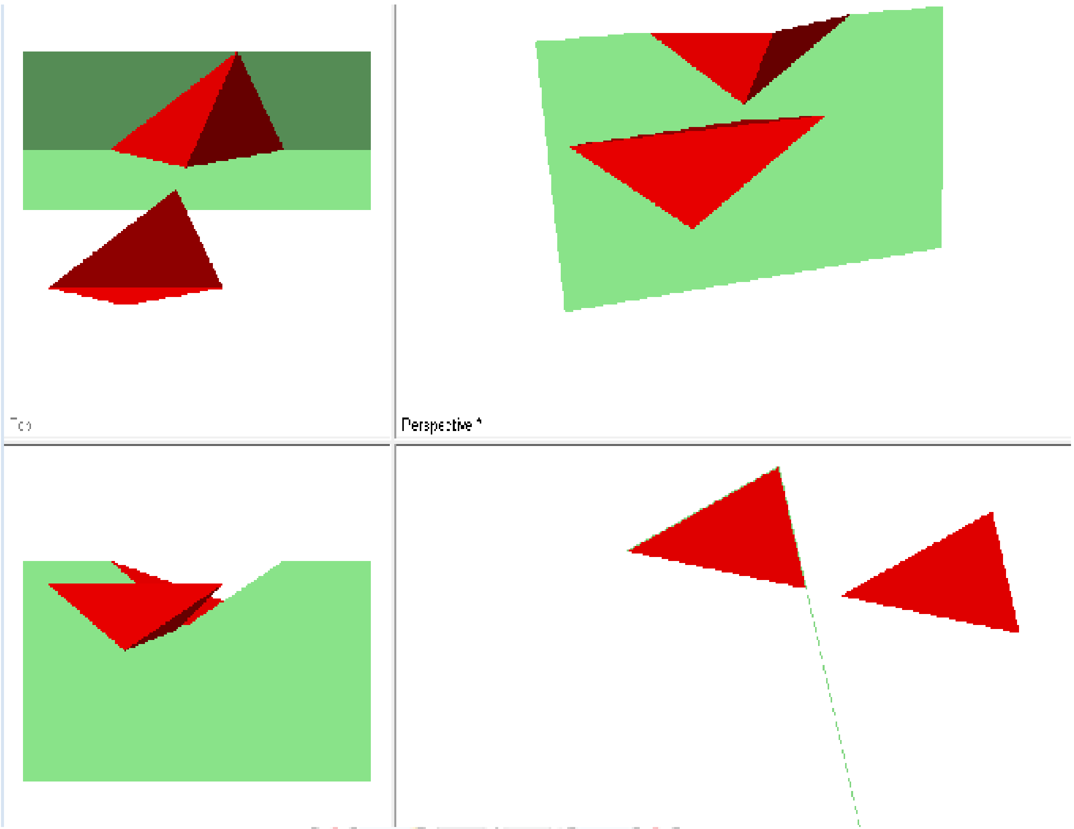

Figure 6.7 Determination of Volume of Wedges using "SWEDGE"

The width of the berm required to contain any block of failed wedge from the wall was determined by means of "SWEDGE". The width of the catch berm is determined from the volume of failed wedge material using the relationship $SBW(m) = \sqrt[3]{Vol * 1.5}$ (Table 6.5 and Figure 6.6).

Table 6.5 Calculated SBW from Volumes of Wedges

Volume (m^3)	136.85	157.42	24.92
SBW (m)	5.89	6.18	3.34

From the table above, the largest value of the SBW was 6.18 meters. Hence the smallest berm should be larger than 6.18 meters to be effective. Taking into consideration the type of equipment available, the catch berm width was taken to be 8 meters.

From open pit berm design recommendations by Haines et al. (2002), berm width are designed such that at least 90% of the failed rock material are retained within at least two berms. Simulation carried out to determine the volume of failed wedge material returned a maximum estimated value of 157.42 m^3 (Table 6.5). This could conveniently be contained on one berm. The choice of a support system for an open pit slope depends on the volume of failed rock supposed to be retained on a berm. The above value suggests either shotcreting or wire meshing as the most effective and cost efficient support system for the proposed pit.

6.5 Probability of Failure

Probability of failure analysis was conducted using a numeric tool referred to as "Phase Two" software. Results generated were very close to zero percent. A check was conducted by comparing the "phase two" results with empirically generated data. An SRK consulting report by Haines et al., (2002) gave a table (Table 6.6) for determining the Probability of failure once the Factor of Safety has been determined by limit equilibrium analysis for a given Pit Slope architecture.

Table 6.6 FoS and Pf for Pit Slope Architecture

Slope Profile Element	Factor of Safety (FoS)	Probability of Failure (Pf)
Individual Bench	1.05 – 1.10	< 35%
Bench Stack	1.20 – 1.25	10 %– 15%
Overall Slope	1.35 – 1.50	<5%

From the limit equilibrium analysis, the minimum factor of safety for overall slope was 1.59 for the north wall. The corresponding Pf is less than 5%. It can therefore be stated, generally, that the Probability of failure for all sectors of the proposed pit has less than five percent Probability of failure.

From the analysis and discussions, the parameters generated are presented in Table 6.7.

Figure 6.7 Pit Wall Architecture for the Geotechnical Domains

Domain	Parameter	North	East	South
Oxide	Bench Face Angle	55	55	55
	Bench Width	6	6	6
	Bench Height	12	12	12
	Overall Slope Angle	45.0	45.2	46.1
Transition	Bench Face Angle	70	70	70
	Bench Width	8	8	8
	Bench Height	18	18	18
	Overall Slope Angle	51.0	50.4	51.0
Fresh	Bench Face Angle	75	75	75
	Bench Width	8	8	8
	Bench Height	18	18	18
	Overall Slope Angle	54.5	54.5	56.7

KNOWLEDGE, TRUTH AND EXCELLENCE

CHAPTER 7

CONCLUSIONS AND RECOMMENDATIONS

7.1 Conclusions

The scope of this thesis was to design optimum slope parameters for the mine design of the proposed Kobeda pit at Tarkwa Gold Mine of Gold Fields Ghana Limited. From geotechnical logging of rock cores, the rock mass conditions were assessed with classification systems by Bieniawski (1989), Laubscher (1990) and Romana (1985).

From the Bieniawski's approach, the Rock Mass Rating (RMR) for the various lithologies were; 49.31 for sandstone, 40.03 for lithic sandstone, 58.41 for conglomerate and 55.34 for mafic intrusive.

The RMR for Oxide material for the three geotechnical sectors were 42.73 for the North Wall, 42.50 for the East Wall and 43.82 for the South Wall. The Transition gave RMR values of 57.05, 56.89, and 57.32 for the north, east and west walls respectively. The Fresh Rock MRM values estimated for the North, East and South Walls were respectively 64.05, 63.23, and 67.72

The Laubscher's (1990) classification system was used in evaluating the Mining Rock Mass Rating (MRMR). The MRMR for the North, East and South Walls were 31.43, 31.30 and 32.70 respectively for Oxide material. Transition rock indicated MRMR values of 41.03,40.91 and 41.22 for the north, east, and south walls respectively. The MRMR values for the Fresh Rock in the North, East and South Walls were 50.85, 50.07, and 53.58 respectively.

The average values for the Indicative Overall Slope Angles (IOSA) corresponding to the MRMR for the Oxide, Transition and the Fresh Rock were 45.43^0, 50.69^0, and 55.78^0 respectively.

From the kinematic analysis conducted, the result indicated higher potential for both planar and wedge failure in the north and east walls. The potential for planar sliding is higher in the north wall than in the east. Also, the east wall was more susceptible to wedge failure than the north wall. The north and east walls have low potential to toppling instabilities. The south wall gave indications of planar, wedge as well as toppling modes of failure. The optimum slope parameters generated for the proposed Kobeda pit are shown in table 6.7

From the simulation carried out to determine the volume of failed wedge material using "SWEDGE", the maximum volume of failed rock was 157.42 m^3 (Table 6.5). This could conveniently be contained on one berm. This informs the choice of support systems for open pit slopes. The volume of failed material from the walls suggest either shotcreting or wire meshing as the most effective and cost efficient support systems for the proposed pit.

Slope monitoring to measure rock mass displacement was done by a combination of visual monitoring of tension cracks, wire extensometers, and the use of survey prisms.

7.2 Recommendations

Vigorous groundwater monitoring programmes should be designed and implemented to mitigate the effect of groundwater on slope instability.

Diversion ditches should be constructed to divert storm water from entering the pit.

Rock face mapping programs should also be implemented to determine the rock mass strength at depth and the presence of adverse structures that were possibly not captured during the geotechnical core logging. It also has the added advantage of optimizing the overall slope angle and decreasing the stripping ratio.

Blasting, excavation and surcharging will result in redistribution of stresses within the pit wall. Hence numerical analysis should be conducted to ascertain the amount of deformation within the pit wall.

As probability of failure approaches 10%, a more comprehensive slope monitoring will be required. As survey prims and berms become inaccessible, a real time slope monitoring system will have to be procured for use.

Horizontal drains will be required for pit wall depressurisation as mining progresses.

REFERENCES

Abramson, L, W., Lee, T. S., Sharma, S., and Boyce, G. M. (2002), *Slope Stability and Stabilization Methods*, Wiley and Sons. *An International Conference on Geotechnical & Geological Engineering*, 19-24 November, Melbourne, Australia, Vol. 2, 41 pp.

Anon., (1990). Swedge, Probabilistic Analysis of the Geometry and Stability of Surface Wedges; User's Guide. Rocscience Inc. 76 pp.

Anon (1991) Tarkwaian Palaeoplacer deposit of Ghana, Geology on Observer, Gold Fields Ghana Limited, pp. 17-26

Anon (1995), "FLAC: Fast Lagrangian Analysis of Continua, Version 3.3, Itasca Consulting Group Inc., Minneapolis, USA", www.itasca.com. Accessed: October15, 2017.

Anon. (1996), "UDEC: Universal Distinct Element Code, Version 3.0, Itasca Consulting Group Inc., Minneapolis, USA", www.itasca.com. Accessed: January 2016.

Anon., (1998). "Dips, Plotting, Analysis and Presentation of Structural Data Using Spherical Projection Techniques; User's Guide. Rocscience Inc. 56 pp.

Anon (2006a) "Environmental Impact Assessment for the Tarkwa Gold Mine", Metago Project T002-02 Report No. 1 Draft, Gold Fields Ghana Limited, Tarkwa, pp.12, 13, 22, 23.

Anon (2006b). Sedimentological and basal setting of Tarkwaian Banket Series on the Tarkwa Mine Concession (Unpubl.) Ref., Gold Fields Ghana Limited pp. 87-98.

Anon, (2008a), "Slope Stability Analysis for Open Pits", www. rocscience.com. Accessed: October 10, 2017.

Anon. (2008b), "Advanced Numerical Techniques in Rock Slope Stability Analysis Application and Limitations", www.eos.ubc.ca. Accessed: October 20, 2017.

Anon (2015), "Production Report", Gold Fields Ghana Limited, Tarkwa pp. 1-6

Barton, N. And Choubey, V. (1977), "The Shear Strength of Rock Joints in Theory and Practice" Rock Mechanics, 10, pp. 1-5.

Bieniawski, Z.T. (1976), "Rock Mass Classifications in Rock Engineering", *Proceedings Symposium on Exploration for Rock Engineering*, Rotterdam, pp. 97 106.

Bieniawski, Z.T. (1989), *Engineering Rock Mass Classifications*, John Wiley & Son, 251 pp.

Bishop, A.W. (1955), "The Use of the Slip Circle in the Stability of Slopes" *Geotechnique*, London, U.K., 5 pp. 7-17.

Broadbent, C.D. And Zavodni, Z.M. (1982), "Influence of Rock Structures on Stability - Stability in Surface Mining," Volume 3, *Society of Mining Engineers*, 60 pp.

BS 1377: (1990), *Methods of Test for Soils for Civil Engineering Purposes*, Thomson Learning Inc. 38 pp.

Bucek, R. (1995), "Toppling Failure in Rock Slopes" *Unpublished PhD Thesis Report*, University of Alberta, 120 pp.

Bukovansky, M., Rodriguez, M. and Cedrun, G. (1974), "Three Slides in Stratified and Jointed Rocks", *Proc, the 3rd Congress*, ISRM, Denver, Vol. II, Part B, pp. 854-859.

Call, R.D. (1982), "Monitoring Pit Slope Behaviour" *Proceedings 3rd International Conference on Stability in Surface Mining*, SMEAIME, New York, pp. 229-248.

Call, R.D., Savely, J.P. And Nicholas, D.E. (1990), "Estimations of Joint Set Characteristics from Surface Mapping Data" *Proceedings 17th US Symposium on Rock Mechanics*, Utah Engineering Experiment Station, University of Utah, Salt Lake City, pp. 2 B2-1 to 2 B2-9.

Chen, Z.Y. (1995), "Recent Developments in Slope Stability Analysis" Proc. ISRM 8th Int. Cong. Rock Mech., Tokyo, Herausgeber Ed., Vol.3, pp. 1041-1048.

Coats, DF. (1977), Pit Slope Manual, CANMET Report 77-5, CANMET Energy, Mines and Resources, Ottawa, Canada, 126 pp.

Dight, P.M. (1982), "Improvements to the Stability of Rock Walls in Open Pit Mines" PhD. Thesis, Duran, A. and Douglas, K.J. (2000), "Experience with Empirical Rock Slope Design" *ISRM International Symposium*, pp. 10 – 15.

Eberhardt, E., Kaiser P.K., and Stead, D. (2003), "Numerical Analysis of Initiation and Progressive Failure in Natural Rock Slopes – the 1991 Randa Rockslides" *International Journal of Rock Mechanics & Mining Sciences. Pp 13 – 21.*

Eberhardt, E., Willenberg, H., Loew, S and Stead, D, (2001), "Active Rockslides in Switzerland – Understanding Mechanisms and Processes". *International Conference on Landslides*, pp. 25-34.

Freeze, R.A, and Cherry, J.A. (1979), "Groundwater", Prentice Hall Inc., Englewood Cliffs, Vol. 7632, 604.

Freitas de, M.H. And Watters, R.J. (1973), "A Comparison of Four Slip Surface Search Routine" *Proc., the Sixth Int. Conference on Numerical Methods in Geomechanics,* Insbruck, Vol. III, pp. 2151-2156

Gibson, W.H., de Bruyn I.A., and Walker D.J.H., (2017),, "Considerations in the Optimization of Bench Face Angle and Berm Width Geometries for Open Pit Mines" *The South African Institute of Mining and Metallurgy International Symposium on Stability of Rock Slopes* , Australasia, SRK Consulting, 25 pp.

Goodman R.E. (1989), "Introduction to Rock Mechanics", John Wiley & Sons, New York, 561 pp.

Goodman, R.E. and Bray, J.W. (1976), "Toppling Failure of Rock Slopes" *Proceedings, Specialty Conferences on Rock Engineering for Foundation and Slope*s, ASCE, Boulder, Colorado, pp. 201 – 234.

Gordon, S. (2006), "Damang Cutback East Wall Failure Report'', Ref. No: 20070511, Damang Goldfield International, Perth (Unpublished).

Griffiths, R. J., Barning, K., Agezo, F. L., & Akosah, F. K. (2002). "Gold Deposits of Ghana", Ghana Minerals Commission.

Haines, A. And Terbrugge, P.J. (1991), "Preliminary Estimation of Rock Slope Stability Using Rock Mass Classification Systems" *7th International Conference on Rock Mechanics Proceedings, Vol. 2,* Aachen, Germany, pp. 887-892.

Haines, A., Engelsman, B., Theron, E., (2002). "Review of Slope Stability and Associated Mining Geotechnical Conditions at the Tarkwa Open Pit Operations, Ghana". SRK Consulting Report, pp. 7-22

Haswanto, W.A and Abd-Ghani, R. (2008), "Kinematic and Block Theory Applications to Rock Slope Stability Analysis at Fraser's Hill Pahang Malaysia", Department of Mining, Faculty of Mineral and Technology, Trisakti University, and Faculty of Science and Technology, National University of Malaysia.

Hirst, T. (1938), "The Geology of the Tarkwa Goldfields and Adjacent Country" Gold Coast Geological Survey Bulletin 10.

Hoek E and Brown, E.T. (1988), "The Hoek – Brown Failure Criterion – 1988 Update" *In Proceedings of the 5th Canadian Rock Mechanics Symposium*, Department Of Civil Engineering, University Of Toronto, Canada, pp. 31 –38,.

Hoek, E. (1981), "Geotechnical Design of Large Openings at Depth, Rapid Exc. & Tunn., Conf. AIME 1981.

Hoek, E. and Bray, J. W., (1974). "Rock Slope Engineering", The Institution of Mining and Metallurgy, London. Rev 3rd edition, pp. 341-351.

Hoek, E., and J.W. Bray. (1981). "Rock Slope Engineering". London: Institute of Mining and Metallurgy, London. Rev 4th Edition, 425 pp.

Hoek, E., Rippere, K. H., Stacey, P.F., (1988). "Large Scale Slope Designs– A Review of the State of the Art ". Golder's Associate, pp. 3-5.

Hudson J.A. (1993), "Rock Engineering System", Publ. Ellis Horwood Ltd., England, 185 pp.

Hudson J.A. and Harrison J.P. (1997), "Engineering Rock Mechanics" *An Introduction to the Principles*, UK, Pergamon, 506 pp.

Hvorslev, J. (1951), "Time Lag and Soil Permeability in Groundwater Observations", Corps of Engineers, US Army, Waterways Expt, Station, Bulletin 36, Vicksburg Pa, USA,

ISRM. (1985), "International Society of Rock Mechanics Commission on Testing Methods, Suggested Methods for Determining Point Load Strength, Int. J. Rock Mech. Min. Sci. and Geomech. Abstr. 22, 1985, pp. 51-60.

KNOWLEDGE, TRUTH AND EXCELLENCE

Janbu, N. (1973), “Application of Composite Slip Surface for Stability Analysis”, Proceed of the Conference on Slope Stability of Earth Slopes, Stockholm, pp. 42-58.

Jiao, J.J. and Nandy, S. (2001), “Confined Groundwater Zone and Slope Instability in Hillsides of Weathered Rock in Hong Kong”, Hong Kong Geologist, 2001, Chapter 7: pp. 31-37*Journal of Rock Mechanics and Mining Sciences, Vol 41 (1*), pp. 68-87.

Junner, N.R. (1942), “Geological of the Gold Coast and Western Togoland”, *Gold Coast Geological Survey Bulletin*, Vol. 11. 40 pp.

Karpeta W. P. (2001). “The Structural evolution of the Tarkwa basin in the Tarkwa Mine Area” Bastillion Limited report, pp. 7-11.

Karpeta W. P. (2002), A Review of the Geology, Mining and Exploration of the Tarkwa Mine Area, pp. 15, 40.

Kayesa, G. (2006), “Prediction of Slope Failure at Lethlhakane Mine with Geomos Slope Monitoring System”, *International Symposium on Stability of Rock Slopes in Open Pit Mining and Civil Engineering Situations*, SAIMM, Johannesburg, 2006, 12 pp.

Kesse, G. (1985). “The Mineral and Rock Resources of Ghana”, A. A. Balkema Publishers, Rotterdam, 610 pp.

Kliche, C. (1999), “Assessing and Monitoring Open Pit Highwalls”, Rock Slope Stability, Society for Mining, Metallurgy and Explorations, Inc. 215 pp.

Kovari, K. and Fritz, P. (1989), “Slope Stability with Plane, Wedge and PolygonalSliding Surfaces”, *Proc. Symp, Rock Mechanics Related to Dam Foundation*, Rio de Janeiro, Brazil, 22 pp.

Krishna P.A. (2006), “Slope Stability Evaluations by Limit Equilibrium and Finite Element Methods” *Unpublished PhD Thesis Report*, Norwegian University of Science and Technology, 2006, 66 pp.

Laubscher, D. H. (1990), “A Geomechanics Classification System for the Rating of Rock Mass in Mine Design”, *Journal Of The South African Institute Of Mining and Metallurgy*, Vol. 90, No 10, (South Africa), pp. 257-273.

KNOWLEDGE, TRUTH AND EXCELLENCE

Laubscher, D.H. (1977), “Geomechanics Classification of Jointed- Mine Application” Tran. Istn. Min. Metal., Vol. 86, pp. A 1-8.

Mandzic, E.H. (1999 And 2003), “Mine Water Risk in Open Pit Slope Stability” Mine Water Environ, Wollongong. 11(4), pp. 35-42,

Marston, R.J., Woolrich, P. and Kwesie, J. (1992), “Closely Associated Stockwork and Palaeplacer Gold Mineralization in the Early Proterozoic Tarkwaian System of Abosso, SW Ghana.” In: Peters, J.W., Kesse, G.O., Acquah, P.C. (Eds.), Regional Trends in African Geology. Proceedings of the 9th International Geological Conference, Accra, pp. 243-271.

McMahon, B.K. (1975), “Probability of Failure and Expected Volume of Failure in High Rock Slope”, Proceedings of the 2nd Australia- New Zealand Conference on Geomechanics, Brisbane, pp. 308-313.

Morton, K.L., Muresan, M.C. and Ramsden, F. (2008), Importance of Pore Pressure Monitoring in High Wall”, The Journal of South African Institute of Mining and Metallurgy, pp. 1-7.

Muller, L. (1963), “Application of Rock Mechanics in the Design of Rock Slope*” Proc. Intnl. Conf. On State of Stress in Earth’s Crust*, Santa Monica. Ed. W.R. Judd, Elservier Publishers, New York, pp. 575-598.

Nash, D. (1987), “A Comparative Review of Limit Equilibrium Methods of Slope Stability Analysis” *Geotechnical Engineering and Geomorphology*, Anderson M.G. & K.S. Richards (eds), John Wiley and Sons. pp. 11-75.

O’ Bryan, P. (2007), “Blasting for Stable Slope” *Unpublished Lecture Notes, Short Course,* Australia centre for Geomechanics, 2007, Perth, Australia, 131 pp.

Priest S.D. and Brown, E.T. (1983), “Probabilistic Stability Analysis of Variable Rock Slopes” Transaction Instn. Min. Metal. Vol. 92.

Robertson, A.M. (1988), “Estimating Weak Rock Strength”, Society of Mining Engineers, SME Annual Meeting, Phoenix, Arizona, Preprint No. 88-145, pp. 1-5.

Romana M. (1985), “New Adjustment Rating for Application of the Bieniawski Classification to Slopes”, *Proc. Int. Symp. Rock Mechanics Mining Civ. Works*. ISRM, Zacatecas, Mexico, pp 59-63.

Rowe, J. and Beale, G. (2007), "Relieving the Pressure; Core Concepts and Solutions in Open Pit Water Control", Water Management Consultants, A Schlumberger Company, Denver, CO. Article Published In June 2007 issue of Mining Magazine. Saayman, A. F., (2006). "Standard Practice Instructions", Geotech Africa Report, pp 14.

Savely, J.P. (1993), "A Rock Mass Strength Classification Mining Innovative Mine Design for The 21th Century", Kingston, August 23-26, pp. 25-34.

Selby M.J. (1980), "A Rock Mass Strength Classification for Geomorphic Purpose with Tests from Antarctica and New Zealand" Zeitschrift fur Geomorphologie. 23, pp. 31-51.

Sjőberg, J. (1999), "Analysis of Large Scale Rock Slopes" *Unpublished PhD Thesis Report,* Lulea University of Technology, Sweden, 788 pp.

Spencer, R. (1967). "A Method of Analysis of the Stability of Embankment Assuming Parallel Inter-Slice Forces," Geotechnique, London, U.K., 17, 11-26 pp.

Sullivan, T.D. (2006), "Pit Slope Design and Risk- A View of the Current State of the Art," *International Symposium on Stability of Rock Slopes in Open Pit Mining And Civil Engineering Situations*", SAIMM, Johannesburg, 30 pp.

Tapia, M., Secanelle, R., Berti, D., Martin, C., Goula X., Susagna, T., Dominique, P., Carbon, D. and Fleta, J. (2007 and 2008), "Probabilistic Seismic Hazard Assessment of the Pyrenean Region, J., Seimol, 12, pp 323-341. *Unpublished PhD Thesis Report*, Monash University, Clayton, Vic, Australia, 409 pp.

Zaruba, Q. and Mencl, V. (1969), *"Landslides and Their Control*" Elsevier, Amsterdam, Robinson, C. Publication, 205 pp.

Ziggah Y.Y., Hu Y. C., Odutola A. and Kumi-Boateng B. (2012), "Regression Models for 2-Dimensional Cartesan Coordinates Prediction"; A Case Study

APPENDICES

Appendix A: Base Angle Measurement

Appendix B: Shear Stress vrs Displacement

Appendix C: Stability Analysis

Appendix D: Structural Mapping Data

Appendix E: Rock Mass Rating Data

Appendix A

Base Angle Measurement

HOLE ID	GDKD069				DATE	10/11/2016					
LOGGED BY:		IOA/EHV									
FROM	TO	DRY				WET				WEATHERING	LITHOLOGY
		T1	**T2**	**T3**	AVERAGE	**T1**	**T2**	**T3**	AVERAGE		
43.73	44.87	44	44	45	44.33	44	44	40	42.67	MW	S
46.3	47.5	42	40	42	41.33	42	43	42	42.33	SW	S
50.97	51.82	35	36	34	35.00	41	40	35	38.67	UW	S
54	55.13	40	40	36	38.67	42	45	45	44.00	UW	IM
59.02	60.83	38	35	34	35.67	40	38	38	38.67	UW	IM
61.38	63	39	37	40	38.67	41	42	40	41.00	UW	IM
64.12	65.07	38	38	36	37.33	40	40	40	40.00	UW	S
68.79	70.01	38	40	42	40.00	45	47	44	45.33	UW	S
71.58	72.91	40	39	39	39.33	40	42	42	41.33	UW	S
91	92.86	44	43	41	42.67	44	46	45	45.00	UW	S
95.83	96.49	40	42	40	40.67	44	45	45	44.67	UW	S
98.4	99	39	39	41	39.67	43	45	41	43.00	UW	S
99.15	99.93	40	42	42	41.33	45	45	45	45.00	UW	S

KNOWLEDGE, TRUTH AND EXCELLENCE

HOLE ID	GDKD070				DATE	02/11/2016					
LOGGED BY:		IOA/ABP									
FROM	TO	DRY				WET				WATHERING	LITHOLOGY
		T1	**T2**	**T3**	AVERAGE	**T1**	**T2**	**T3**	AVERAGE		
29.04	29.96	45	45	45	45.00	35	45	45	41.67	S	SW
29.96	31.13	44	45	43	44.00	47	43	45	45.00	S	SW
32.02	33.01	40	44	48	44.00	45	35	43	41.00	S	SW
33.01	34.01	50	39	44	44.33	40	45	43	42.67	S	SW
35.73	36.6	43	43	48	44.67	42	42	42	42.00	S	SW
36.6	37.31	42	43	40	41.67	38	38	40	38.67	S	SW
37.43	38.27	50	43	45	46.00	43	47	43	44.33	S	SW
40.2	41.03	38	38	38	38.00	47	43	46	45.33	S	SW
43.09	43.83	44	46	51	47.00	43	42	44	43.00	S	SW
50.16	51.4	39	43	40	40.67	43	43	48	44.67	S	SW
51.4	59.93	43	43	40	42.00	41	40	40	40.33	S	SW
52.93	53.94	41	41	40	40.67	40	40	41	40.33	S	SW
53.94	54.53	41	41	44	42.00	41	43	43	42.33	S	SW
54.87	56.24	35	43	39	39.00	41	42	50	44.33	G	SW
56.24	57.16	40	43	40	41.00	40	43	42	41.67	G	SW
57.21	58.18	40	42	40	40.67	39	43	42	41.33	G	SW
71.45	72.2	36	37	36	36.33	36	36	40	37.33	S	UW
72.4	73.36	34	38	37	36.33	38	38	39	38.33	S	UW
74.6	75.27	36	34	35	35.00	36	40	38	38.00	S	UW
75.4	76.36	37	37	38	37.33	40	38	37	38.33	S	UW
82.37	83.13	34	40	37	37.00	37	38	37	37.33	S	UW
83.13	83.98	37	37	38	37.33	38	36	38	37.33	S	UW

HOLE ID	GDKD072				DATE						
LOGGED BY:		IOA/PNA									
FROM	TO	DRY				WET				WEATHERING	LITHOLOGY
		T1	T2	T3	AVERAGE	T1	T2	T3	AVERAGE		
4.04	6.75	49	45	50	48.00	50	55	40	48.33	MW	S
34.75	35.48	43	45	41	43.00	44	42	43	43.00	SW	S
35.48	36.47	40	41	43	41.33	44	40	40	41.33	UW	IM
36.84	37.45	39	39	38	38.67	41	41	39	40.33	UW	IM
39.29	40.88	40	42	40	40.67	42	41	41	41.33	UW	IM
43.1	43.97	41	42	41	41.33	41	42	43	42.00	UW	IM
45.6	46.35	44	38	40	40.67	44	44	44	44.00	UW	IM
47.48	48.22	40	41	40	40.33	42	40	42	41.33	UW	S
53.37	54.33	43	43	41	42.33	41	44	43	42.67	UW	S
56.38	57.33	43	43	44	43.33	43	43	42	42.67	UW	S
63.52	64.5	45	43	45	44.33	45	43	45	44.33	UW	S
68.33	69.15	43	43	43	43.00	45	45	45	45.00	UW	S
77.38	78.92	45	42	43	43.33	43	42	42	42.33	UW	S

HOLE ID	GDKD075				DATE	12/11/2016					
LOGGED BY:		IOA/PNA									
FROM	TO	DRY				WET				WEATHERING	LITHOLOGY
		T1	T2	T3	AVERAGE	T1	T2	T3	AVERAGE		
19.9	21.27	47	47	47	47.00	45	49	45	46.33	MW	S
23.6	25.67	40	38	40	39.33	40	42	44	42.00	UW	S
26.57	27.52	45	42	40	42.33	41	42	41	41.33	UW	IM
28.36	29.21	40	44	40	41.33	41	41	43	41.67	UW	S
29.21	30.18	41	41	40	40.67	40	40	40	40.00	UW	S
32.32	33.58	40	39	39	39.33	41	41	40	40.67	UW	S
33.58	34.82	40	35	38	37.67	40	36	38	38.00	UW	S
37	39.36	40	40	36	38.67	39	41	41	40.33	UW	S
42.84	44.78	36	41	41	39.33	39	40	40	39.67	UW	S
46.78	47.55	40	40	40	40.00	41	40	40	40.33	UW	S
49.97	52.15	40	40	40	40.00	40	41	40	40.33	UW	S
57.07	58.69	42	40	40	40.67	48	42	43	44.33	UW	S
73.4	75.65	41	40	40	40.33	42	42	42	42.00	UW	S

HOLE ID	GDKD076			DATE	15/11/2016						
LOGGED BY:		IOA/PNA									
FROM	TO	DRY				WET				WEATHERING	LITHOLOGY
		T1	T2	T3	AVERAGE	T1	T2	T3	AVERAGE		
13.57	16.5	49	42	38	43.00	47	43	42	44.00	MW	S
17.18	20.31	39	42	41	40.67	45	41	43	43.00	UW	S
20.95	22.94	40	39	41	40.00	42	41	40	41.00	UW	S
27.2	28.32	38	40	38	38.67	42	40	42	41.33	UW	S
32.78	33.13	41	42	43	42.00	42	45	45	44.00	UW	S
39.7	44.07	41	40	43	41.33	41	44	42	42.33	UW	S
45.48	46.54	40	41	40	40.33	40	41	45	42.00	UW	IM
53.92	54.75	38	41	41	40.00	40	42	41	41.00	UW	S
60.79	62.76	44	42	41	42.33	45	41	43	43.00	UW	S
69.05	69.92	45	43	43	43.67	45	45	43	44.33	UW	S
72.53	76.81	42	45	44	43.67	42	41	40	41.00		Q
77.81	81.5	44	43	45	44.00	43	45	40	42.67		Q
82.69	55	43	41	41	41.67	44	41	40	41.67		IM

KNOWLEDGE, TRUTH AND EXCELLENCE

HOLE ID	GDKD077				DATE	18/11/2016					
LOGGED BY:		IOA/PNA									
FROM	TO	DRY				WET				WEATHERING	LITHOLOGY
		T1	**T2**	**T3**	AVERAGE	**T1**	**T2**	**T3**	AVERAGE		
38.72	39.51	41	40	44	41.67	42	41	45	42.67	MW	IM
47.9	49.02	40	41	42	41.00	42	42	40	41.33	UW	S
49.53	50.83	44	41	41	42.00	45	41	40	42.00	UW	IM
52.9	53.73	40	39	36	38.33	41	40	41	40.67	UW	S
54.78	55.68	37	40	41	39.33	40	40	40	40.00	UW	S
56.66	57.63	36	39	39	38.00	40	40	35	38.33	UW	S
59.91	61.85	40	36	35	37.00	39	39	40	39.33	UW	S
65	66.42	39	35	36	36.67	39	40	40	39.67	UW	S
68.48	71.45	38	35	35	36.00	39	40	39	39.33	UW	S
76.38	77.34	36	35	35	35.33	40	40	39	39.67	UW	S
78.49	79.81	40	39	35	38.00	40	43	40	41.00	UW	S
84.31	87.84	45	49	44	46.00	45	45	41	43.67	UW	S
88.56	90.42	43	42	40	41.67	42	42	41	41.67	UW	S
90.9	91.59	41	40	40	40.33	40	42	43	41.67	UW	S
99.31	100.09	45	45	45	45.00	48	45	49	47.33	UW	S

Appendix B

Shear Stress vs Displacement

KNOWLEDGE, TRUTH AND EXCELLENCE

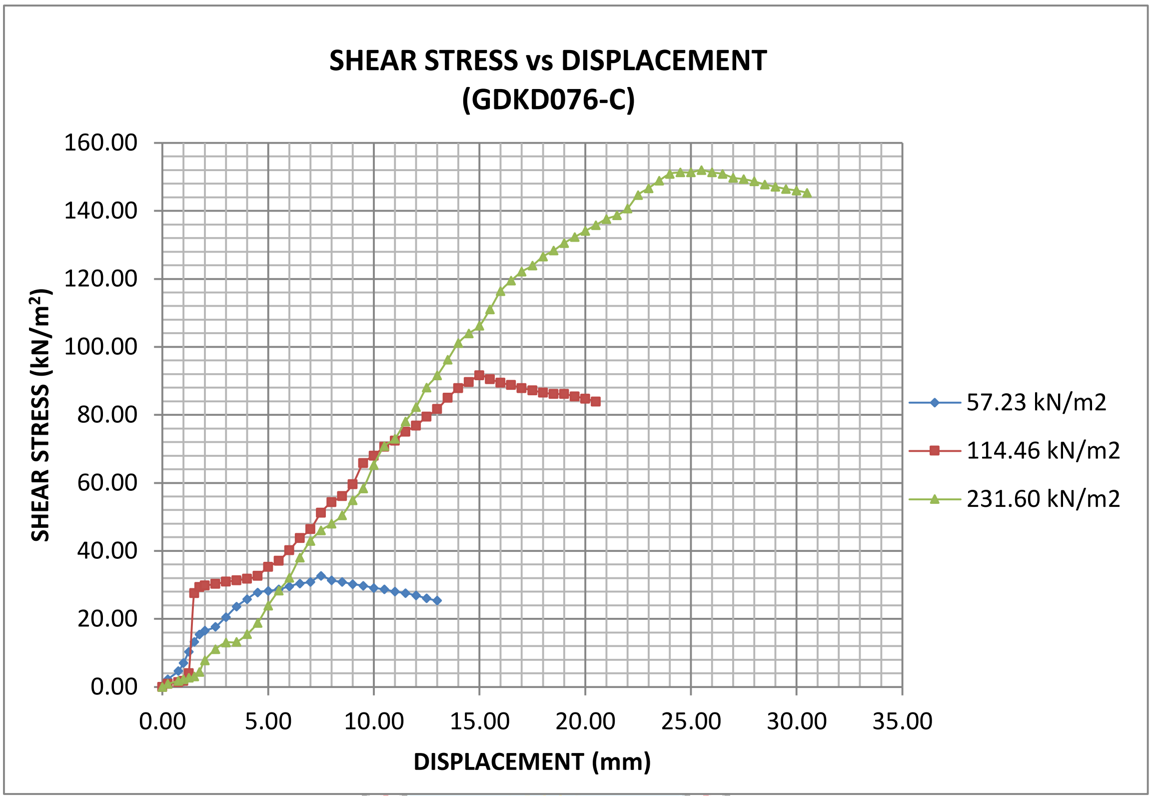
SHEAR STRESS vs DISPLACEMENT
(GDKD076-C)
SHEAR STRESS (kN/m²)
DISPLACEMENT (mm)
57.23 kN/m2
114.46 kN/m2
231.60 kN/m2

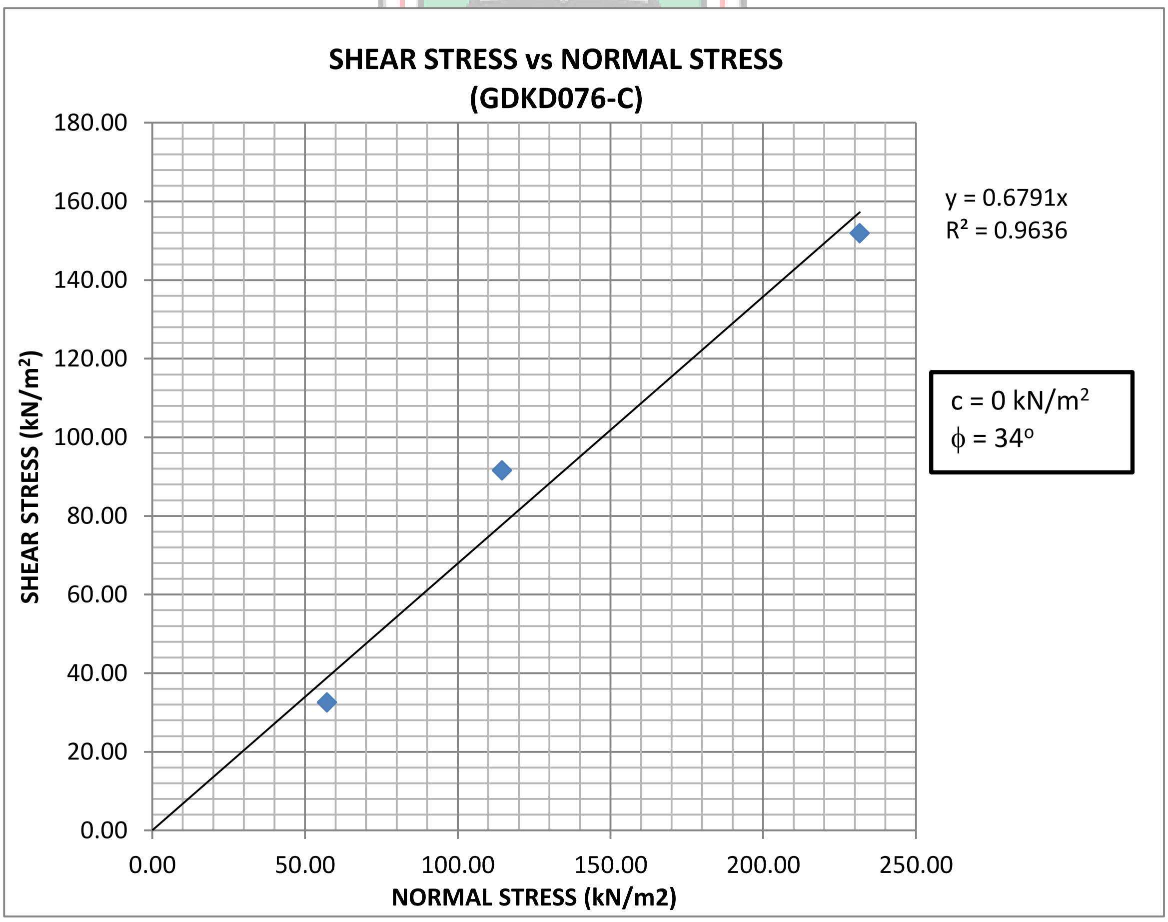
SHEAR STRESS vs NORMAL STRESS
(GDKD076-C)
SHEAR STRESS (kN/m²)
NORMAL STRESS (kN/m2)
y = 0.6791x
R² = 0.9636
c = 0 kN/m²
ϕ = 34°

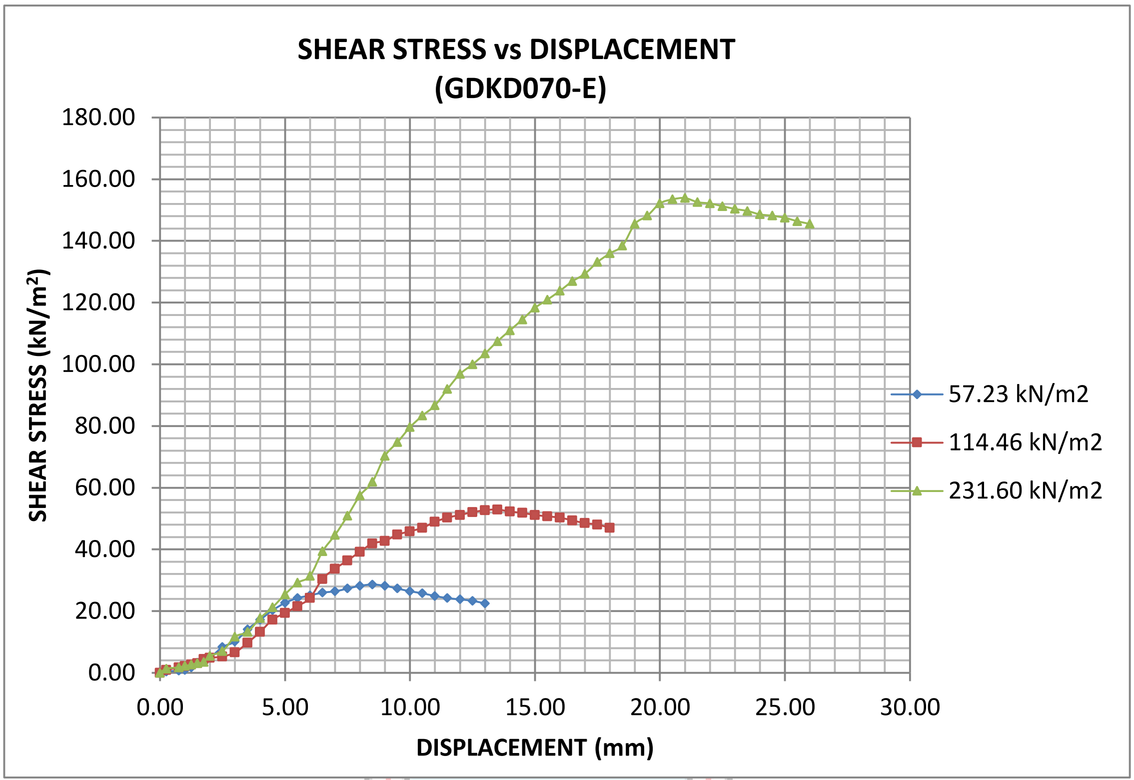
SHEAR STRESS vs DISPLACEMENT
(GDKD070-E)
SHEAR STRESS (kN/m²)
180.00
160.00
140.00
120.00
100.00
80.00
60.00
40.00
20.00
0.00
0.00
5.00
10.00
15.00
20.00
25.00
30.00
DISPLACEMENT (mm)
57.23 kN/m2
114.46 kN/m2
231.60 kN/m2

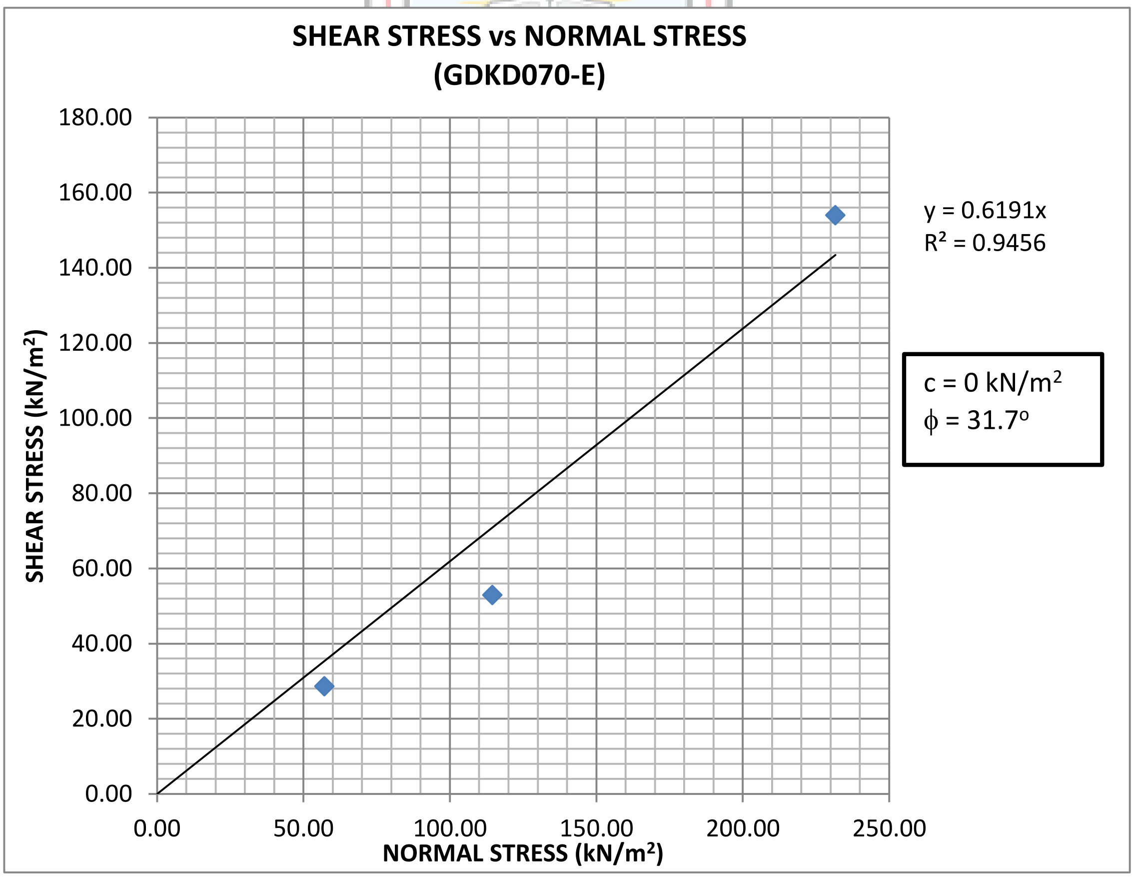
SHEAR STRESS vs NORMAL STRESS
(GDKD070-E)
SHEAR STRESS (kN/m²)
180.00
160.00
140.00
120.00
100.00
80.00
60.00
40.00
20.00
0.00
0.00
50.00
100.00
150.00
200.00
250.00
NORMAL STRESS (kN/m²)
y = 0.6191x
R² = 0.9456
c = 0 kN/m²
ϕ = 31.7º

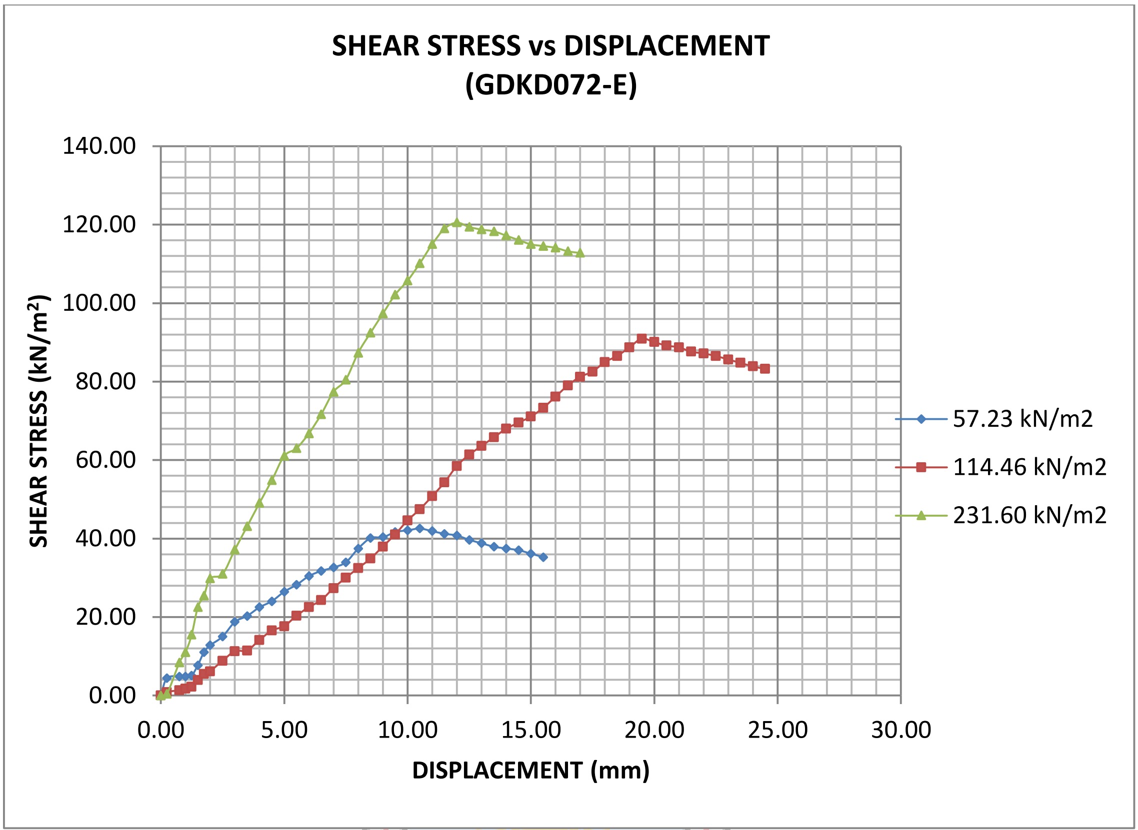
SHEAR STRESS vs DISPLACEMENT
(GDKD072-E)
SHEAR STRESS (kN/m²)
DISPLACEMENT (mm)
140.00
120.00
100.00
80.00
60.00
40.00
20.00
0.00
0.00
5.00
10.00
15.00
20.00
25.00
30.00
57.23 kN/m2
114.46 kN/m2
231.60 kN/m2

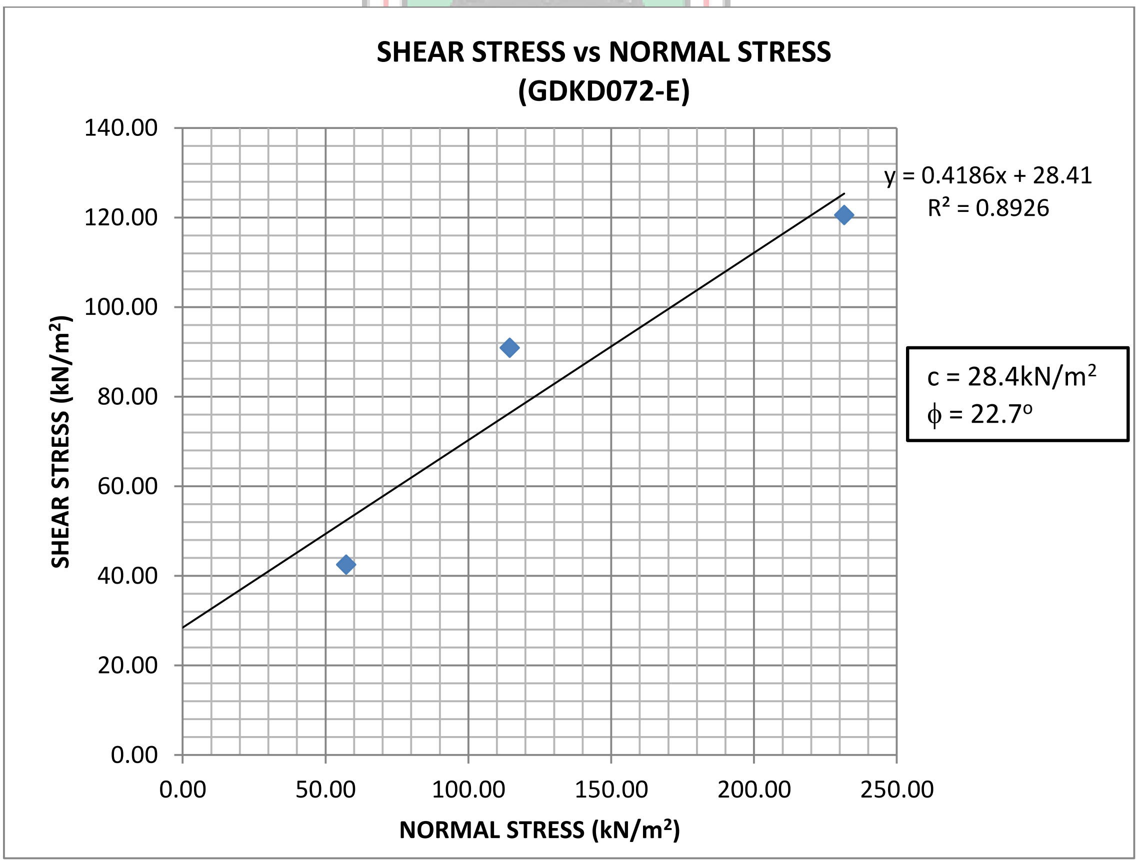
SHEAR STRESS vs NORMAL STRESS
(GDKD072-E)
SHEAR STRESS (kN/m²)
NORMAL STRESS (kN/m²)
140.00
120.00
100.00
80.00
60.00
40.00
20.00
0.00
0.00
50.00
100.00
150.00
200.00
250.00
y = 0.4186x + 28.41
R² = 0.8926
c = 28.4kN/m²
ϕ = 22.7°

Appendix C

Stability Analysis

KNOWLEDGE, TRUTH AND EXCELLENCE

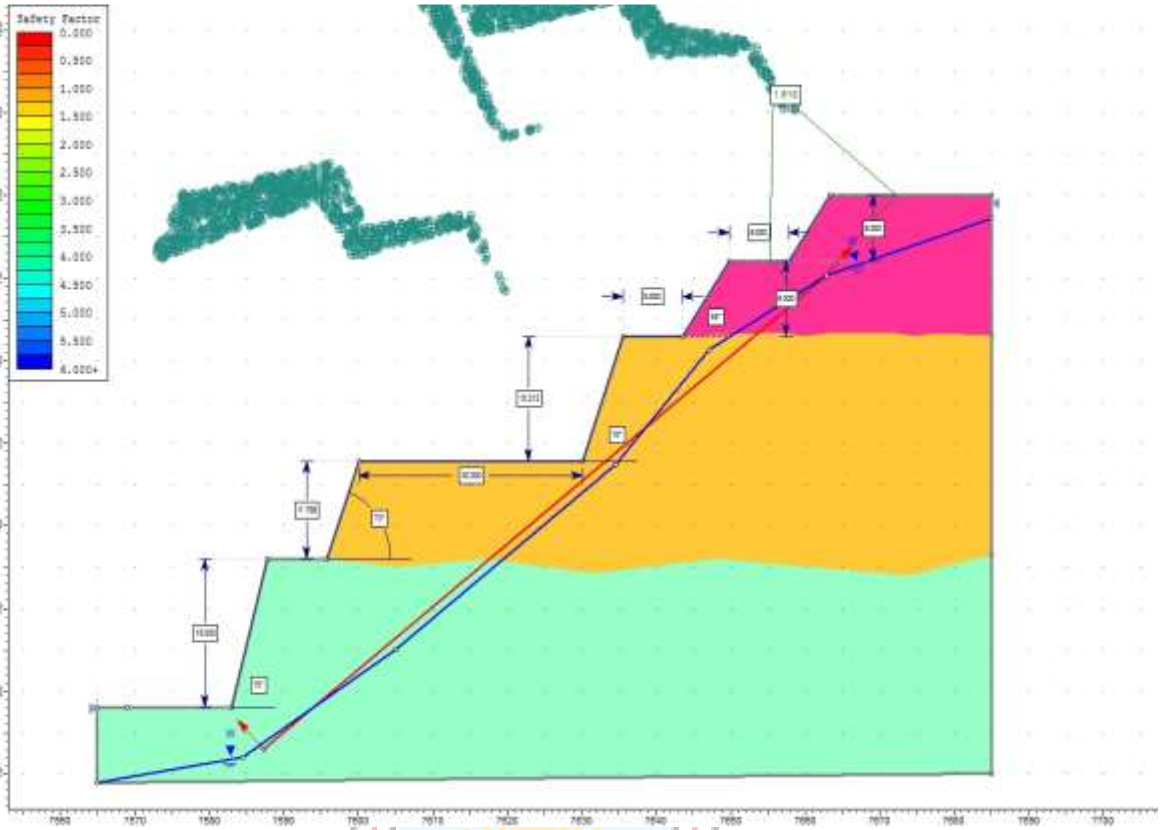
Safety Factor
0.000
0.500
1.000
1.500
2.000
2.500
3.000
3.500
4.000
4.500
5.000
5.500
6.000+

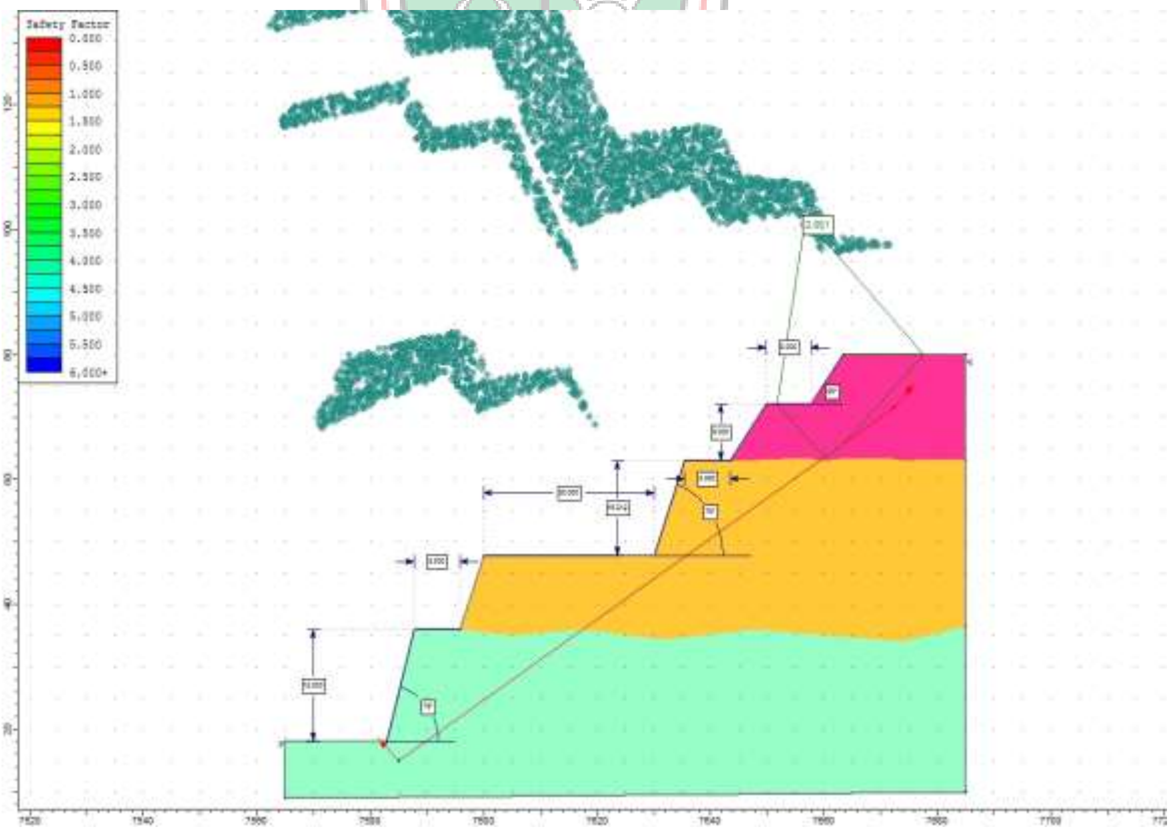
Safety Factor
0.000
0.500
1.000
1.500
2.000
2.500
3.000
3.500
4.000
4.500
5.000
5.500
6.000+

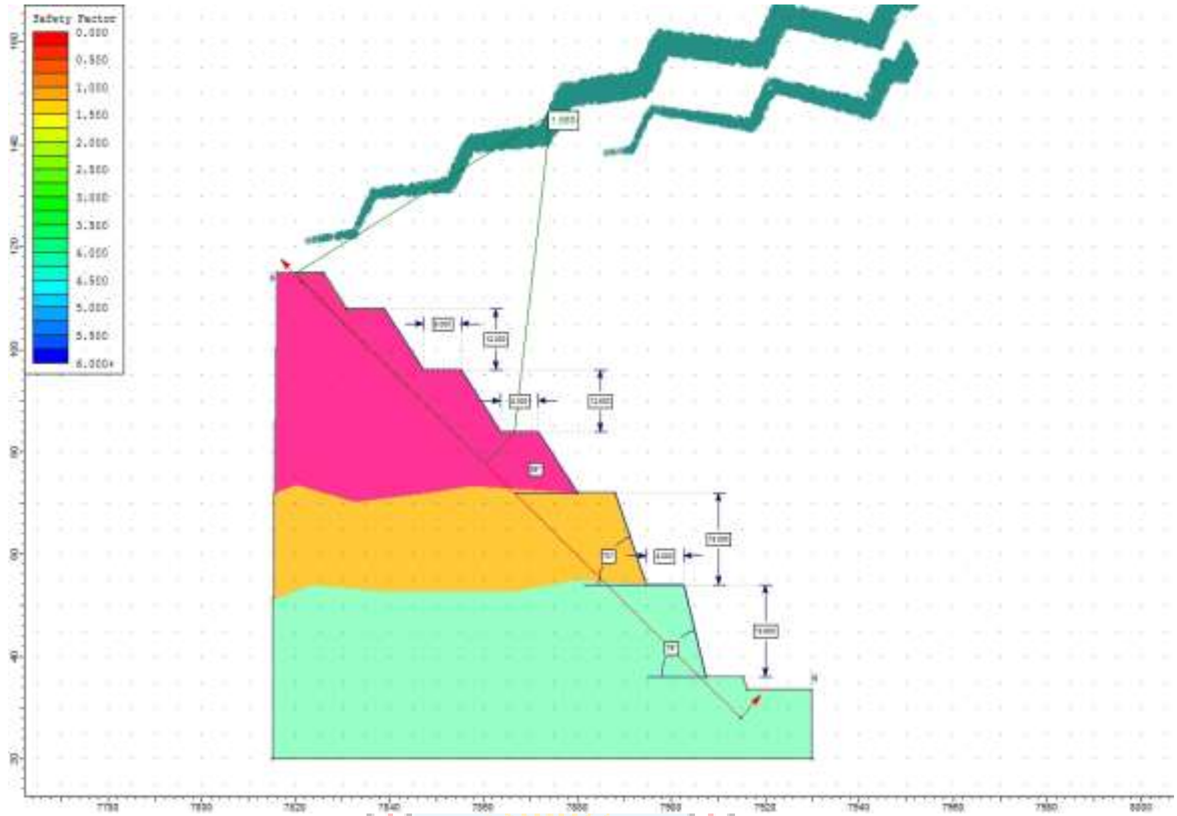
Safety Factor
0.000
0.500
1.000
1.500
2.000
2.500
3.000
3.500
4.000
4.500
5.000
5.500
6.000+

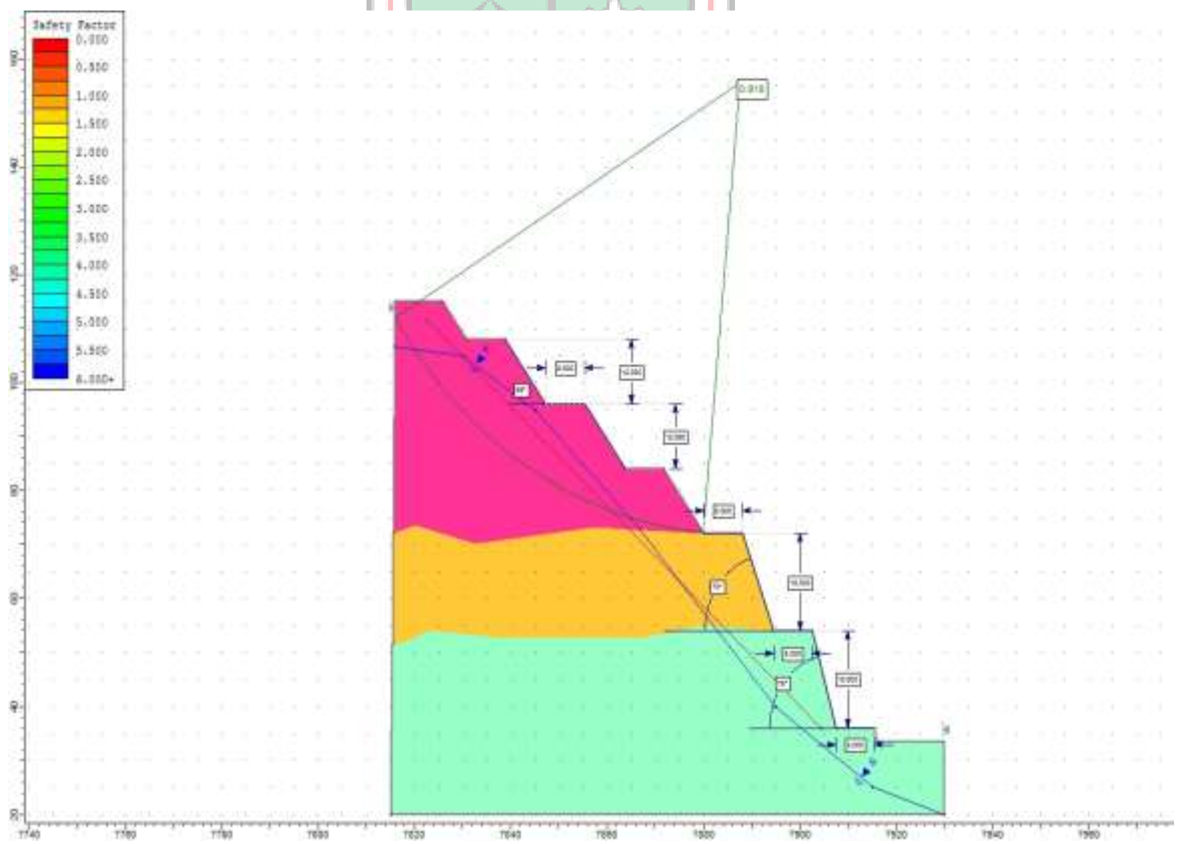
Safety Factor
0.000
0.500
1.000
1.500
2.000
2.500
3.000
3.500
4.000
4.500
5.000
5.500
6.000+

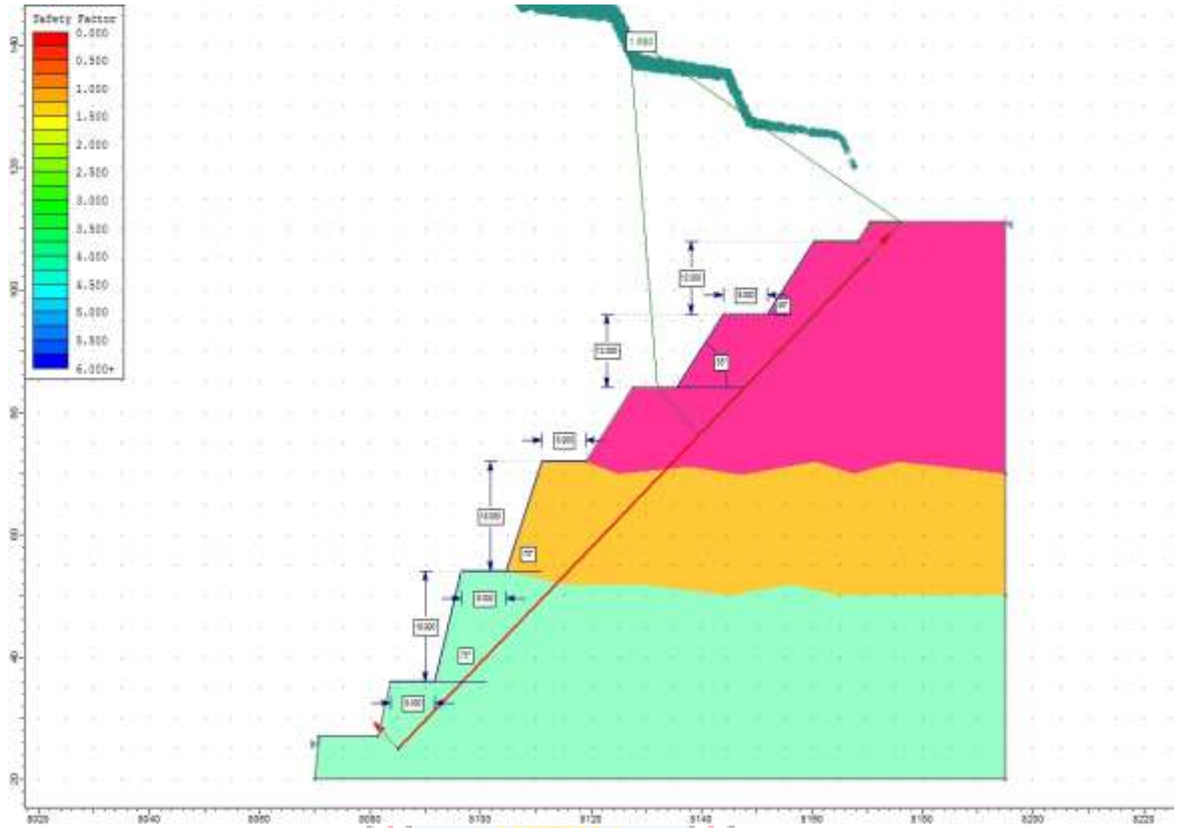
Safety Factor
0.000
0.500
1.000
1.500
2.000
2.500
3.000
3.500
4.000
4.500
5.000
5.500
6.000+


Safety Factor
0.000
0.500
1.000
1.500
2.000
2.500
3.000
3.500
4.000
4.500
5.000
5.500
6.000+

Appendix D

Structural Mapping Data

depth_from	depth_to	recovery_m	rqd_m	rock_type	hardness	weathering	matrix_m	matrix_type	matrix_solid_m	lith descrip.
0.00	2.22	1.02	0.00	RSSP	0.3	CW				Reddish brown completely weathered overburden
2.22	4.30	1.70	0.00	RSSP	0.5	CW				Reddish brown completely weathered quartzite
4.30	5.46	0.56	0.00	SSSS	0.8	CW				Yellowish brown completely weathered quartzite
5.46	5.70	0.24	0.00	SSSS	0.8	CW				Greyish brown completely weathered quartzite
5.70	7.12	1.02	0.00	SSSS	0.5	CW				Brown completely weathered quartzite
7.12	9.40	0.98	0.00	SSSS	1	HW				Greyish brown highly weathered quartzite
9.40	10.04	0.64	0.00	SSSS	1	HW				Light brown highly weathered quartzite
10.04	10.90	0.56	0.00	SSSS	1	HW				Yellowish brown highly weathered quartzite
10.90	11.88	0.98	0.23	SSSS	30	MW				Pinkish moderately weathered quartzite
11.88	12.16	0.28	0.13	SSSS	35	MW				Brown moderately weathered quartzite
12.16	12.24	0.08	0.00	SSSS	1	HW				Whitish grey highly weathered quartzite
12.24	13.30	1.06	5.03	SSSS	30	MW				Yellowish brown moderately weathered quartzite
13.30	14.19	0.89	0.00	SSSS	25	MW				Pinkish brown moderately weathered quartzite
14.19	15.10	0.71	0.13	SSSS	35	MW				Reddish brown moderately weathered quartzite
15.10	15.71	0.61	0.60	SSSS	40	MW				Whitish grey to pale yellow moderately weathered
15.71	16.43	0.72	0.36	SSSS	38	MW				Greyish yellow moderately weathered quartzite
16.43	16.63	0.20	0.00	SSSS	35	MW				Greyish white moderately weathered quartzite
16.63	17.57	0.94	0.75	SSSS	36	MW				Yellowish grey moderately weathered quartzite
17.57	17.79	0.22	0.00	SSSS	20	HW				Pinkish red highly weathered quartzite
17.79	18.56	0.77	0.54	SSSS	45	MW				Moderately weathered whitish grey to pale yellow
18.56	18.82	0.26	0.00	SSSS	45	MW				Whitish grey moderately weathered quartzite
18.82	19.57	0.75	0.40	SSSS	45	MW				Light reddish brown moderately weathered quartzit
19.57	21.72	2.15	0.89	SSSS	50	MW				Greyish white to pale yellow moderately weathered
21.72	22.26	0.54	0.00		25	MW				Broken yellowish grey quartzite
22.26	23.62	1.36	1.25	SSSS	70	SW				Whitish grey slightly weathered quartzite
23.62	25.00	1.38	1.02	SSSS	35	MW				Dark yellowish grey moderately weathered quartzit

25.00	26.56	1.56	1.17	SSSS	45	MW	Pale yellowish grey to dark yellowish grey m quartzite
26.56	27.80	1.24	0.62	SSSS	50	MW	Whitish grey moderately weathered quartzite
27.80	27.94	1.06	0.22	SSSS	40	MW	Yellowish grey moderately weathered quartzite
27.94	30.24	2.30	1.82	SSSS	68	SW	Whitish grey slightly weathered quartzite
30.24	30.59	0.35	0.00	SSSS	60	MW	Whitish grey moderately weathered quartzite
30.59	31.21	0.69	0.65		75	SW	Whitish grey slightly weathered quartzite
31.21	32.13	1.33	0.92		80	SW	Pale yellow slightly weathered quartzite
32.13	33.02	0.79	0.71	SSSS	85	UW	Whitish grey unweathered quartzite
33.02	33.47	0.55	0.53	SSSS	85	UW	Pinkish to whitish grey quartzite
33.47	33.74	0.27	0.00	SSSS	80	HW	Whitish grey hightly weathered quartzite
33.74	34.41	0.67	0.59	SSSS	80	SW	Whitish grey slightly weathered quartzite
34.41	34.66	0.25	0.00	SSSS	75	MOD	Whitish grey moderately weathered quartzite
34.66	35.78	1.12	0.81	SSSS	90	SW	Pale yellow to whitish quartzite
35.78	37.01	1.23	1.14	SSSS	95	UW	
37.01	38.01	1.00	0.78	SSSS	95	UW	Whitish grey unweathered quartzite
38.01	38.76	0.75	0.44	SSSS	95	UW	Whitish grey unweathered quartzite
38.76	39.25	0.49	0.49	SSSS	100	UW	Whitish grey unweathered quartzite
39.25	39.56	0.31	0.00	SSSS	80	MW	Whitish grey moderately weathered quartzite
39.56	40.02	0.46	0.32	SSSS	85	SW	Whitish grey slightly weathered quartzite
40.02	41.02	1.00	1.00	SSSS	110	UW	Greyish white unweathered quartzite
41.02	42.00	0.98	0.83	SSSS	110	UW	Greyish white unweathered quartzite
42.00	43.54	1.44	1.44	SSSS	110	UW	Greyish white unweathered quartzite
43.54	44.08	0.54	0.31	SSSS	110	SW	Greyish white unweathered quartzite
44.08	44.61	0.53	0.35	SSSS	115	SW	Greyish white unweathered quartzite
44.61	45.52	0.79	0.17	SSSS	118	MW	Greyish white pebbly quartzite
45.52	46.89	1.37	1.18	SSSS	118	SW	Greyish white slightly weathered quartzite

KNOWLEDGE, TRUTH AND EXCELLENCE

Appendix E

Rock Mass Rating Data

RMR Joint Spacing (Js)																						
setSG Js*SG00	set2 Js*SG00	set3 Js*SG00	Js Joint Sets	Js rating 0 sets	Js rating SG sets	Js rating 2 sets	Js rating 3 sets	IRS rating	RQD rating	Js rating	Macro rating	Micro rating	Infill rating	Alter rating	Jc rating	RMR	Weathing	Orien-tation	Stress	Blasting	MRMR	IOSA
0.0	0.0	0.0	0	25	0	0	0	0	0	25	1.00	1.00	1.00	1.00	40	0.00	0.62	0.85	1.00	0.94	0	30
0.0	0.0	0.0	0	25	0	0	0	0	0	25	1.00	1.00	1.00	1.00	40	0.00	0.62	0.85	1.00	0.94	0	30
0.0	0.0	0.0	0	25	0	0	0	0	0	25	1.00	1.00	1.00	1.00	40	0.00	0.62	0.85	1.00	0.94	0	30
0.0	0.0	0.0	0	25	0	0	0	0	0	25	1.00	1.00	1.00	1.00	40	0.00	0.62	0.85	1.00	0.94	0	30
0.0	0.0	0.0	0	25	0	0	0	1.089	0	25	1.00	1.00	1.00	1.00	40	0.00	0.78	0.85	1.00	0.94	0	30
0.0	0.0	0.0	0	25	0	0	0	1.416	0	25	1.00	1.00	1.00	1.00	40	0.00	0.78	0.85	1.00	0.94	0	30
0.0	0.0	0.0	0	25	0	0	0	0	0	25	1.00	1.00	1.00	1.00	40	0.00	0.62	0.85	1.00	0.94	0	30
0.0	0.0	0.0	0	25	0	0	0	0	0	25	1.00	1.00	1.00	1.00	40	0.00	0.62	0.85	1.00	0.94	0	30
0.0	0.0	0.0	0	25	0	0	0	2.544	3	25	1.00	1.00	1.00	1.00	40	70.20	0.90	0.85	1.00	0.94	50	55
0.0	0.0	0.0	0	25	0	0	0	3	15	25	1.00	1.00	1.00	1.00	40	82.93	1.00	0.85	1.00	0.94	66	63
0.0	0.0	0.0	0	25	0	0	0	1.416	0	25	1.00	1.00	1.00	1.00	40	0.00	0.78	0.85	1.00	0.94	0	30
0.0	0.0	0.0	0	25	0	0	0	3.55	0	25	1.00	1.00	1.00	1.00	40	68.48	1.00	0.85	1.00	0.94	55	57
0.0	0.0	0.0	0	25	0	0	0	9.55	0	25	1.00	1.00	1.00	1.00	40	74.48	1.00	0.85	1.00	0.94	60	60

Index

B

C

KNOWLEDGE, TRUTH AND EXCELLENCE

E

P

KNOWLEDGE, TRUTH AND EXCELLENCE

KNOWLEDGE, TRUTH AND EXCELLENCE

W